PHOTOSYNTHETIC CAPACITY ALONG A GRADIENT OF TRACE ELEMENT CONTAMINATION IN A SPONTANEOUS URBAN FOREST COMMUNITY

By

ALLYSON SALISBURY

A dissertation submitted to the

Graduate School-New Brunswick

Rutgers, The State University of New Jersey

In partial fulfillment of the requirements

For the degree of

Doctor of Philosophy

Graduate Program in Environmental Science

Written under the direction of

Jason Grabosky

And approved by

_____

_____

_____

_____

_____

_____

New Brunswick, New Jersey

MAY 2017

ABSTRACT OF THE DISSERTATION

Photosynthetic Capacity along a Gradient of Trace Element Contamination in a Spontaneous Urban Forest Community

By Allyson Salisbury

Dissertation Adviser

Jason C. Grabosky

Trace element (TE) pollution of soil is a pervasive global problem which affects both human health and ecosystem function. However there is a lack of mechanistic understanding in the ways TE effects on individual organisms ultimately alter ecosystem function. The goal of this dissertation was to explore the effects of TE contamination on primary productivity in a hardwood forest which spontaneously established in an urban brownfield. Given the age of the site, the study first compared a set of measurements made on soil data collected at the site over the course of 20 years. This analysis revealed that pseudo-total concentrations of copper, lead, and zinc in the soil remained fairly stable in this time period. However between 2005 and 2015 concentrations of arsenic and chromium increased. Next, the study measured photosynthesis rates and other related leaf level biophysical parameters over the course of two growing seasons in *Betula populifolia* which were growing in plots with low or high TE concentrations (trees were at least 10 years old). The maximum carboxylation rate and electron transport rate of trees growing in high TE plots was significantly lower than those in low TE plots during July 2014 and May 2015. TE alone was not a significant predictor of photosynthesis parameters. These findings suggest TE effects on photosynthesis apparatus in these trees may transient and seasonal in nature and that photosynthesis is fairly robust along the gradient of TE contamination at the research

site. In the third study, leaf area index (LAI) measured over the course of seven years was compared between two low and two high TE plots within the study site. In the first three years of LAI measurements, one high TE plot consistently had the highest LAI while the second high TE plot had the lowest LAI. The LAI results suggest that other factors such as soil nutrient availability, facilitative mycorrhizal interactions, stand age and plot history may also be important drivers of canopy productivity in addition to TE stress. These studies, taken together with other research conducted at the site, highlight the challenge of developing a mechanistic understanding of TE impact on hardwood primary productivity. TE may play a more important role earlier in assemblage development by acting as an abiotic filter on species establishment, though more work is needed to confirm this hypothesis. These findings also demonstrate the potential of such ecosystems to function in spite of severe abiotic stress.

Acknowledgements

This dissertation would not have been possible without help from a large number of people. First and foremost, I have to thank my advisers Drs. Jason Grabosky and Frank Gallagher for the opportunity to lead this project and their trust to allow me to make it my own. Throughout this project my committee members Drs. Daniel Gimenez, Chris Obropta, and John Reinfelder provided guidance and support which really improved the quality of this research. And special thanks to my outside member Dr. Jennifer Krummins who was willing to join the team last minute but still had a wealth of insight to contribute.

I have had the privilege to work with an outstanding group of students who helped me conduct field work. In spite of the hot weather, rain, snow, poison ivy, ticks, mosquitos and hornets, they were always amazing: Isabella Cocuzza, Catherine Dillon, Booker George, Longjun Ju, Michael Martini, and Han Yan.

Drs. John Reinfelder and Silke Severman and the members of their respective labs made Chapter 2 possible: Amy Christiansen, Sarah Janssen, and Phil Sontag. Also thanks to Maria Rivera for letting me utilize the Environmental Science Teaching Lab.

The USDA NRCS Somerset Lab let me test soil samples with their portable XRF on multiple occasions.

The Rutgers Soil Testing Lab allowed me to use equipment to test samples and also graciously analyzed a large set of samples with very short notice.

Dr. Karina Schaffer shared equipment and personnel and also provided input on the setup of the photosynthesis study.

Dr. Josh Caplan provided much needed assistance on statistical analysis.

The New Jersey Department of Environmental Protection Park and Forestry Division have kindly been allowing researchers to make the most of an incredible site for well over a decade, enabling a very large body of research to be developed.

This project was funded by a grant from the McIntyre-Stennis Federal Program, a fellowship from the Graduate Assistance in Areas of National Need (GAANN) program, and the Rutgers Urban Forestry Kuser Endowment. For several years at Rutgers I also worked part time as a graduate mentor with the Douglass Project for Women in Math, Science, and Engineering which is an outstanding program that taught me a lot about mentoring and leadership.

The technical support staff at LI-COR biosciences also deserves a huge thanks for helping me perform repairs on our LI-6400 multiple times.

It has been a joy to be a part of the Rutgers Urban Forestry Lab Group for the past six years. I have been extremely fortunate to be able to show up to work every day with the nicest, most supportive bunch of coworkers anyone could ask for.

Last but certainly not least, I owe an enormous debt of gratitude to my family and friends who have provided me with so much love and support through this entire endeavor. I am blessed beyond measure by all of the wonderful people in my life, I hope this work make you proud.

Contents

List of Tables

List of Figures

Chapter 1 - Introduction and Background

INTRODUCTION

Trace Element Contamination in Soil

Trace element pollution of soils is a significant global health threat, with exposure risk increasing as more of the global population moves into urban environments. Hundreds of thousands of contaminated sites have been identified in the United States and Europe alone (Panagos et al. 2013; United States General Accounting Office 1987), while Chinese reports estimate over 3.33 million hectares of the country's cropland are no longer suitable for food production because of pollution (Larson 2014). A meta-analysis of 96 cities around the globe found a wide range of trace element concentrations in urban soils with many city soils containing trace element concentrations above remediation standards (Ajmone-Marsan and Biasioli 2010).

Soil trace element contamination can come from a variety of sources and be found in a variety of places. These sources include, but are not limited to, leftover materials from smelting (Derome and Nieminen 1998) and mining activities (Moreno-Jiménez et al. 2010; Wong 2003), industrial processes such as chromium plating (Castro-Rodríguez et al. 2015), aerial deposition from industrial and mobile sources (Gandois et al. 2010), and irrigation with wastewater (Guédron et al. 2014). While there are many historic sources of trace element pollution, this is not simply a problem of the past. Increasing global use of vehicles and demand for electronics will continue to generate soil pollution well into the foreseeable future (Ajmone-Marsan and Biasioli 2010; Tang et al. 2010). As the list of possible sources suggests, trace element contamination can be found in a range of environments, from dense city centers to rural forests downwind of industrial operations. For the purposes of this dissertation, the phrase urban soils will be used in its broadest sense to encompass not only soils in city environments, but soils in industrial,

transportation, and mining areas as well (collectively called SUITMAs (Morel et al. 2014)) which have been affected by anthropogenic activity. Brownfields can be considered a sub-group or an alternate name for contaminated sites. Brownfields are abandoned land considered derelict from lack of use and are often not redeveloped because of concern for potential soil contamination (Linn 2013). Most brownfield studies referenced in this project have confirmed cases of contamination.

Phytostabilization and Natural Attenuation

Trace element pollution is particularly difficult to manage because of its elemental nature, it cannot be degraded into less toxic components. Once in the soil, trace element ions are influenced by sorption/desorption processes with clay, (hydr)oxides, and organic matter; oxidation/reduction reactions; precipitation/dissolution reactions; plant uptake; volatilization; and leaching through mass flow in the soil solution (Sparks 2003). These processes determine whether trace element ions will remain in place, immobilized by soil material, or will become mobile and leave the immediate soil system. Phytostabilization is one of many options for managing soil contamination. This process allows or facilitates the establishment of a stable vegetative cover instead of capping or removing the soil (Hartley et al. 2012). This dissertation defines a phytostablization project as any contaminated site covered by a plant community. The process utilizes vegetation to limit contaminant transport by reducing erosion, maintaining an aerobic soil environment, and binding some types of contaminants through the addition of organic matter (Robinson et al. 2009). However, since trace elements are left on site there remains a risk of leaching deeper into the soil profile or water table and of trace elements entering the food web at potentially toxic concentrations through plant and/or macroinvertebrate uptake (Dickinson et al. 2009).

An ongoing challenge with the practice of phytostabilization is understanding how to promote the growth of plants while limiting trace element mobilization (Li and Huang 2015; Mendez and Maier 2008). In addition to toxicity from elevated concentrations of trace elements, soils in contaminated or severely disturbed sites may have poor drainage, low nutrient availability, extreme pH (too high or too low), and high bulk density (Wong 2003). Organic matter and associated nutrients needed to enable or enhance plant growth may also be able to mobilize trace elements, though this effect is highly variable. Additionally, organic matter will accumulate in the soils of contaminated sites as plant communities develop. Beesley et al., (2010) found the application of greenwaste compost and biochar increased Cu and As concentrations 30 fold in pore water, though Zn and Cd availability decreased likely because of changes in soil pH and dissolved organic carbon. Ruttens et al., (2006) found the addition of compost and cyclonic ash reduced Zn and Cd leaching but increased the leaching of Cu and Pb in a lysimeter study. These different responses to the application of organic matter is a function of both the hydrolysis and binding properties of each trace element as well as the composition of the organic matter (Sparks 2003). Trace element binding affinity varies by functional group in organic matter so the chemical composition of the material exerts a strong influence on its ability to retain trace element ions.

The bioavailability of trace elements in soil is another important component of plant establishment on a contaminated site and is influenced by the soil's mineralogy, physical characteristics, and biologic activity. Minerals such as Fe- and Mn-(hydr)oxides (Contin et al. 2007; Hartley et al. 2009), carbonates (Bolan et al. 2003; Gray et al. 2006), and phosphates (Chlopecka and Adriano 1997; Madrid et al. 2008) can contribute to the ability of a soil retain trace elements. Though the ability of these materials to immobilize trace elements is highly sensitive to pH and redox conditions – a site must maintain optimal conditions in order to ensure

the longevity of immobilization (Madrid et al. 2008). Bolan et al. (2014) suggest more field studies are needed to gage the long term effectiveness of immobilizing amendments.

Mendez and Maier (2008) point out that there is generally a lack of studies lasting more than one to two years on the success of phytostabilization projects or studies. The authors suggest that successful revegetation projects are able to self-propagate, produce equivalent biomass and cover in comparison to an uncontaminated site, and have above ground plant tissue trace element concentrations below toxicity limits for domestic animals. A survey of brownfield greening projects in the United Kingdom found many case studies had limited success in establishing habitat, usually because of poor soil conditions (Doick et al. 2009).

Spontaneous Urban Vegetation

Vegetative assemblages can also develop on contaminated or severely disturbed soil without the aid of human activity. There are several studies which document cases of spontaneously vegetated contaminated sites or urban soils – places where an ecosystem becomes established without human intervention, despite poor growing conditions (e.g. Desjardins et al., 2014; Olson and Fletcher, 2000; Schadek et al., 2009). The unique and sub-optimal soil conditions at these sites resulted in the development of unique plant community composition (Olson and Fletcher 2000) which can change over time as the community modifies soil conditions (Schadek et al. 2009). These sites not only demonstrate the capacity of systems to thrive in spite of limiting conditions, they can also provide clues about the conditions necessary to develop a self-sustaining ecosystem (Frouz et al. 2008). In some cases, spontaneous urban vegetation may have higher plant and insect diversity compared to managed landscapes (Robinson and Lundholm 2012), though diversity can be strongly dependent on microsite conditions (Cervelli et al. 2013). Del Tredici (2010) has argued that it may be more advantageous to improve our understanding

and management the ecosystem functions of spontaneous urban vegetation instead of spending effort to restore ecosystems to their pre-urban states.

Contaminated Soils and Ecosystem Function

Ecosystem functions are a broad category of processes and pools of material that emerge from the interactions of organisms with each other and with their environment. Some authors modify this definition to include ecosystem goods – ecosystem properties with market value – and ecosystem services – properties which benefit human society (Hooper et al. 2005). This dissertation will primarily focus on the processes aspect of ecosystem function, though many sources it references utilize an ecosystem service based perspective. Understanding the responses of ecosystem functions to anthropogenic disturbances such as soil pollution is highly relevant to large scale biosphere models (Medvigy et al. 2009), natural resource management (Cox et al. 2013), and the practices of ecological restoration and environmental risk management (Hooper et al. 2016).

Understanding the effects of stress on both the structure and functions of ecosystems is necessary in order to mitigate the impacts of human activities on ecosystems (Gessner and Chauvet 2013). Increasing concentrations of trace elements in the environment have been shown to reduce leaf litter decomposition (Oguma and Klerks 2015), soil respiration and plant biomass (Ramsey et al. 2005), and alter hydrologic cycles (Derome and Nieminen 1998). However more research has focused on the effects of pollution on lower levels of biological organization rather than community and ecosystem level responses (Clements and Kiffney 1994; De Laender et al. 2008; Mysliwa-Kurdziel et al. 2004). There is a need to be able to draw connections and extrapolate individual responses to community and ecosystem level responses to trace element exposure (Munns et al. 2009; Rohr et al. 2016).

Contaminated Soils and Ecosystem Response to Climate Change

Little is known about the ways plant communities stressed by soil contamination will also be affected by climate change. Climate change will significantly influence the growth and distribution of plants in all environments in complex ways. While greater availability of CO_2 can enable higher net primary productivity, these benefits may be limited by nutrient and water availability as well as increased temperatures (Pastor and Post 1988). Additionally some regions of the world may also experience more frequent extreme weather events (Romero Lankao et al. 2014) which can have severe impacts on forest structure and function (Wang et al. 2010). It has also been hypothesized that trace element speciation and mobility will be affected as changing temperature and rainfall patterns alter soil pH and redox conditions (Al-Tabbaa et al. 2007). It is important to understand how phytostabilization and spontaneous urban plant communities will respond to the dual stresses of climate change and trace element contamination in order to ensure their long term stability.

Aim of Research

In an increasingly urbanizing world, it is critical to understand and predict ecosystem level responses to anthropogenic activities and disturbances. However as Rohr et al. (2016) pointed out, assessing contaminant effects at high levels of biological organization can be very challenging. Consequently research is lacking on the mechanisms connecting individual level responses to ecosystem responses in terrestrial environments. Though ecosystem functions encompass a wide range of processes, this dissertation will focus on aboveground primary productivity in plants because it is a foundational process for terrestrial ecosystems. Additionally,

given current concerns about global climate change there is particular interest in documenting carbon sequestration in biomass as part of mitigation efforts for climate change (Nowak and Crane 2002)**.**

This dissertation used Liberty State Park in Jersey City, NJ, which is a spontaneously vegetated urban brownfield contaminated with a suite of trace elements, to explore the following question: What are the mechanisms connecting soil trace element contamination to primary forest productivity?

Previous research at this brownfield documented reduced coarse scale forest productivity and tree basal growth rates in areas with high soil trace element concentrations (Dahle et al. 2014; Gallagher et al. 2008a; Radwanski et al. 2017). To complement these studies, this dissertation assessed the photosynthetic capacity of a dominant tree species at this site to determine the effects soil trace element concentrations have on photosynthesis in this species. This research was based on the hypothesis that if photosynthetic capacity is a primary driver of forest productivity and forest productivity at Liberty State Park decreases with increasing trace element concentration, then photosynthetic capacity should decrease as well.

The first project assessed temporal changes in soil trace element concentrations measured over the past 20 years. Since trees are long lived organisms, it is important to understand how their exposure to trace element contamination may or may not have changed over time. Additionally, while restoration and phyostabilization type projects implicitly assume trace element concentrations will remain stable in the long term, little research has actually documented whether or not this is actually the case (Mendez and Maier 2008). The age of the Liberty State Park's forest and the body of soil data available provide a prime opportunity to explore this issue.

The next project measured the response of leaf level photosynthetic capacity along a gradient of soil trace element contamination. A suite of photosynthetic gas exchange parameters were measured for two growing seasons on specimens of *Betula populifolia* which were at least 10 years old and growing in high or low concentrations of trace elements. While many other researchers have documented the negative effects of trace element contamination on photosynthetic rates and related gas exchange parameters, these studies are typically limited to highly controlled environments (Mysliwa-Kurdziel et al. 2004). This study was fairly unique in its use of self-seeded trees in a field setting which had been growing in trace element contaminated soil for many years. Since this study lasted for two growing seasons, it also assessed the effects of stressful weather patterns such as drought and a heat wave on the photosynthetic capacity of these trees.

The third project assessed trace element effects on canopy productivity using leaf area index (LAI) as a metric. As LAI is measured from the ground up, it captures the extent of the tree canopy at the stand scale and provides context for the photosynthesis measurements made at the leaf scale. Since LAI has been tracked at this site since 2010, it also provides insight into temporal variability in responses to TE contamination. The LAI data was also used to assess the effects of the Hurricane Sandy storm surge which occurred in October 2012, in the middle of the sampling period.

The synthesis chapter presents the findings of these three projects in the context of a conceptual model which describes the effects of trace element soil contamination on hardwood primary productivity. This model assesses trace element effects on different levels of biological organization as well as the interactions which occur between levels in order to understand their impacts on productivity.

BACKGROUND

Study Site

In the early 1800s, Liberty State Park was a coastal marsh located along the Hudson River (Figure 1-1). Over the course of 60 years the marsh was bound with three sea walls and filled in with rubble, construction debris, dredge material, slag, cinder, several barges, and other wastes. This created a peninsula of dry land and improved access to the deeper water of the Hudson River (U.S. Army Corps of Engineers 2005). These sea walls create a unique hydrologic setting where there is little groundwater movement in or out of the site (U.S. Army Corps of Engineers 2004). The site became an expansive rail yard, marina, and industrial area. These activities and historic fill resulted in a soil with high trace element concentrations exceeding both residential (New Jersey Department of Environmental Protection 1999) and ecological (United States Environmental Protection Agency 2003) soil screening criteria. The State of New Jersey opened the site as a park in 1976. Its perimeter and water front were capped and now host several million visitors a year. The park now serves as a gateway to the Statue of Liberty and Ellis Island. The 210 acre interior was left alone in its vegetated state and has since enabled research on the ability of a spontaneously developed ecosystem to establish on a contaminated site. As of the writing of this dissertation, 24 papers have been published based on research at the site and several projects remain ongoing.

Total Metal Load

The concentrations of the five most prevalent trace elements at the site exhibit high spatial variability (Figure 1-2) throughout the interior which has had important implications for plant community development (Gallagher et al. 2008b). In order to study the combined effects of

these trace elements, prior research created a total metal load index for study plots within the site. The total metal load (TML) is a rank sum index of the log normalized concentrations of As, Cu, Cr, Pb, and Zn at 22 plots in the interior. The index ranges from 0 (very low concentrations) to 5 (very high concentrations) and is unique to Liberty State Park. Modeled after Juang et al. (2001) this method provides a unique metric which allows for relative comparisons within the site. Study plots are classed as low metal load for TML values ranging from 0 to 2, medium metal load for 2-3, and high metal load for 3-5. This division was based on an assessment of patterns of primary productivity and TML distribution at the site (Gallagher et al. 2008b).

While this dissertation will primarily use the phrase trace element to refer to the soil contamination both at the study site and more broadly, the terms metal or metal load will also be used when referring to the total metal load index calculated specifically for Liberty State Park.

FIGURES

Figure 1-1: Location map of Liberty State Park in Jersey City, New Jersey. From United States Army Corps of Engineers (2004)

Figure 1-2: Distribution of total metal load within the Liberty State Park interior. Lower TML score indicates lower overall trace element concentration. Markers and associated numbers on the map indicate location and identifiers of plots used in various studies at the site. From Gallagher et al. (2008).

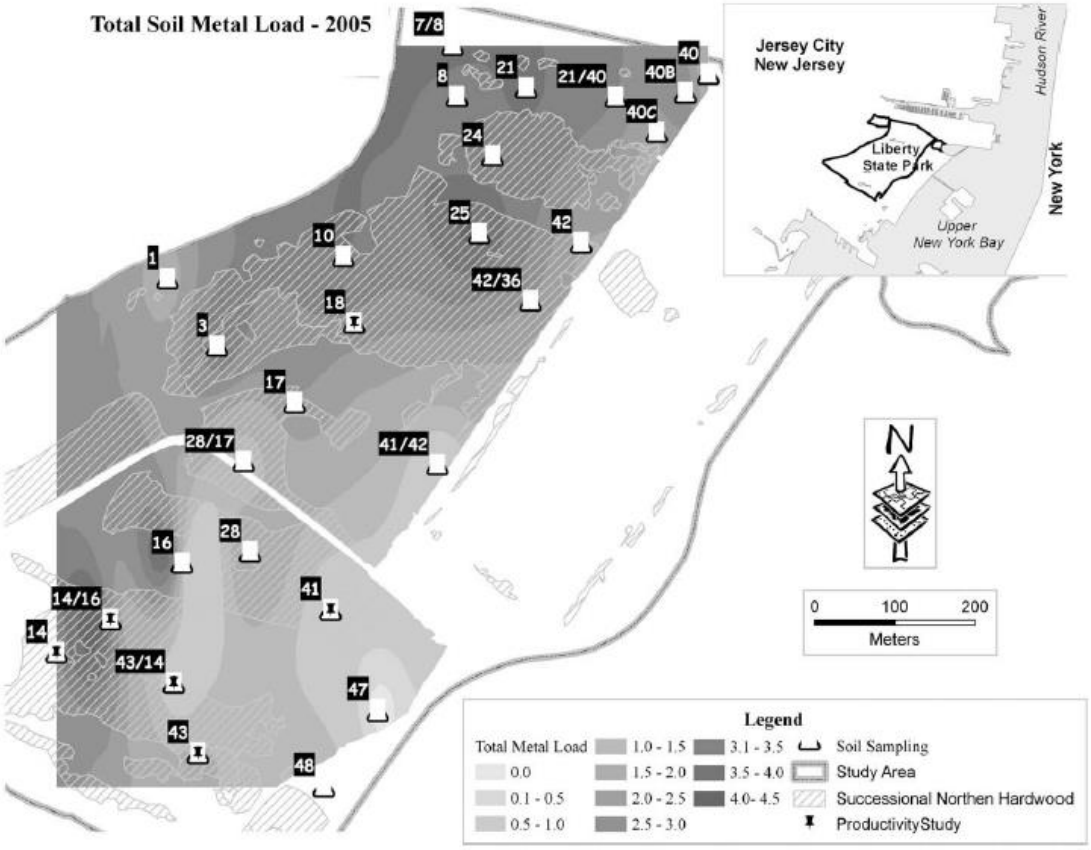

Chapter 2 - Long term stability of trace element concentrations in a spontaneously-vegetated urban brownfield with anthropogenic soils

This study was published in *Soil Science* (2017, vol. 182, iss. 2). A. Salisbury collected the 2015 soil samples, analyzed the data, and wrote the manuscript. F. Gallagher and J. Grabosky provided edits and revisions to manuscript.

INTRODUCTION

Trace element (TE) contamination of soils is a significant global health threat. TEs can be found in both urban and agricultural soils at concentrations greater than background levels, posing multiple risks to human health (Larson 2014; Liu et al. 2013; Micó et al. 2006; Nabulo et al. 2006; Panagos et al. 2013). TEs have been identified in urban soils across the globe, with many present in concentrations exceeding soil screening criteria (Ajmone-Marsan and Biasioli 2010). Sources of TEs include, but are not limited to, leftover materials from smelting (Derome and Nieminen 1998) and mining activities (Moreno-Jiménez et al. 2010; Wong 2003), industrial processes such as chromium plating (Castro-Rodríguez et al. 2015), aerial deposition from industrial and mobile sources (Gandois et al. 2010), and irrigation with wastewater (Guédron et al. 2014). Additionally, increasing global use of vehicles and demand for electronics will continue to increase soil TE concentrations beyond ambient levels well into the foreseeable future (Ajmone-Marsan and Biasioli 2010; Tang et al. 2010).

In cities the reuse of abandoned land is often hindered by soil contamination from TEs, among other contaminants (Linn 2013). These properties (often referred to as brownfields) can be converted to green space, with potential benefits such as recreation opportunities, wildlife habitat, and soil and water conservation (DeSousa 2003; Doick et al. 2009; Moffat and Hutchings 2007). Phytostabilization, also known as natural attenuation, is the most cost effective of several strategies for managing soil contamination (Mench et al. 2010). Effective phytostabilization

requires the establishment of a plant community that will limit TE movement off site by reducing erosion, and maintaining an oxic soil environment. These communities may be spontaneously vegetated or intentionally designed and planted. The immobilization of TE contamination is generally accomplished through adsorption/absorption to organic matter (Robinson et al. 2009), stabilization at or within the rhizosphere and the associated microflora (Ma et al. 2011; Sessitsch et al. 2013), or sequestration within specific plant tissue (MacFarlane and Burchett 2000; Vesk et al. 1999). The long term condition of brownfields and contaminated sites is subject to physical, biological, and social processes. The social aspects of management are beyond the scope of this study, although no less important. While phytostabilization approaches assume long term stability of TE concentrations in a soil, research is lacking on TE concentrations in soils at phytostabilization sites several decades after their establishment (Bolan et al. 2014; Kumpiene et al. 2008; Mendez and Maier 2008).

Few studies have documented changes in metal concentrations or availability in the soils of phytostabilization sites for more than a few years. Longer studies tend to involve the application of amendments such as alumino-silicates, lime, or zero-valent iron grit to improve soil conditions (Ascher et al. 2009). After four years of growing grass on mining spoils amended with beringite, steel shot, and organic matter, water extractable As concentrations decreased (Bleeker et al. 2002). At brownfield sites in the UK, bioavailable concentrations of As, Cu, Ni, and Pb stayed constant over the course of three years of coppiced tree growth, though Salix spp. exhibited high concentrations of Cd and Zn (French et al. 2006). Seven years after a pyritic sludge spill, total As concentrations and (NH4)2SO4-extractable Mn and Zn decreased because of leaching in non-amended soil (Vázquez et al. 2011). Twenty years after atmospheric deposition ceased, Cu, Pb, and Sb concentrations were stable in the soil surface of a forest due to binding with organic matter, while Cd and Zn showed evidence of leaching (Clemente et al. 2008). The importance of pH in maintaining stable metal concentration is a common theme in these studies

(e.g. Blake and Goulding 2002; Clemente et al. 2006; Vázquez et al. 2011). While much research has focused on the initial conditions and short-term response of phytostabilization projects, the fate of contamination at these sites after decades of plant growth remains unclear.

Plant uptake can play an important role in influencing the fate of soil TE concentrations. Plant uptake has been shown to reduce TE concentrations (phytoextraction) under very specific conditions with active management (Dickinson et al. 2009; Mench et al. 2010). In the absence of active removal of aboveground biomass, litterfall can be an important component of TE budgets in forested catchments affected by atmospheric deposition (Gandois et al. 2010; Itoh et al. 2007) as well as in grasslands on mine tailings (Milton et al. 2004). In several cases, the litterfall contribution of TEs to soil exceeded concurrent atmospheric inputs (Johnson et al. 2003; Landre et al. 2009; Navrátil et al. 2007). TEs can also cycle between fine roots and soil (Johnson et al. 2003). There is concern that the cycling of TEs through plants could have negative impacts on terrestrial food webs (Milton et al. 2004; Niemeyer et al. 2012; Tack and Vandecasteele 2008). However, it has been proposed that the uptake and temporary storage of TEs in plants, and the subsequent return of TEs to the soil upon plant litter decomposition, could enable long term stability of soil TEs (Gallagher et al. 2011).

The aim of this study was to determine the long-term stability of TEs in a self-seeded, untreated brownfield by analyzing samples from the upper soil profile of a contaminated anthropogenic soil 28, 38, and 48 years after abandonment. In so doing, we ask the question, how do TE concentrations in the upper soil horizon of a contaminated site change over the course of 20 years? To address this question, our study takes advantage of soil data collected by other organizations in previous sampling campaigns 10 and 20 years prior to compare their results with current soil samples.

We hypothesized that TE concentrations in the upper soil horizon of a contaminated brownfield site would stabilize at steady-state values within 20 to 40 years after establishment of

a novel forest community, through the translocation of soil TEs through plant biomass, the production and accumulation of TE-binding plant organic matter, as well as through intrinsic sorption properties of the soil. However, plant communities are dynamic and may undergo changes in composition and structure over time, both influencing and being influenced by the soil contamination. In addition, if translocation pathways differ among TEs and plant species, the stability of soil TE concentrations cannot be generalized and may change over time. To test our hypothesis, we 1) compared concentrations of five soil TEs in a reforested brownfield in 1995, 2005, and 2015; 2) assessed the spatial variability of TE concentrations among study plots at this site in 2005 and 2015; 3) assessed the current vertical distribution of the five TEs in the top of the soil profile; and 4) examined the relationships between pH, total Fe, Mn, S, C and N and the five TEs in the soil. Sampling primarily focused on the top 30 cm of this profile (excluding the thin organic horizon), which has a high density of roots.

METHODS

Site Background

This study was conducted in the 82 ha interior natural area of Liberty State Park (LSP), in Jersey City, New Jersey, USA (centered at 40o 42’ 14” N; 74o 03’ 14” W). In the early 1800s, the area was a Hudson River coastal marsh . The marsh was filled in with rubble, construction debris, dredge material, slag, cinder, and other wastes, and was bound with three sea walls to create a peninsula of dry land, improving access to deeper waters (U.S. Army Corps of Engineers 2005). These sea walls create a unique hydrological regime where there is little groundwater movement in or out of the site (U.S. Army Corps of Engineers 2004). The use of the site as a rail yard, marina, and industrial area, along with the historic fill, resulted in a heterogeneous soil with high total TE concentrations exceeding both residential (New Jersey Department of Environmental Protection 1999) and ecological (United States Environmental Protection Agency

2003) soil screening criteria. After abandonment in 1967, vegetation spontaneously colonized the site and by the mid-1970s had created a patchwork of meadows, marshes, and hardwood forest (Gallagher et al. 2011). Today much of the site has been converted to managed parkland. During park construction, 101.5 ha of the abandoned freight yard were left undisturbed, and now serve as a long term study site for the unassisted revegetation of TE contaminated soil. Figure 2-1 shows the areal extent of the site as well as the location of research plots that will be referenced throughout the paper.

This study focuses on the top 30 cm of soil at the site, which contain three distinct mineral horizons created by the deposition of debris: the A, C1, and C2 horizons which are approximately 5, 20, and 10 cm thick, respectively, though thickness varies by location. LSP is classed by the US Natural Resource Conservation Service as a sandy-skeletal over loamy, mixed, mesic Typic Udorthent, with 0 to 3% slope as part of the LadyLiberty soil series (Soil Survey Staff 2010). The historical fill at the site resulted in a soil profile consisting of several unique debris horizons. The soil's organic horizon is 1-2 cm thick. All three layers of interest are a loamy sand and are differentiated by their colors –black (10YR 2/1) and very dark brown (10YR 2/2) – and by the amount of coal and boiler slag fragments along abrupt and clear boundaries. The horizons are typically strongly acidic (pH 5.0-5.2). The A horizon has a coarse granular structure while C1 and C2 have massive structure. According to its soil series and a study by U.S. Army Corps of Engineers (2004), depth to groundwater in most of the site is 1.2 to 1.5 m; additionally no redoxymorphic features were observed during soil sampling. Soil samples collected for a separate project at the site had fairly low electrical conductivities (ranging from 0.07 to 0.14 mS cm-1) and loss on ignition values that were much higher than would be expected for mineral soils, with a mean of 9.3% and a maximum of 21.3% (Table 1, Salisbury, unpublished).

Much of the prior research at LSP has focused on the effects of the elevated soil TE concentrations on the site's flora and fauna. Plant community guild – grass/forbe, shrub, and

forest – correlates fairly strongly with TE distribution. Early successional hardwood forests at the site are found in both areas of high and low TE concentrations. Interestingly, analysis of historic aerial photography shows that high TE areas were colonized by early successional hardwoods more quickly than low TE areas, showing the competitive advantage of this guild in highly degraded soils (Gallagher et al. 2011). The site also contains pockets of wetlands that formed on perched water tables, although these areas were excluded from the present study. Increasing metal loads decreased hardwood forest productivity (based on analysis of hyperspectral imagery) and plant diversity (Gallagher et al. 2008), and altered community guild trajectories (Gallagher et al. 2011). The TE gradient was found to decrease the basal area growth rates of B. populifolia (Dahle et al. 2014) and P. deltoides (Renninger et al. 2012), but not their allometry or photosynthetic capacities. Bioconcentration factors for eight herbaceous and woody species at LSP varied by metal and by plant species, although in general, metal concentrations were higher in the root system compared to aerial compartments (Qian et al. 2012). Troglodytes aedon (house wren) nestlings at LSP had higher concentrations of Pb, As, Cr, Cu, and Fe in their feathers in comparison to a reference site, although these concentrations had little effect on their size or fledge rates (Hofer et al. 2010). TE concentrations affected ectomycorrhizal fungi community composition (Evans et al. 2015) and had a direct relationship to microbial enzymatic activity (Hagmann et al. 2015). In spite of these effects, the LSP community appears to be robust, as forest cover continues to increase and new tree species are beginning to colonize the site. Characterizing the temporal changes in the site's soil conditions is an important part of understanding the complex nature of plant-soil-microbe feedbacks in metal contaminated soils at sites such as LSP (Krumins et al. 2015).

Early successional hardwood (SNH) assemblage is one of several habitat types in LSP and is dominated by gray birch (Betula populifolia Marsh.), eastern cottonwood (Populus deltoides Bart.), and quaking aspen (Populus tremuloides Michx.) with smaller populations of red

oak (Quercus rubra L.), red maple (Acer rubrum L.), tree of heaven (Ailanthus altissima Mill.), and three sumac species (Rhus copallinum L., R. glabra L., R. typhina L.). For the past 50 years the area covered by this assemblage has been increasing at LSP and it is possible this assemblage could represent an alternate steady state which could persist for many years (Gallagher et al. 2011). Additionally the dominant plant species in this assemblage have been shown to accumulate the TEs of interest to this study (Qian et al. 2012). Consequently, the SNH assemblage is relevant to understanding the long term dynamics of TEs at LSP.

Soil Sampling – 2015

While there are many long term study plots set up in the LSP interior, this study focuses on seven, which contain SNH assemblages (Table 2). Plot identifiers L, M, and H indicate relatively low, medium and high TE concentrations, respectively. The plots were selected for this project because their SNH community has been established for at least 10 years (Gallagher et al. 2011). These plots also represent a range of high and low TE concentrations.

In late 2014 and mid-2015, the seven SNH plots were each sampled in five locations using a hand trowel or soil corer from three different horizons: the A (approx. 5 cm thick), the C1 (approx. 20 cm thick), and the C2 (approx. 15 cm thick). The three horizons were sampled in order to better understand the vertical distribution of TEs in the plots. Each sample is a composite of soil from five pits within 1 m2 at each location. Samples were brought back to the lab where they were air dried for a minimum of 48 hours. Large plant material and gravel > 2 mm were removed from the samples, which were then ground with a mortar and pestle to break up aggregates and sieved through a 2 mm screen. Samples (< 2 mm) were analyzed for pH using a 1:1 ratio by volume of soil to water with an S975 Seven Excellence Multiparameter pH meter (Mettler Toledo, Columbus, OH).

In order to generate measurements of soil TE concentrations comparable to the 2005 data set, the C1 horizon soil samples were extracted following a procedure similar to the one used in

2005 (Gallagher et al. 2008a). For this analysis, 0.5 g from the <125 μm fraction was mixed with 10 mL of trace metal grade HNO3 and heated to >175o C for 30 minutes in Teflon bombs with an Anton-Paar Multiwave 3000 microwave digester (Anton Paar, Austria). Method blanks and a standard reference material (National Institute of Standards and Technology Standard Reference Material 1944, "New York-New Jersey Waterway Sediment") were also run with the samples. Extracts were then analyzed for As, Cr, Cu, Pb, and Zn using a Thermo Scientific iCAP 7600 ICP-OES (Thermo Scientific, Waltham, MA). Although different analytical methods were used in 2005 and 2015, several authors have found that maintaining the same sample digestion and preparation methods has greater influence on accuracy and comparability (Chen and Ma 1998; Munroe et al. 2012; Pyle et al. 1996).

The vertical distributions of TE, Fe, Mn, and S concentrationswere analyzed in the top three mineral soil horizons (A, C1, C2) in this study using an Innov-X Delta X-ray Fluorescence (pXRF) handheld analyzer (DS-4000; Olympus NDT, Waltham, MA). Each sample was measured four times to obtain a representative measurement of the sample. The pXRF was calibrated with a #316 stainless steel chip every 50 measurements. Numerous studies comparing the performance of AAS, ICP-AES, and pXRF on the same set of soil samples or reference materials have generally found good correlation between these techniques, though several found the pXRF may not be as accurate as other analytical methods (e.g. Anderson et al. 1998; McComb et al. 2014; Radu and Diamond 2009; Wu et al. 2012). Since a subset of 2015 samples were measured with two techniques, correlations between ICP-OES and pXRF results are presented below.

Total carbon (TC) and total nitrogen (TN) were determined in 350 (± 50) mg subsamples of soil for the 2015 A, C1, and C2 samples using a dry combustion method at 900o C with a vario MAX cube C/N analyzer (Elementar Americas Inc., Mt. Laurel, NJ) and helium as a carrier gas. The upper horizons of LSP soils have high coal dust and fragment content (Soil Survey Staff

2010), which would have inflated traditional loss on ignition (LOI) measurements made at a lower temperature by combusting some, but not all, of the coal carbon (Rawlins et al. 2008). Instead the TC analysis completely measures both recent soil organic carbon and coal carbon (Ussiri et al. 2014). To help discern the effects of recent soil organic carbon, measurements of total nitrogen (TN) were included, presuming TN could be a reasonable representation of recent soil organic matter.

Soil Sampling – 1995, 2005

To assess temporal changes in soil TE concentrations, this study utilized subsets of data collected in 1995 (3rd decade post-abandonment) by the U.S. Army Corps of Engineers (USACE) and in 2005 (4th decade post-abandonment) by the New Jersey Department of Environmental Protection (NJDEP). While a large number of samples were collected in 1995 and 2005, only data from the seven SNH plots described in the previous section were analyzed for the 2015 comparison. In the earlier studies, only one horizon was sampled, since their focus was on characterization of the horizontal distribution of TEs.

The 1995 soil data was part of a site characterization study, and so sampled broadly following transects across the site collecting a total of 98 samples (New Jersey Department of Environmental Protection 1995). Aerial photographs from this time period reveal that the entire site was vegetated by several types of plant guilds, making it reasonable to assume all sample plots were vegetated as well. These sample locations were later used as the plot locations for other studies. In 1995 one composite sample was collected from each plot by split spoon as a composite of the A and C1 horizons and was analyzed for TE content using graphite furnace atomic absorption spectrometry (GFAA).

In 2005, 32 of the original 98 plots sampled were selected to be representative of each plant guild in order to better assess the relationship between TE concentrations and the dominant plant communities established on the site. . During this sampling, three cores were collected at

each plot with a soil borer to a depth of 10 to 25 cm (C1 horizon), the depth of greatest root density (Gallagher et al. 2008a). In 2005 the plant communities of this study's seven plots were all SNH. The air-dried and sieved samples were treated with trace-metal grade HNO3 using a microwave extraction procedure and analyzed for Cr, Cu, Pb, V, and Zn by flame atomic absorption spectroscopy (AAS) in a Perkin-Elmer 603 atomic absorption spectrophotometer. Arsenic was analyzed with a Mg(NO3)2/Pb(NO3)2 matrix modifier in a Perkin-Elmer Z5100 GFAA (Perkin-Elmer, Waltham, MA). Method blanks and National Institute of Standards and Technology (NIST) Standard Reference Material (SRM) 1944 (urban sediment) were used for quality control. Soil pH was measured using a LaMotte colorimetric field pH meter (LaMotte Company, Chestertown, MD).

Soil data from 2005 was previously used to generate a total metal load (TML) index for each study plot in the site as described in Gallagher et al. (2008b). TML is a rank-sum index based on the 2005 concentrations of As, Cr, Cu, Pb, and Zn for 32 study plots in LSP. High TML reflects higher concentrations of the five metals.

Estimation of soil-water partition coefficients

The soil-water partition coefficient (Kd) of TEs is a useful indicator of the degree of element sorption in a given soil (Tipping et al. 2003), although it does not necessarily reflect bioavailability or biological uptake (Watmough 2008). While Kd is influenced by a number of factors, several studies have shown that pH can serve as a reasonable predictor (Buchter et al. 1989; Sauve et al. 2000; Tyler and Olsson 2001; Watmough 2008). Mean, minimum, and maximum Kd of Cu, Pb and Zn in LSP soil C1 horizons were estimated based on pH measurement made in 2005 and 2015 using equations derived by Sauve et al. (2000) from a review of over 70 studies of metal contaminated or metal spiked soils:

$$\text{Log(Kd-Cu)} = 0.27\ (\pm 0.02)\ \text{pH} + 1.49\ (\pm 0.13) \quad (1)$$

$$\text{Log(Kd-Pb)} = 0.49\ (\pm 0.04)\ \text{pH} + 1.37\ (\pm 0.25) \quad (2)$$

$$\text{Log(Kd-Zn)} = 0.62\ (0.03)\ \text{pH} - 0.97\ (0.21) \quad (3)$$

For the purposes of their review, Sauve et al. (2000) defined Kd (L kg-1) as the ratio of total soil metal concentration (mg metal kg-1 soil) to metal concentration in the soil solution (mg metal L-1 solution). In the experiments they reviewed, total metal content was determined based on acid digestion procedures. Soil solution metals were determined based on several procedures, including extractions using distilled water or dilute salt solutions. While regression equations relating Kd to pH for As and Cr exist (Watmough 2008), they were derived from soils with As and Cr concentrations much lower than the values observed in this study, and consequently may not be applicable to soils at LSP.

Statistical Analysis

For all analyses, each TE of interest (As, Cr, Cu, Pb, and Zn) was tested separately. A natural log transformation was applied to normalize the residuals of the acid extracted TE data and improve its homogeneity of variance. Differences in TE concentrations between sample years were tested using a one-way ANOVA; year was used as the treatment variable. While sample number varied in 1995, 2005, and 2015 (n = 7, 21, and 35, respectively), when normality and homoscedasticity assumptions are met, one-way ANOVA is fairly robust against differences in sample size (Oehlert 2010). Plot level variation in temporal changes in TE between the seven plots was tested using a two-way ANOVA (Type III) where year and plot were treatment variables since a Type III ANOVA can accommodate unequal sample sizes among two factors (Oehlert 2010). Since there was no within plot replication in the 1995 data set, only the 2005 and 2015 data sets were used in the two-way ANOVA analysis. To test if TE concentrations and pH varied between horizons in 2015 within each plot, the pXRF data set was also tested with a two-

way ANOVA (Type III) with horizon nested within plot. Additionally the correlation between pXRF and ICP-OES measurements was assessed with a linear regression using data from the 2015 C1 horizon samples since those samples were analyzed using both methods. All pairwise comparisons were conducted using a Tukey Honestly Significant Difference (HSD) test which constructs simultaneous confidence intervals to control the overall significance level and is appropriate for use with unbalanced data (Oehlert 2010). The relationships between TE and Fe, Mn, S, TC, TN and pH in 2015 were assessed using the pXRF data and Pearson correlation coefficients. All data analyses were performed using the R environment for computing (R Core Team 2016) utilizing the car (Fox and Weisberg 2011), lattice (Sarkar 2008) and agricolae (de Mendiburu 2016) packages.

RESULTS

Across the seven LSP study plots concentrations of all five soil TEs varied over several orders of magnitude (Supplementary Table, A-1). Comparisons of TE concentrations from 1995, 2005, and 2015 revealed two distinct temporal trends. No significant differences in the average soil concentrations of Cu, Pb, and Zn in the C1 horizon were observed between 1995, 2005, and 2015 when data from all seven plots was pooled together (Figure 2-2, $p = 0.113$, 0.21, 0.08, respectively). However As and Cr concentrations in the C1 horizon were significantly higher in 2015 compared to 1995 and 2005 ($p = 0.003$, and $p < 0.001$ respectively). From 1995 to 2015 Cu and Pb concentrations in the C1 horizon generally increased, however the difference between years was not significant.

Since heterogeneity of TE spatial distribution is a common issue in anthropogenic and contaminated soils (Hartley et al. 2009, 2012; Nowack et al. 2010), it is important to assess the interacting effects of spatial and temporal variability in long term studies. Some variation in the

temporal changes in TE concentrations was observed between plots from 2005 to 2015 (Figure 2-3). The increasing trend in As from 2005 to 2015 was seen in plots L1, L2, L3, M1, and H2, but was less pronounced in H1 and H2. Plot H2 was the only plot where Cr concentration did not increase from 2005 to 2015. Within all plots there is a generally increasing trend in the concentration of Cu from 2005 to 2015, though none of these differences were significant. Pb concentrations were fairly similar in L2, L3, M1, H1, and H2 from 2005 to 2015, though a significant increase over time was observed in L1, while there was a significant decrease in H3. Zn concentrations increased significantly in plot L2, while there were also non-significant increases in L1, L3, and H1.

When comparing the 2015 soil TE concentrations measured by pXRF between the three sampled soil horizon, the only significant difference observed was in the higher concentration of Cr in the A horizon compared to the C2 horizon (Figure 2-4). In plots H2 and H3, As and Cr concentrations decreased with depth, though these differences were not significant. Cu and Zn decreased with depth in M1 as well, although the differences between horizons were not significant. Zn also decreased with depth in L2 and H1, although again the differences were not significant.

Correlations were observed between pH, total Fe, Mn, S, total carbon (TC) and total N (TN) and the five TEs in the 2015 soil samples from all three horizons. Total Fe, Mn, S, TC, and TN ranged widely across the samples (Table 3). Zn was the only TE that correlated significantly with pH (Table 4). Arsenic, Cr, Cu, and Pb were all positively correlated with both total Fe and total Mn, but Zn was only correlated with Mn. Correlations were also observed between S and As, Pb, and Zn. Of the five TEs, only Cr had a significant correlation with TC and TN. Fe had a significant correlation with TC as well. Additionally all five TEs had significant positive correlations with each other.

Soil pH remained fairly consistent between 2005 and 2015 in the C1 horizon (Figure 2-5, $p = 0.57$). For 2015 samples soil pH did not vary significantly across the three horizons (Figure 2-6, $p = 0.61$). Kd values were estimated for Cu, Pb, and Zn based on soil pH. Kd values for these three TEs increased from 2005 to 2015, in all of the plots except M1 (Table 5). Overall, predicted Kd values were highest for Pb, followed by Cu then Zn.

The pXRF and ICP-OES analyses for the three soil horizons sampled in 2015 produced comparable results for soil concentrations of Zn (slope confidence interval contained 1, Table 6) and fairly good results for Cu and Pb (slope confidence intervals are close to 1). The pXRF method underpredicted As and overpredicted Cr compared with the ICP-OES analysis.

DISCUSSION

Understanding temporal trends in the vertical distributions of TEs is important for understanding the stability of TEs within specific soil horizons, the long-term bioavailability of TEs to shallow- and deep-rooted vegetation in recovering landscapes, and the potential for TEs to migrate out of a system via groundwater. Aside from atmospheric deposition, there have been no new inputs of TEs into the soil system at LSP during the study period. In addition, since the site grade is relatively flat, ranging from 0 to 2% (U.S. Army Corps of Engineers 2004), lateral flow of pore water was unlikely to have influenced the redistribution of TEs among individual plots. Consequently the observed increases in As and Cr in the C1 horizon must have resulted from the amount of As and Cr leaching into the C1 horizon (presumably from horizons above) being greater than that leaching out. On the other hand, the stability of Cu, Pb, and Zn concentrations in the A and C horizons over time suggests that either there was no vertical movement of these metals or inputs and outputs of these TEs in these horizons were approximately balanced. In the

latter case, TE uptake by plants would need to have been approximately equal to subsequent TE release as a result of leaf litter decomposition.

The analysis of soils collected from the seven hardwood LSP plots in 1995, 2005, 2015 supports the initial hypothesis that TE concentrations were stable for three of the five TEs examined. The concentrations of Cu, Pb, and Zn did not significantly change in the surface soils of the seven hardwood plots studied over this time period. These findings are supported by other work showing that changes in metal concentrations are more likely to occur in the first few years following the cessation of pollution input, and that in subsequent years concentrations stabilize (Clemente et al. 2008; Ramos Arroyo and Siebe 2007). However, concentrations of As and Cr increased significantly in the C1 horizon from 2005 to 2015 (Figure 2-2).

Small spatial scale variability in temporal trends of TE concentrations in highly heterogeneous reforested brownfield sites is not unexpected (French et al. 2006). Indeed, while the seven LSP study plots show consistent temporal trends in TE concentrations when analyzed in aggregate, some variation between study plots was observed. In most cases plot L1 exhibited the greatest increases in TE concentrations, while H3 exhibited no change or slight decreases in TE concentrations. H2 was an outlier for Cr, exhibiting no change while Cr increased in every other plot. The most dramatic difference between L1 and H3 (as well as H2) is their TML index. It is possible that since L1 started with lower TE concentrations, it has been able to accumulate TE at a higher rate. On the other hand, with its significantly higher TE concentrations, soil in the H3 plot may be close to saturation with respect to the amount of TE it can sorb. These results highlight the challenges of monitoring and predicting temporal trends of TE concentrations in highly heterogeneous, contaminated soils.

Fe- and Mn- (hydr)oxides, Al-oxides, soil humics, and clays are all potential sorbents for As, Cr, Cu, Pb, and Zn (Sparks 2003). All seven plots had low clay content, but high total Fe and Mn concentrations. The concentration of total Fe in particular was at the high end of the typical

range found in soils (Bodek et al. 1988). Although concentrations of total Fe and Mn rather than their (hydr)oxides were quantified, soil at the LCP site is oxic and a previous mineralogical analysis of three soil pits at LSP identified the presence of Fe oxides (3 to 12% of optical grain count) (Soil Survey Staff 2010). This, and our observation of positive correlations between all five TEs and Fe or Mn (Table 4) strongly suggests that Fe and Mn (hydr)oxides play an important role as TE sorbents at this site.

Organic matter (OM) plays a complex role in TE geochemistry. Depending on OM form and environmental conditions such as pH, OM can immobilize or mobilize TEs in soil (e.g. Bolan et al. 2014; Brown et al. 2000; Li et al. 1999; McBride et al. 1997; Ruttens et al. 2006). Total organic matter measured by loss on ignition (LOI) in LSP soil (Table 1) is much higher than expected for mineral soil (Jones 2012), most likely because of the presence of coal dust and fragments in the soil (Soil Survey Staff 2010). Given the difficulties of measuring recent soil organic carbon in soils with high coal content, care should be taken in the interpretation of the TC correlation data (Rawlins et al. 2008). Only Cr showed significant correlations with both TC and TN, suggesting organic matter could be an important sorbent for Cr. Jardine et al. (2013) similarly observed higher Cr sorption rates in the A-horizon of soils which correlated with increasing total organic carbon and decreasing pH. While it is somewhat surprising, correlations were not observed between TC and the other four TEs, it is possible that weaker relationships between organic matter and the TE could be obscured by the high coal-carbon content in the soil.

The two elements which increased from 2005 to 2015 – As and Cr – would be present as oxyanions given the oxic conditions in the plots as well as their pH (Takeno 2005). We assume oxic conditions for all samples since they were collected from the unsaturated zone of upland soils. Thus As(V) and Cr(VI) should have been the dominant oxidation states. The pXRF TE results show that there were pools of As and Cr in the horizon closest to the surface that may have served as a source to enrich the C1 horizon. While total Fe and Mn concentrations were fairly

constant through the soil profile, NRCS pedon data suggests Fe-oxide distribution may be more uneven and there could be more Fe-oxide in the lower horizons (Soil Survey Staff 2010). Oxyanion sorption decreases with increasing pH as soil particles and organic matter lose their positive charges (Smith 1999). The increase in As and Cr from 2005 to 2015 coincides with an increase in pH in six of the seven plots, suggesting that a change in soil pH may have contributed to the mobilization of As and Cr in this time period. Similar results were observed by Clemente et al. (2008) when twenty years after cessation of adjacent smelter activities, As showed evidence of moving downward into the soil profile and then becoming immobilized by Fe and Al (hydr)oxides. Arsenic immobilization has also been observed in forested catchments and mining soils (Huang and Matzner 2007; Moreno-Jiménez et al. 2010).

The three elements which showed no overall change in concentration from 1995 to 2015 – Cu, Pb, and Zn – are expected to be present as divalent cations in the oxic and slightly acidic conditions in these plots (Takeno 2005). Estimated Kd values for Cu, Pb, and Zn in each plot are all lower than mean values reported in the literature, although they are at least two orders of magnitude greater than the reported minimum values (Table 3). This suggests a moderate degree of mobility of these TEs in the soil solution. Greater mobility in soil solution means these elements could be more available for plant uptake (Bolan et al. 2014).

The cycling of Pb (Heinrichs and Mayer 1980; Watmough and Dillon 2007), Mn (Navrátil et al. 2007), Cd, and Zn (Landre et al. 2009) through forest biomass and return to the forest floor has been documented in forests affected by atmospheric pollution and in unpolluted environments. This is consistent with prior research on plant TE bioaccumulation at LSP showing that plant translocation is an important driver of Cu, Pb, and Zn soil concentrations over time (Gallagher et al. 2008b; Qian et al. 2012). With some variation among species, these LSP studies showed that TE concentrations in above and belowground plant tissue decreased in the order: Zn > Pb > Cu > Cr > As. The three TEs present in the highest concentrations in the site's plants –

Cu, Pb, and Zn – correspond to the TEs with whose concentrations were constant in soil from 1995 to 2015. These patterns were observed despite the fact that the route of TE accumulation in plants varies among metals. In a forest contaminated with Cu, Ni, Pb, and Zn from smelter emissions, fine roots were important for Cu and Pb plant-soil transfer, while foliage was more important for Zn (Johnson et al. 2003). Similarly, Qian et al. (2012) found Zn had the highest bioconcentration factors in the leaves of B. populifolia and P. deltoides, while bioconcentration factors for As, Cr and Cu were higher in the roots (Pb was not analyzed in this study).

CONCLUSIONS

While there is an expectation and need for phytostabilization or natural attenuation sites to retain TE contamination for prolonged time periods, there is a paucity of follow up studies that track TE concentrations beyond the first decade of plant community establishment. By utilizing soil data collected 28 to 48 years after site abandonment, this study documented changes in soil TE concentrations in a spontaneously vegetated urban brownfield over the course of 20 years. The results demonstrate that in this time period, Cu, Pb, and Zn concentrations in the upper mineral horizons remained fairly stable, but that As and Cr concentrations increased deeper in the soil profile. Bioaccumulation in plant material (and later decomposition), favorable pH, as well as mineral and organic sorbents in the soil, all play an important role in retaining TEs in soil over the long term. The apparent transfer of As and Cr from the surface to deeper in the soil profile may have been driven by changes in pH at the soil surface, and highlights the need, at least for these elements, to continue monitoring soil conditions in vegetated brownfields through longer time periods.

TABLES

Table 2-1: Soil electrical conductivity, total organic carbon (measured by loss on ignition), and soil texture from composite of A and C1 horizons in plots L1, L2, L3, H1, H2, and H3 as part of a separate study in Fall 2015.

	Min	**Median**	**Max**	**Mean**	**Std. Dev.**
Organic Carbon (loss on ignition, %)[a]	2.4	7.8	21.3	9.3	4.5
Electrical Conductivity (mS cm^{-1})[b]	0.07	0.08	0.14	0.09	0.02
Sand (%)[c]	72	80	93	81	5
Silt (%)[c]	4	15	24	15	5
Clay (%)[c]	0.1	4	6	4	2

[a] Loss on ignition temperature of 400^{o}C

[b] 1:1 by volume water to soil

[c] Soil texture was determined using a hydrometer method with 50 g of soil (sieved to < 2mm) dispersed with 50 mL of 10% Na-Hexametaphosphate

Table 2-2: 2015 study plot names used in current paper along with names used in previous studies and total metal load (composite index based on concentrations of As, Cr, Cu, Pb, and Zn measured in 2005, see Gallagher et al. (2008).

Plot	**Previous label**	**Total Metal Load**
L1	TP-41	0.85
L2	TP-48	1.56
L3	TP-43	1.64
M1	TP-18	2.85
H1	TP-14	3.08
H2	TP-14/16	3.56
H3	TP-25	4.31

Table 2-3: Range, median and mean concentrations of total Fe, total Mn, and total S of samples collected from the A, C1, and C2 in 2015 (n = 98). Fe, Mn, and S were measured using a pXRF, total carbon (TC) and total nitrogen (TN) were measured using an elemental analyzer.

	Min	**Median**	**Max**	**Mean**	**Std. Dev.**
	(mg/kg)				
Fe	18,828	62,682	448,348	82,087	61,166
Mn	112	276	1,509	359	231
S	1,384	5,336	26,063	6,281	3,974
	(%)				
TC	0.3	21.5	35.7	21.2	6.8
TN	0.008	0.362	1.163	0.432	0.242

Table 2-4: Pearson correlation coefficients for pH and Ln-transformed element concentrations based on pXRF analysis of samples from A, C1, and C2 horizons (n = 98).

	Ln(Cr)	**Ln(Cu)**	**Ln(Pb)**	**Ln(Zn)**	**Ln(Mn)**	**Ln(Fe)**	**Ln(S)**	**TC%**	**TN%**	**pH**
Ln(As)	0.61***	0.75***	0.83***	0.59***	0.53***	0.59***	0.35***	0.1	0.11	0
Ln(Cr)		0.56***	0.52***	0.42***	0.37***	0.38***	0.05	0.4***	0.34***	-0.05
Ln(Cu)			0.8***	0.66***	0.63***	0.46***	0.14	0.05	-0.05	0.14
Ln(Pb)				0.68***	0.59***	0.45***	0.21*	0.12	0.17	0.05
Ln(Zn)					0.71***	0.07	-0.26*	-0.18	0.1	0.49***
Ln(Mn)						0.49***	0.05	-0.04	0.09	0.25*
Ln(Fe)							0.77***	0.25*	0.02	-0.36***
Ln(S)								0.18	-0.08	-0.51***
TC%									0.79***	-0.54***
TN%										-0.31**

*** $p < 0.001$, ** $p < 0.01$, * $p < 0.05$

Table 2-5: Mean with minimum and maximum solid-solution partition coefficients (K_d) estimated for Cu, Pb, and Zn in soil from plots sampled in 2005 and 2015 (based on pH and Equations 1, 2, 3). Minimum and maximum K_d values calculated based on standard error of equation coefficients. For comparison mean, minimum, and maximum values for various soil types reported in the literature are also provided (Sauve et al. 2000).

	Copper		**Lead**		**Zinc**	
Plot	**2005**	**2015**	**2005**	**2015**	**2005**	**2015**
L1	1288 (724-2291)	1424 (794-2552)	20417 (6607-63096)	24733 (7866-77795)	562 (229-1380)	722 (290-1798)
L2	1371 (767-2449)	1380 (771-2468)	22856 (7328-71285)	23451 (7486-73497)	649 (262-1603)	677 (273-1681)
L3	887 (513-1535)	948 (545-1649)	10375 (3548-30339)	11911 (4016-35343)	239 (101-562)	288 (121-687)
M1	1288 (724-2291)	1112 (629-1967)	20417 (6607-63096)	17291 (5581-53707)	562 (229-1380)	488 (197-1210)
H1	783 (457-1343)	906 (522-1574)	8279 (2884-23768)	11402 (3834-33958)	179 (77-417)	280 (117-671)
H2	783 (457-1343)	1234 (696-2188)	8279 (2884-23768)	18980 (6174-58361)	179 (77-417)	514 (210-1258)
H3	1459 (813-2618)	1746 (959-3180)	25586 (8128-80538)	36421 (11193-118596)	748 (301-1862)	1192 (466-3048)
	Mean (min-max) from literature					
	4799 (6.8 – 82,850)		171,214 (60.56 – 2,304,762)		11,615 (1.4 – 320,000)	

Table 2-6: Results of regression analysis comparing ICP-OES (as independent variable) and pXRF (as dependent variable) TE concentrations in horizon C1 collected in 2015 using a 95% confidence interval. LCL = lower confidence limit, UCL = upper confidence limit. (n = 35)

Element	Slope	Slope LCL	Slope UCL	Intercept	Intercept LCL	Intercept UCL	r^2
As	0.7	0.62	0.78	1.15	-12.36	14.66	0.9
Cr	1.7	1.27	2.14	11.59	-84.17	107.35	0.64
Cu	0.92	0.85	0.98	-31.78	-72.33	8.78	0.96
Pb	0.72	0.54	0.9	-22.16	-209.23	164.92	0.66
Zn	0.91	0.71	1.12	-48.65	-170.88	73.57	0.7

FIGURES

Figure 2-1: Aerial photograph of Liberty State Park (LSP), Jersey City, New Jersey with interior boundary of unmitigated natural area and seven study plots highlighted.

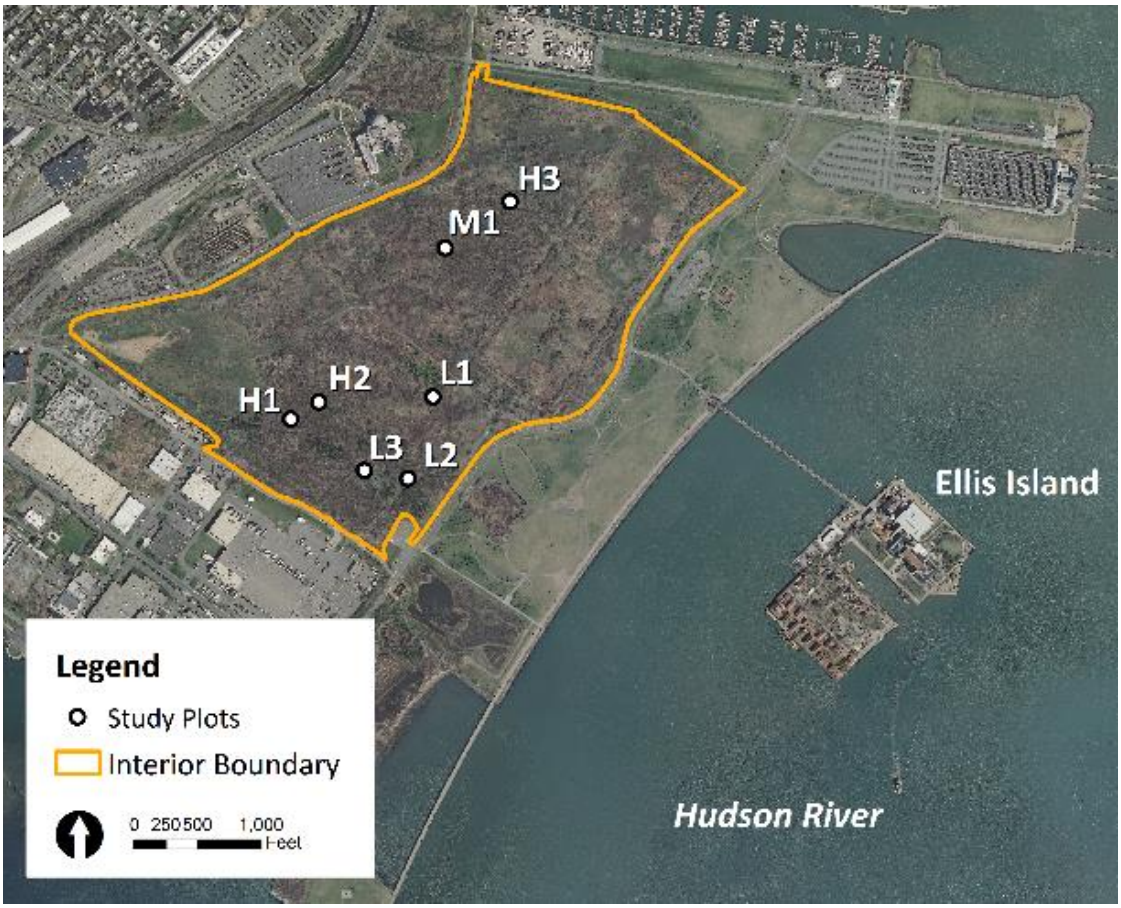

Figure 2-2: Soil TE concentrations (mg/kg) in the C1 horizon from 1995, 2005, and 2015 for seven study plots (n = 6, 21, and 35, respectively). Groups which share the same letters are not statistically different ($p < 0.05$) according to a Tukey HSD test. Note that concentrations of all TE are shown on a logarithmic scale.

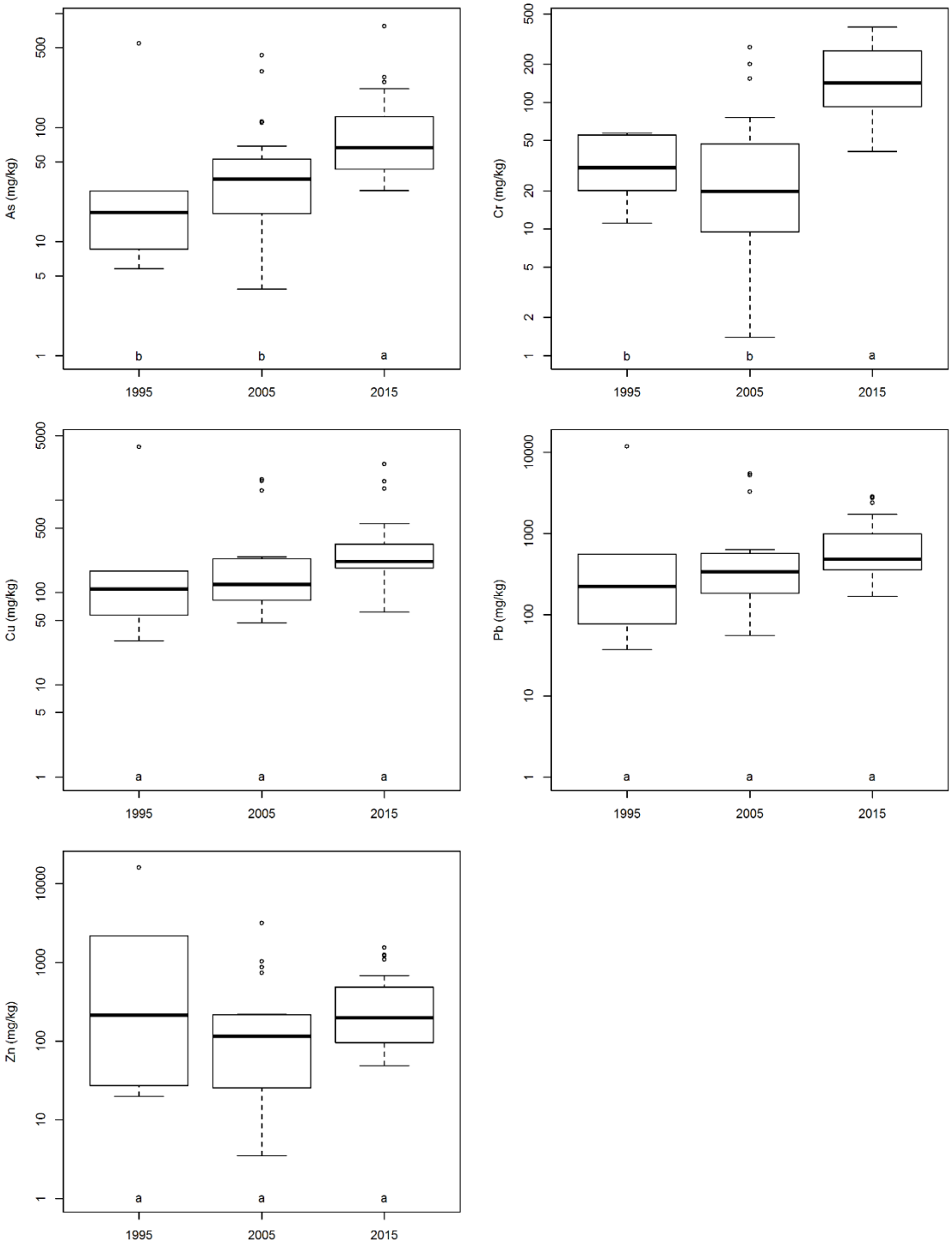

Figure 2-3: Soil TE concentrations (mg/kg) in the C1 horizon from 2005 (n = 3 per plot) and 2015 (n = 5) for seven study plots. Concentrations within plots which share the same letters are not statistically different ($p < 0.05$) according to a Tukey HSD test. Note that concentrations of all TE are shown on a logarithmic scale.

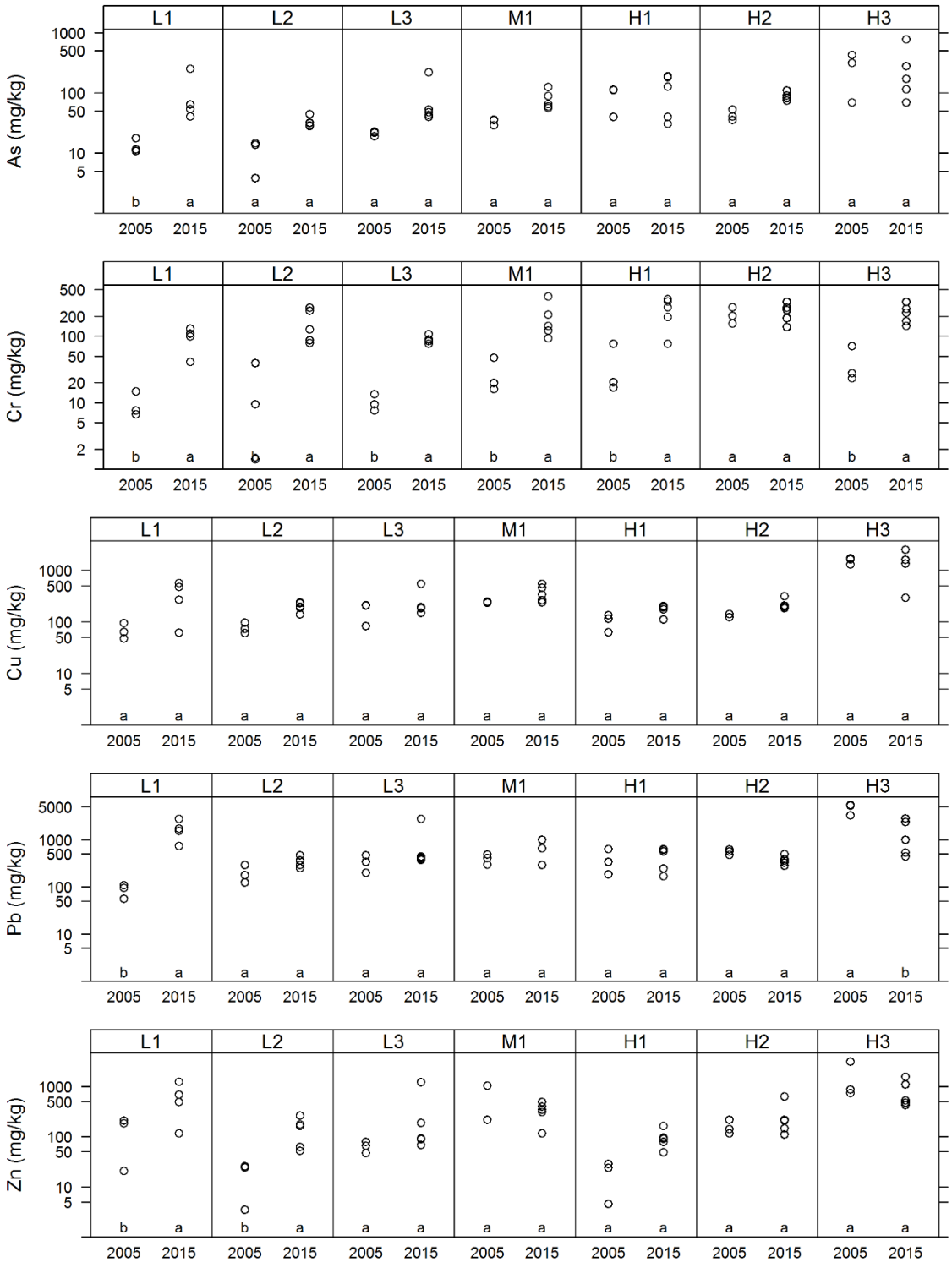

Figure 2-4: Soil TE concentrations (mg/kg) in 2015 samples from the A, C1, and C2 horizons measured by pXRF (n = 5 per horizon per plot). Solid triangles represent mean concentrations, open circles represent individual concentrations.

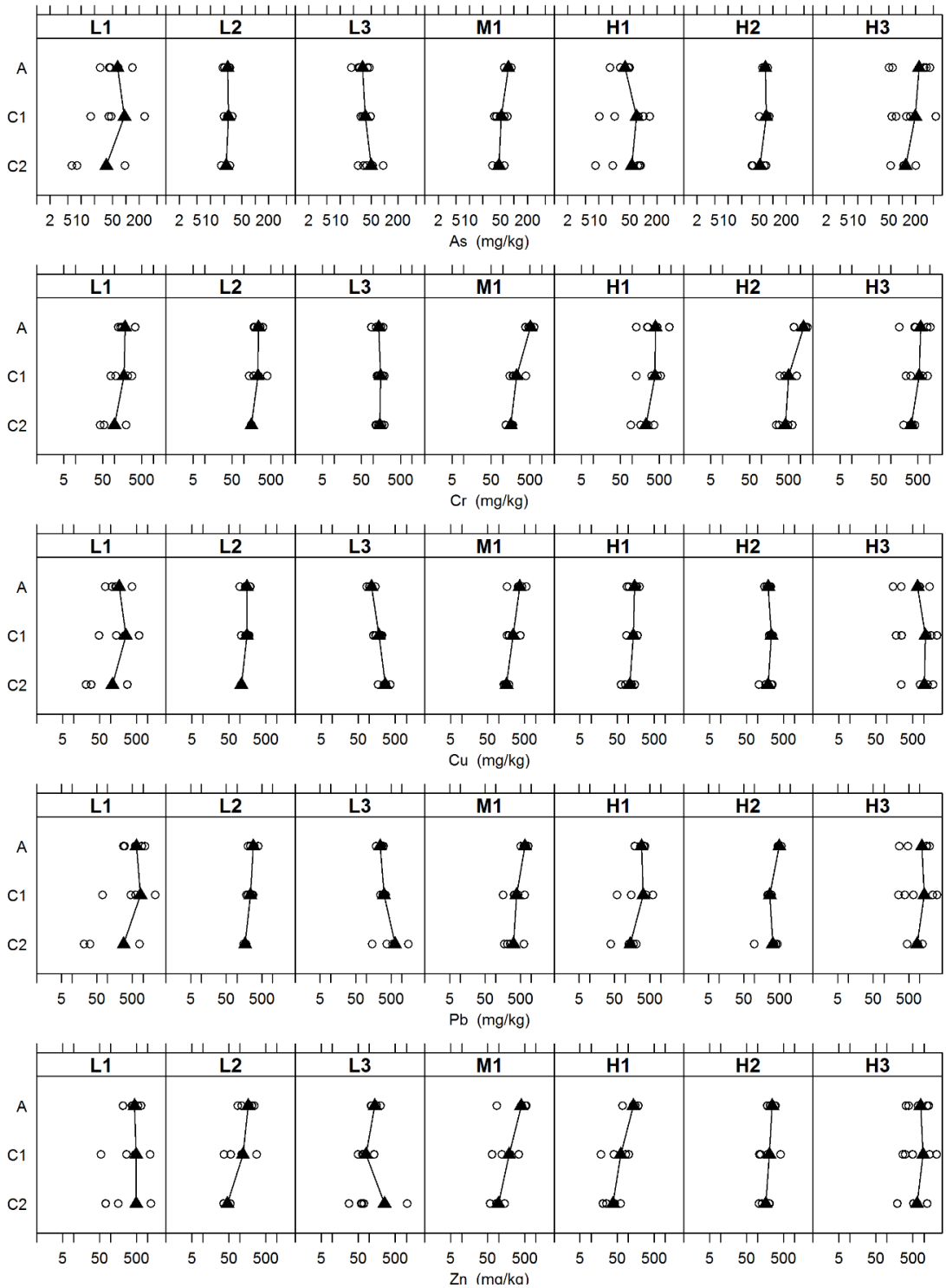

Figure 2-5: Soil pH measured in the C1 horizon in 2005 (n = 7) and 2015 (n = 35) for seven study plots.

Figure 2-6: Soil pH of the A, C1, and C2 horizons in 2015 (n = 5 per horizon). Solid triangles represent mean pH, open circles represent individual pH measurements.

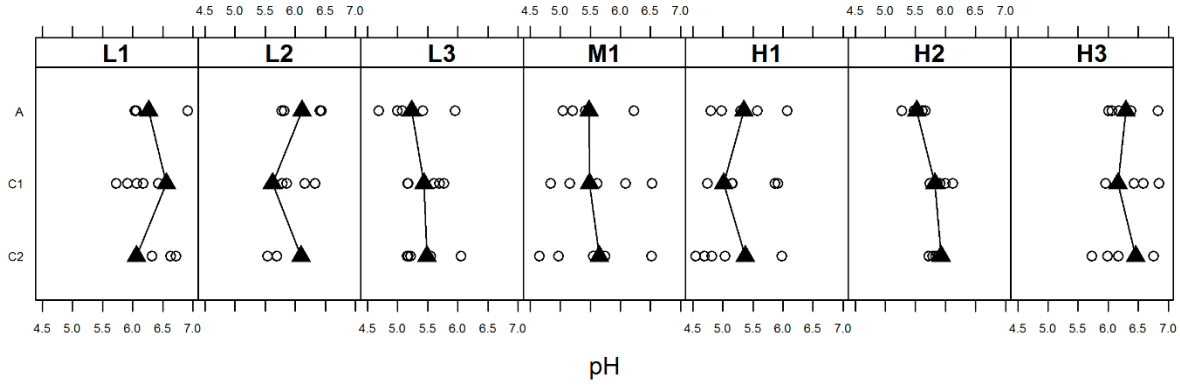

Chapter 3 - Photosynthetic rates and gas exchange parameters of Betula populifolia growing in trace element contaminated soils

INTRODUCTION

Prior research at Liberty State Park found inverse correlations between soil trace element concentrations and tree growth rates. Tree coring data showed that over the course of six years, there was a significant negative curvilinear relationship between total metal load (TML, see Chapter 1) and cumulative cross sectional trunk area added (Gallagher et al. 2008a). A second study found significant differences in the relationships of *Betula populifolia* trunk diameter and tree age between high and low metal load plots (Dahle et al. 2014). Similarly, when comparing *Populus deltoides* at Liberty State Park with similar trunk diameter at high and low metal load plots, the high metal load trees tended be older than their similarly sized low metal load counterparts (Renninger et al. 2012).

One possible explanation for the observations of decreased growth rates in these trees is a decrease in photosynthesis leading to a decrease in biomass production. Direct and indirect effects of trace elements on photosynthesis are well documented. Trace elements can reduce the production of chlorophyll, interact with enzymes such as Rubisco, change the function of chloroplast membranes, interact with both the electron donor and acceptor components of photosystem I and photosystem II, impair stomatal function, and interfere with the photosynthetic carbon reduction cycle (Mysliwa-Kurdziel et al. 2004). However, all of these responses are element and species specific. Frequently laboratory studies which were designed to investigate interactions at a molecular level do not necessarily represent the response of the whole plant to the concentrations of trace elements found in the environment. Plants are able to survive elevated concentrations of trace elements using a variety of mechanisms, including active exclusion (to a limit), isolation in vacuoles, and binding with chelating complexes and ligands (Greger 2004).

The interaction between trace elements and plant water relations are complex, particularly when drought is involved. Trace elements have been shown to affect water transport through roots (Maggio and Joly 1995), decrease the diameter and number of xylem vessels (Robb et al. 1980), induce stomatal closure (Moustakas et al. 1997), and create a stress response which is similar to water-deficiency stress (de Silva et al. 2012). All of these responses vary among metals and plant species. Interestingly, some of these effects may confer drought resistance. Changes in xylem structure, higher stomatal resistance, smaller and fewer leaves, and enhanced abscission effectively promote water conservation by the plant, countering the effects of drought (Poschenrieder and Barcelo 2004). However, these changes are beneficial to some species but not others (Santala and Ryser 2009; de Silva et al. 2012).

One of the dominant hardwoods at Liberty State Park, *Betula populifolia*, is an early successional species, able to colonize lower quality sites though it prefers moist, well drained soils and is not tolerant to prolonged saturation (Wennerberg 2004). Exposure to Cu and Ni appears to confer drought tolerance to *Betula papyrifera* seedlings grown in a greenhouse setting (Santala and Ryser 2009). Since the photosynthetic and stomatal conductance rates of *B. populifolia* and *B. papyrifera* responded similarly in a drought study (Ranney et al. 1991), perhaps trace element exposure may enable greater drought tolerance in *B. populifolia* as well.

Given previous broad scale observations of primary productivity and *B. populifolia* basal growth rates, I hypothesized that soil metal load is the primary limitation on leaf gas exchange and photosynthesis parameters of *B. populifolia* at Liberty State Park (Hypothesis 1). I also hypothesized that high metal load would exacerbate the effects of short heat wave and drought on gas exchange parameters (Hypothesis 2). Additionally, I hypothesized that other soil properties such as soil nutrients and water content would also influence gas exchange (Hypothesis 3). Specifically, it was expected that in response to stress HML trees will have lower net photosynthetic assimilation (A_{net}), transpiration (E), stomatal conductance (g_s), intrinsic water use

efficiency (iWUE), intercellular to ambient CO_2 concentration ratio (C_i/C_a), maximum carboxylation efficiency (V_{cmax}), electron transport rate (J_{max}), light saturated photosynthetic rate (A_{max}), and quantum efficiency (φ) but higher CO_2 compensation point (Γ^*), light compensation point (I_{comp}), and dark respiration (R_{dark}).

BACKGROUND

Members of the *Betula* genus can be found throughout the Northern Hemisphere in both boreal and temperate zones (Jarvinen et al. 2004). Many *Betula* species are characterized as pioneer or colonizer species and tend to be shade intolerant. This study focuses on *B. populifolia* which spontaneously colonized the abandoned rail yard at Liberty State Park. *B. populifolia* is not particularly well studied, though several other members of *Betula* from Europe, Northeastern Asia, and North America have been the subject of both photosynthesis and trace element studies (Table 3-1). Phylogenetic analysis of *Betula* suggests the closest relatives to *B. populifolia* are *B. platyphylla, B. papyrifera,* and *B. pendula* (Jarvinen et al. 2004; Li et al. 2007).

Several species within the *Betula* genus have been found growing at or were planted in soils with high concentrations of trace elements, including *B. populifolia* in abandoned rail yards (Gallagher et al. 2008a; Murray et al. 2000); *B. pendula* in coal mining spoil heaps (Frouz et al. 2008; Good et al. 1985), former industrial sites (Dickinson 2000), mine spoils (Borgegard and Rydin 1989; Margui et al. 2007) and As contaminated soils (Gustafsson and Jacks 1995; Moreno-Jiménez et al. 2010); *B. papyrifera* in forests affected by acid deposition (Landre et al. 2010); *B. alba* in As contaminated mine spoils (Bleeker et al. 2002); and *B. pubescens* in copper mine spoils (Borgegard and Rydin 1989). Additionally *Betula pendula* is a commonly planted species for brownfield greening projects in the UK (Doick et al. 2009; French et al. 2006). However within a species there can be a high degree of genotypic variation in the establishment and growth

rate responses to high metal concentrations (Gaudet et al. 2011; Good et al. 1985; Kopponen et al. 2001; Utriainen et al. 1997).

Some evidence suggests metal tolerance in *Betula* comes from an exclusion based mechanism, though no precise mechanism has been identified. Denny and Wilkins, (1987) hypothesize that *Betula* tolerance of Zn lies in its ability to exclude Zn uptake at the root endodermis based on their observations of a threshold type response by *B. pendula* and *B. pubescens* to increasing Zn concentrations, excluding it up to a point then becoming inundated by it. This work was also supported by Kopponen et al., (2001) who found that clones of *B. pendula* and *B. pubescens* with the greatest reduction in growth when grown in Cu and Zn contaminated soils tended to have the highest aboveground concentrations of the two elements. However, at Liberty State Park *B. populifolia* and *Populus deltoides* have both been observed to hyperaccumulate Zn in their leaves (Qian et al. 2012).

Betula species have been shown to tolerate exposure to elevated levels of several trace elements and in some situations accumulating some of the elements in high concentrations. Elevated concentrations of Cd and Cu have been documented in *B. papyrifera* (Landre et al. 2010) as well as high concentrations of Cd, Pb, and Zn in *B. pendula* and *B. pubescens* (Borgegard and Rydin 1989). Though in contrast *B. pendula* had the lowest concentrations of Cu in aboveground biomass (leaves and stem) compared to other species of trees (*Alnus* and *Salix* spp.) in a brownfield afforestation study (Dickinson 2000). *Betula* spp. may be more resistant to As uptake since wild growing *Betula pendula* at an abandoned mine site had the lowest transfer and bioaccumulation factors (ratio of shoot to soil concentrations) for As of the woody species sampled by the study (Moreno-Jiménez et al. 2010). For *B. populifolia* growing at Liberty State Park, Zn hyperaccumulates in the leaf (as evidenced by a leaf-soil bioconcentration factor greater than 1) while As, Cr, and Cu had much lower bioconcentration factors in the leaf (Qian et al. 2012).

Little field research has been conducted exploring the responses of photosynthesis in *Betula* to trace element exposure. Hydroponically grown seedlings of *Betula ermanii* were able to maintain relatively high net assimilation, carboxylation efficiency and quantum yield when exposed to increasing concentrations of manganese (Kitao et al. 1997). In an open top chamber experiment, exposure to soil contaminated with Zn, Cu, and Cd laden filter dust reduced the evapotranspiration rates of a community of forest plants which included *Betula pendula* (Menon et al. 2005); presumably such a reduction in evapotranspiration would correlate with a reduction in net photosynthetic assimilation of CO_2 as well.

In addition to toxic effects from elevated levels of trace elements in degraded sites, frequently poor soil conditions such as low nutrient availability can also limit plant growth in these environments. Consequently there is a strong interest in understanding the role soil amendments may play in both negating the effects of metal toxicity as well as enabling improved plant growth (Kumpiene et al. 2008). The application of fertilizer on study plots in opencast coal sites did little to influence the growth of *B. pendula* and *B. pubescens* (Good et al. 1985). However *B. aurata* (a pioneer species) planted in slate rock waste tips did exhibit increased growth rates in response to the addition of clay and organic waste (Williamson et al. 2011). Williamson et al., (2011) suggest amendments must address both water holding capacity and nutrient availability in concert in order to be effective. The addition of lime and fertilizer enhanced root growth of *B. populifolia* at the study site (Gallagher et al. 2015).

METHODS

Study Site

Study plots (20 x 50 m) were located in the interior area of Liberty State Park, Jersey City, New Jersey (40º42’16” N x 74º03’17” W). The site was formerly a rail yard and industrial

area built on filled tidal marsh. The site's history resulted in concentrations of trace elements (TE) that exceed background levels and both residential and ecological screening criteria (New Jersey Department of Environmental Protection 1999; United States Environmental Protection Agency 2003). Contamination varies spatially over the site which facilitates the comparison of trees growing in both high and low concentrations of TE**.** Plots within Liberty State Park have been compared using a rank composite index based on soil concentrations of As, Cr, Cu, Pb, and Zn called the total metal load index (TML, See Chapter 1).

This study focused on four hardwood plots at Liberty State Park, two with soils below a previously defined critical TML threshold of 3 (Gallagher et al., 2008) and two above the threshold (Table 3-2**).** All four study plots were located in early successional hardwood stands which are predominantly composed of *Betula populifolia* along with *Populus deltoides* and *Populus tremuloides.*

Gas Exchange measurements

Measurements of leaf gas exchange were made monthly from May to September in 2014 and 2015. Within each of the four plots, five mature *B. populifolia* trees were selected based on their diameter at breast height (DBH) to ensure individuals represented the 2nd to 4th DBH quartiles previously determined for the population (Dahle et al. 2014). When possible, the same trees were measured from month to month, however some trees had to be cycled out of the study due to deteriorating conditions in canopy (high number of dead branches). All measurements were made on excised branches collected from approximately 5 m above the ground, which were immediately placed in water and recut while submerged to maintain a hydraulic connection for the leaves (Joesting et al. 2009; Kubiske and Pregitzer 1996; Reich et al. 1995). Preliminary excision experiments at Liberty State Park in 2014 showed the excision procedure did not influence photosynthesis rates.

To quantify leaf photosynthetic traits, two sets of gas exchange measurements were made typically between the hours of 8:00 and 13:00, using a LI-COR 6400XT portable gas exchange system (LI-COR Biosciences, Lincoln, Nebraska). These were made using the first and second fully expanded leaves (i.e. most apical and second-most apical) with minimal damage on each excised branch. For the first set, light availability measured as photosynthetic active radiation (PAR) was varied from saturating to darkness using the instrument's LED chamber. These "light curves" were generated using the following photosynthetic photon flux density (PPFD) sequence: 2000, 1500, 1000, 500, 200, 100, 50, 20, 0 μmol photons m^{-2} s^{-1}. During these measurements reference CO_2 was maintained at 400 μmol CO_2 mol^{-1} air. The second set of measurements, "A-C_i" curves, maintained constant saturating light at 1500 μmol photons m^{-2} s^{-1} and varied ambient CO_2 concentrations using the following sequence: 400, 300, 200, 100, 50, 400, 400, 600, 700, 800, 900, 1000, 1500 μmol CO_2 mol^{-1} air. Relative humidity in the sample chamber was maintained between 60 and 80% and chamber temperature was set to 25ºC for both sets of measurements.

To determine if soil metal loads compounded or increased the effects of high temperature, an additional set of A-C_i curves were collected on July 25 and 26, 2014 Five trees from high metal plot H3 and five trees from low metal plot L1 were used in the temperature study (none of these trees were used in the primary study). Temperature was controlled by setting the LI-6400 block temperature to 25, 30, and 35ºC (note that the highest leaf temperature achieved was 34.4ºC). A different branch was excised for each temperature level and acclimated in the cuvette until readings stabilized. All other settings for the A-C_i curves were the same as the procedures described above.

Three days of high temperatures (19-21 July 2015) occurred in the middle of the sampling period; daily maximum temperatures ranged from 33 to 36ºC. A total of 1.8 cm of rain had fallen in the preceding two weeks and daily reference evapotranspiration (ETo) ranged from

1.3 to 4.7 mm day^{-1} on these three days (see Weather Data subsection for explanation of ETo calculation). Preliminary measurements made on July 21 indicated photosynthetic rates were much lower than normal. Consequently additional survey measurements – single gas exchange measurements – were made on July 22 and 23 (daily maximum temperature 30°C, ETo 8.7 and 8.3 mm day^{-1}) in order to capture net photosynthetic assimilation (A_{net}), transpiration (E), and stomatal conductance (g_s) from all of the study trees in a short amount of time.

Survey measurements were made on leaves of excised branches at 400 μmol CO_2 mol^{-1} air and 1500 μmol photons m^{-2} s^{-1}. A leaf was placed in the sample chamber, then once CO_2 and H_2O concentrations stabilized a single measurement was made. While there is no single agreed upon definition of a heat wave (Smith et al. 2013), the July 19-21 period of high heat dry weather will be referred to as the July 2015 heat wave for the purposes of this paper.

Leaf mass per unit area (LMA) was measured for all leaves used in gas exchange measurements in 2015. Leaves were scanned using an Epson Expression 11000XL scanner then the leaf area was measured using ImageJ (imagej.nih.gov/ij/) software. Leaves were oven dried at 60°C for at least 72 hours then cooled in a desiccator and weighed. LMA was calculated by dividing the leaf dry weight (g) by the leaf area (m^2).

Soil properties

To compare soil properties other than heavy metals across the study plots, 3 to 4 samples were collected from random location within each study plot using a slide corer from the top 15 cm of soil (excluding intact leaf litter). The < 2 mm fraction of the soil samples were analyzed by the New Jersey Agricultural Experiment Station (NJAES) Soil Testing Lab for pH, soil texture, electrical conductivity, macro and micronutrients. pH was measured using a 1:1 ratio of soil to liquid (by volume) with S975 SevenExcellence Multiparameter pH meter (Mettler Toledo, Columbus, OH). The hydrometer method was used to determine soil texture with 50 g of soil (<2

mm) dispersed with 50 mL of 10% Na-Hexametaphosphate. Total Kjeldahl Nitrogen (TKN) for total organic nitrogen plus free ammonia was determined following EPA Method 351.1 using an AutoAnalyzer III (wavelength = 667 nm, Bran + Luebbe Analytics, Norderstedt, Germany). Macro and micronutrients (P, K, Ca, Mg, Zn, Mn, Cu, B, and Fe) were extracted using a Mehlich-3 extractant and analyzed using an iCAP 7000 inductively coupled plasma optical emission spectrophotometer (ICP-OES; Themo Scientific, Waltham, MA). Note that the Mehlich-3 extractions approximate plant available element concentrations rather than total or pseudo-total concentrations.

Gravimetric soil water content (θ_g) was measured in the four study plots at the beginning, middle and end of each monthly photosynthesis measurement period in 2015. There were three sample locations in each plot which were sampled repeatedly over the course of the growing season. When possible, all four plots were sampled on the same day. Samples were collected with a core sampler or auger from the top 15 cm of the soil profile and were dried in an over at 110^{o}C for a minimum of 3 days until they reached constant mass. θ_g was calculated as,

$$\theta_g = \frac{M_W - M_D}{M_D} \quad (1)$$

where M_W and M_D are the masses of the soil before and after drying, respectively.

Weather Data

Hourly and daily weather data (temperature, relative humidity, wind speed, and precipitation) for the study period was collected at a weather station at Liberty Science Center, Jersey City, NJ (Station #3411) next to the site (New Jersey Weather & Climate Network 2016). Reference evapotranspiration (ETo) was calculated using the Penman Monteith equation following the procedure outlined by the Food and Agricultural Organization (FAO):

$$ETo = \frac{\Delta\left(R_N - G\right) + 86{,}400\rho_a C_p \dfrac{\left(e_s - e_a\right)}{r_a}}{\lambda\left(\Delta + \gamma\left[1 + \dfrac{r_s}{r_a}\right]\right)} \quad (2)$$

Where Δ is the rate of change for saturated vapor pressure change (kPa $^oC^{-1}$), R_N is net radiation at the crop surface (MJ m^{-2} day^{-1}), G is soil heat flux (MJ m^{-2} day^{-1}, assumed negligible for single day time step), ρ_a is mean air density (kg m^{-3}), C_p is the specific heat of air at constant pressure (MJ kg^{-1} $^oC^{-1}$), e_s is saturation vapor pressure (kPa), e_a actual vapor pressure (kPa), r_a is aerodynamic resistance (s m^{-1}), λ is the latent heat of vaporization (MJ kg^{-1}), γ is the psychrometric constant (kPa $^oC^{-1}$), and r_s is the surface canopy resistance (s m^{-1}). Aerodynamic resistance (r_a, s m^{-1}) was calculated according to:

$$r_a = \frac{\ln\left(\dfrac{z_m - d}{z_{om}}\right)\ln\left(\dfrac{z_h - d}{z_{om}}\right)}{k^2 u_z} \quad (3)$$

Where z_m is the height of wind measurements (10 m), z_h is the height of the humidity measurements (10 m), z_{om} is the roughness length governing momentum transfer (m), z_{oh} is the roughness length governing transfer of heat and vapor (m), d is the zero plane of displacement height (m), k is von Karman's constant (0.41, no units), and u_z is wind speed at height z (m s^{-1}). As recommended by FAO, the equations for calculation for a hypothetical reference crop with an assumed height of 0.12 m, fixed surface resistance (r_s) of 70 s m^{-1} and an albedo of 0.23 (Allen et al. 1998). For this purpose, ETo is intended to represent the atmospheric demand for water, not actual ET.

Data Analysis

Light curves were fitting using nonlinear least squares regression utilizing a procedure described by Lobo et al. (2013). Since several different equations are available for fitting light curve data to determine leaf photosynthetic traits or parameters, Lobo et al. (2013) suggest fitting data with multiple equations and then selecting the equation which produces the lowest sum of squares of the errors. The following equation from Prioul and Chartier (1977) was found to produce the best fit for the greatest number of light curves collected for the study:

$$A_N = \frac{\phi_{(Io)} \times I + A_{g\max} - \sqrt{\left(\phi_{(Io)} \times I + A_{g\max}\right)^2 - 4\theta \times \phi_{(Io)} \times I \times A_{g\max}}}{2\theta} - R_{dark} \quad (4)$$

Equation parameters and their abbreviations are described in Table 3-3. The maximum assimilation rate (A_{max}) was determined from net assimilation (A_{net}) in saturating light at the irradiance level (I) above which no significant change in A_{net} occurred. The light compensation point (I_{comp}), the irradiance at which CO_2 assimilation and respiration are equal, was calculated from the parameterized equation by setting A_{net} equal to zero. Quantum yield (φ, also called quantum efficiency) was taken as $\varphi_{(Io)}$ in Eq. 4. While both are measured at ambient CO_2 and saturating light conditions, A_{max} and A_{net} are treated separately since A_{max} is calculated based on light curves and A_{net} is a direct measurement point which was made both while collecting curve data and single survey measurements.

A-C_i curves were fit according to the Farquhar-Von Caemmerer-Berry (FvCB) model of C_3 photosynthesis (Farquhar et al. 1980). The FvCB model splits the A-C_i curve into two or three regions. The low C_i (intercellular CO_2) portion of the curve (< ~400 ppm) represents Rubisco limited photosynthesis which is described by:

$$A_C = V_{c\max}\left[\frac{C_i - \Gamma^*}{C_i + K_C\left(1 + O / K_O\right)}\right] - R_D \quad (5)$$

The high C_i portion of the curve (> ~ 400 ppm) represents RuBP regeneration limited photosynthesis:

$$A_J = J\frac{C_i - \Gamma*}{4C_i + 8\Gamma*} - R_D \quad (6)$$

At very high C_i, photosynthesis can additionally become limited by triose phosphate use (TPU):

$$A_P = 3TPU - R_D \quad (7)$$

At a given C_i net photosynthetic assimilation (A_{net}) is a function of the most limiting process:

$$A_N = \min\{A_C, A_J, A_P\} \quad (8)$$

Equation variables and their units are listed in Table 3-3. Values of Γ*, K_O and K_C were based on Bernacchi et al. (2001) and were temperature corrected using the following version of the Arrhenius equation:

$$Parameter = e^{\left(c - \frac{\Delta H_a}{R(Tleaf)}\right)} \quad (9)$$

where Tleaf is the leaf temperature in Kelvin and R is the universal gas constant (8.314 J mol^{-1} K^{-1}). Values for c (a scaling constant) and ΔH_a are shown in Table 3-4, based on Bernacchi et al. (2001, 2003).

A-C_i curves were fitted to parameterize maximum carboxylation rate (V_{cmax}), maximum electron transport rate (J_{max}), triose phosphate utilization (TPU), and dark respiration (R_{dark}) using the plantecophys package in R statistics run in the R computing environment (Duursma 2015; R Core Team 2016). One challenge in fitting A-C_i curves is identifying the level of C_i where one limitation transitions to another (the C_i transition point), especially since at some concentrations both Rubisco and RuBP regeneration can be co-limiting (Sharkey et al. 2007). The plantecophys package obviates the need to manually determine the C_i transition point for each curve and has two options for fitting the FvCB model. For curves which were not TPU limited, the program's default non-linear regression approach was used. Curves with all three limitations were fit using

the program's linear method. If a curve had less than three points available to constrain the RuBP regeneration or TPU limited equations, J_{max} and/or TPU were be excluded from further analysis. To facilitate comparison, V_{cmax} and J_{max} were normalized to 25ºC using the constants shown in Table 3-4. While the temperature response constants for K_C, K_O, and Γ* are considered intrinsic properties of Rubisco and are fairly well conserved among species (von Caemmerer 2000), Medlyn et al. (2002) show that there can be greater variability in the temperature responses of V_{cmax} and J_{max}, even within species. While temperature response data for A-C_i curves was collected as part of the study, the temperature range was not wide enough to accurately estimate c and ΔH_a for *B. populifolia* at LSP. The values of c and ΔH_a used in this study do fall well within the range of values found by Medlyn et al. (2002) for deciduous trees. All of the other default settings in plantecophys were used for fitting. The CO_2 compensation point (Γ_{comp}) was calculated by solving the fitted model for $A_{net} = 0$.

Intrinsic water use efficiency (iWUE, also called potential water-use efficiency or physiological water-use efficiency) was calculated as

$$iWUE = A_{net} / g_s \quad (10)$$

Where A_{net} and g_s are the net photosynthetic assimilation rate (μmol CO_2 m^{-2} s^{-1}) and stomatal conductance to water vapor (mol H_2O m^{-2} s^{-1}) at 400 ppm CO_2 and 1500 μmol PPFD m^{-2} s^{-1}.

Statistical Analysis

Photosynthesis parameters were tested using a linear mixed effects model. The effects of metal load (ML) and sample month and year (MY) on each photosynthesis parameter were tested using a linear mixed effects model. The low metal load group included plots L1 and L2 while the high metal load group included plots H2 and H3. Linear mixed effects models account for within-subject or within-group variation by setting random intercepts for each individual and/or cluster.

ML, MY and their interaction were treated as fixed effects while tree and plot were treated as random effects. Three models were tested for each parameter: 1) the full model (ML and MY plus their interaction), 2) ML only, and 3) MY only. J_{max}, Γ_{comp}, I_{comp}, E, and g_s were natural log transformed to achieve normality and constant variance of residuals. Likelihood ratio tests were used to determine the significance of ML, MY and their interaction by testing each of the three models against a null model containing only random effects.

The relationship between A-Ci curve parameters and leaf temperatures from the temperature response study was tested using linear regression with an interaction effect between leaf temperature and metal load (LML or HML). Leaf conductance (g_s) and E were log transformed in order to normalize their residuals. To facilitate interpretation of the linear regression intercept coefficient (which would be 0^{o}C and meaningless in this context) leaf temperature was re-centered on the mean temperature, 30^{o}C, prior to running the regression. Using the re-centered leaf temperatures, the intercept coefficient represents the mean value of a parameter for the low metal load (LML) trees at 30^{o}C. The high metal load (HML) coefficient is then the difference between the LML mean and the HML mean at 30^{o}C.

The effects of weather variables on the photosynthesis parameters were tested using linear and quadratic regressions. Since all measurements were made in the morning, daily maximum and mean temperatures as well as precipitation were based on the 24 hours preceding the morning of the measurement. Precipitation totals were also calculated for the 72 hours preceding the morning of the measurement. For both types of regression photosynthesis parameters were tested for normality and constant variance and were transformed as needed. However no suitable transformation was found for the light compensation point, stomatal conductance, and quantum yield consequently those parameters were excluded from this analysis.

One way ANOVAs were used to compare soil water content (θ_g) between plots on each day soil samples were collected to determine if θ_g varied significantly between plots. Residuals

were normally distributed and had constant variance so no transformations were needed. On dates when the ANOVA indicated a significant difference between plots, a Tukey HSD test was used to assess which plots were significantly different from the others. A linear mixed effects model was also used to test the interacting effects of metal load and θ_g using plot and tree as random effects. On days when photosynthesis was measured but θ_g was not, θ_g was estimated by linearly interpolating between the two closest θ_g measurement dates.

RESULTS

Photosynthesis parameters varied strongly by measurement month-year (MY), but did not show strong differences based on soil metal load (ML) alone – no parameter had a significant ML only model (Table 3-5). There was greater variance between trees than between plots, though within subject variation for all parameters was at least an order of magnitude greater than the variance from either random effect (Table 3-6). However significant interactive effects between MY and ML for were observed for maximum carboxylation rate (V_{cmax}), electron transport rate (J_{max}), quantum efficiency (φ), light compensation point (I_{comp}) and intrinsic water use efficiency (iWUE) (Table 3-7). In July 2014 and May 2015, V_{cmax}, J_{max}, and φ were significantly lower for high metal load trees compared to low metal trees[1] (Figure 3-1). V_{cmax} and φ were also significantly lower for high than low metal load trees in September 2014 as was J_{max} in August 2014 and June 2015. Following the heat wave in July 2015, the iWUE of high metal load trees was significantly lower in that month.

[1] Note that the rephrasing “low metal” and “high metal trees” refers to trees growing in soils with a respectively low or high total metal load (TML) and does not necessarily mean the tree has a high concentration of metals

Though metal load alone was not a significant predictor of any of the photosynthesis parameters, several trends suggest that the high metal load trees were under stress (Figure 3-2). The medians of V_{cmax}, J_{max}, maximum net assimilation (A_{max}), light compensation point (I_{comp}), quantum efficiency (φ), dark respiration rate (R_{dark}), and net assimilation (A_{net}) were all lower in the high metal load trees while CO_2 compensation point (Γ_{comp}), and iWUE were higher. The medians of transpiration (E) and stomatal conductance (g_s) were not different between metal load though the high metal 3rd and 4th quartiles are lower. These results do not provide strong evidence in support of Hypothesis 1 and instead highlight the strong seasonal variation in the photosynthetic physiology of these trees.

Leaf mass per area (LMA) was the only parameter with a significant metal load (ML) only model which indicated that the mean LMA from the low metal load trees (53 ± 1 (standard error) g m^{-2}) was significantly greater than the mean of the high metal load trees (47 ± 2 g m^{-2}). While LMA of the 2015 leaf samples ranged from 11 to 88 g m^{-2}, the low standard deviation (9.3 g m^{-2}) about the mean of all samples (49.9 g m^{-2}) suggests that overall LMA was fairly consistent among the sample leaves. Other authors have found LMA for *B. populifolia* leaves ranging from 74 to 95 g m^{-2} (Chen et al. 2014; Wayne and Bazzaz 1993).

Monthly temperature and precipitation in 2014 were similar to statewide historic monthly averages, although precipitation in August, September, and October 2014 were about 5 to 6 cm below statewide historic averages (Figure 3-3, Table 3-8). During the 2014 growing season mean assimilation values (A_{max} and A_{net}) peaked in June while the maximum carboxylation rate (V_{cmax}) for low metal trees peaked in July (Figure 3-1). Quantum efficiency (φ), light compensation point (I_{comp}), and dark respiration (R_{dark}) means were also low in July 2014. Intercellular to ambient CO_2 ratio (C_i/C_a), transpiration (E), and stomatal conductance (g_s) decreased from May to August 2014 while CO_2 compensation point (Γ_{comp}) and intrinsic water use efficiency (iWUE) increased. July through September 2015 were both hotter and drier than the statewide historic average, with

July and August both having very low precipitation totals (Figure 3-4). ET_o did not vary greatly between the two study seasons.

While June 2015 was wetter than average, a short heat wave (several days of high temperatures and no rainfall) in July 2015 strongly affected photosynthesis parameters. The point sample measurements from the L1 trees suggest that before the heat wave, photosynthesis rates were comparable to rates in 2014 (Figure 3-5). However 3 days after the start of heat wave net assimilation (A_{net}), transpiration (E), stomatal conductance (g_s), intercellular CO_2 (C_i), and intercellular to ambient CO_2 ratio (C_i/C_a) in plot L1 all decrease dramatically while iWUE increases. Additionally in the remainder of the plots measured in the days following the heat wave, maximum carboxylation rate (V_{cmax}), net assimilation (A_{max} and A_{net}), quantum efficiency (φ), dark respiration (R_{dark}), transpiration (E), and stomatal conductance (g_s) were all much lower in July 2015 compared to July 2014 (Figure 3-1). CO_2 compensation point ($\Gamma_{comp)}$ and intrinsic water use efficiency (iWUE) were much higher in July 2015 compared to 2014. In August 2015 V_{cmax}, A_{max}, φ, and R_{dark} remained low while A_{net}, E, and g_s increased slightly and increased again in September to similar levels observed in 2014.

Following the initial hypothesis, the high metal load trees had lower mean iWUE in July 2015 after the heat wave compared to low metal load (Figure 3-6, Table 3-7). iWUE declined for both groups in August and September 2015 as g_s rates increased but A_{net} remained fairly low. High metal load transpiration and g_s were lower in August 2015, which was 7 cm drier than the statewide historic average, but were higher compared to low metal load trees in September 2015.

The relationship between g_s and C_i/C_a can be used to separate the effects of stomatal and non-stomatal limitations on photosynthesis during periods of water stress (Brodribb 1996; Singh and Raja Reddy 2011). For most of the study months, the relationship between g_s and C_i/C_a follows an expected exponential rise to maximum function where higher C_i/C_a is associated with higher g_s but is not affected by metal load (Figure 3-7). However while some measurements show

a very sharp decline in C_i/C_a with decreasing g_s, other measurements made in July and August 2015 show that C_i/C_a increases drastically at very low g_s. These observations of very high C_i/C_a at very low g_s, which occurred in all four study plots, strongly suggest the occurrence of non-stomatal limitations to photosynthesis in these trees (Brodribb 1996).

A_{max}, A_{net}, I_{comp}, R_{dark}, V_{cmax}, and E all had significant relationships with weather variables though all of the model fits are fairly weak (Table 3-9). All of the polynomial regressions for temperature reach a maximum around 15ºC for both maximum and mean daily temperature (Figure 3-8). E and A_{net} had negative relationships with ET_o. R_{dark} was predicted by both temperature and precipitation. Both 24 and 72 hour precipitation totals predicted A_{net}, I_{comp}, and R_{dark} with either a positive linear relationship or a polynomial relationship which reached a maximum around 2 cm (72 hours) or 1 cm (24 hours).

Varying leaf temperatures from 25 to 35ºC altered photosynthesis parameters though no interactive effects with metal load were observed, i.e. metal load did not change the relationship between the parameters and leaf temperature. There were significant relationships between leaf temperature and V_{cmax}, J_{max}, Γ_{comp}, g_s (log transformed), and C_i (Table 3-10). However assimilation and transpiration were not significantly affected by leaf temperature. Positive relationships were observed for V_{cmax}, J_{max}, and Γ_{comp}, while the other significant parameters decreased with increasing temperature (Figure 3-9). J_{max} values from high metal load trees were significantly lower than those from the low metal plot at 30ºC though there were no interactive effects between metal load and leaf temperature. None of the other parameters were significantly affected by metal load. However all high metal load coefficients indicate that the mean value for high metal load trees at 30ºC were lower than the low metal means.

Some differences were observed between the macro and micronutrients and other soil properties of the four study plots (Tables 3-11, 3-12, 3-13). For the most part macronutrient concentrations were similar for the high and low metal load plots, though interestingly L2 and H3

had similarly low phosphorus concentrations in comparison to L1 and H2. Concentrations of Mehlich 3 extractable Zn and Cu were significantly higher in Plot H3 compared to plots L2 and H2.

Gravimetric soil water content (θ_g) in all four plots declined from ~45% to ~10% over the course of the 2015 study period (Figure 3-4) which coincides with the decreasing rainfall from June to September 2015. In June and July 2015 L2 tended to have the highest and L1 the lowest θ_g, while H3 and H2 had fairly similar intermediate θ_g values. In August 2015, θ_g in L2 had decreased to a similar level as H3 and H2 and by September θ_g from all four plots had converged. According to Tukey HSD tests, θ_g was significantly higher in L2 compared to L1 on 2015-07-14 and 2015-07-21. No significant differences were found between the plots for any of the other measurement days. Net photosynthesis (A_{net}), E, and g_s scaled positively with θ_g for measurements made from June to September 2015 (Table 3-14, Figure 3-10). Interactions between θ_g and metal load were observed for $V_{cmax,}$ R_{dark}, and A_{max}. In general these parameters in the low metal group were less sensitive to decreasing θ_g. This apparent lack of sensitivity seems to be driven by Plot L1 (Figure 3-10) which tended to have the lowest θ_g yet higher V_{cmax}, A_{max}, and R_{dark} values compared to the high metal load trees at similar θ_g.

DISCUSSION

Hypothesis 1: Soil metal load is primary limitation on photosynthesis parameters

The effects of soil metal load on the photosynthesis parameters of *B. populifolia* trees growing in LSP were not as drastic as initially hypothesized. Numerous studies have demonstrated that photosynthesis and related gas exchange parameters are diminished with increasing exposure to a variety of heavy metals (e.g. Di Baccio et al. 2009; Gaudet et al. 2011; Pereira et al. 2016; Santana et al. 2012). Differences in methodologies and reporting make it extremely difficult to compare soil trace element concentrations across studies. Consequently it is

possible that the gradient of trace elements in the LSP study plots was not as wide as those assessed in other studies which may account for the smaller differences observed in this photosynthesis study. A large body of research on the effects of heavy metals on plants and photosynthesis has been conducted in lab or greenhouse settings in which leaves and chloroplasts were exposed to metal solutions directly or plants were grown in media with high bioavailable concentrations (Mysliwa-Kurdziel et al. 2004). While these approaches are valuable for elucidating mechanistic responses, they do not reflect complex field conditions where many interacting factors may mediate leaf level TE response, including community level interactions (Krumins et al. 2015) and plant-mycorrhizal associations (Yang et al. 2015).

One of the few significant metal load month-year interactions – the significant decreases in V_{cmax} and J_{max} in July 2014 and May 2015 – could be the result of elevated Zn concentrations in the leaves during these time periods. Gallagher et al. (2008) found *B. populifolia* leaf Zn concentrations changed over the course of the growing season and that in HML plots there were significant positive relationships between leaf Zn and leaf red/green ratio index (an image-based proxy for chlorophyll content). A_{max} and A_{net} also decreased in the HML trees during these two months, though their decreases were not significant. HML R_{dark} was also lower in this month, potentially offsetting the effects of reduced V_{cmax} and J_{max} on net assimilation rates. While these reductions may be transient, it is possible that they occur during a critical part of the year and had substantial effects on overall growth rates (Boone et al. 2004). The significantly lower V_{cmax} and J_{max} observed in HML trees in July 2014 and May 2015 suggest metal stress effects may be transient and seasonal.

The decreasing trend of V_{cmax}, J_{max}, A_{max} and A_{net} with metal load has been observed for many species as a stress response with exposure to various metals (e.g. Van Den Berge et al. 2011; Gaudet et al. 2011; Pereira et al. 2016). The mean value of A_{net} measured at LSP during 2014 (the average growing season), was lower than mean values for *Betula* species from other

sites found in the literature review (Table 3-1). The 2014 means of V_{cmax}, J_{max}, and g_s were all less than the literature values. R_{dark} and I_{comp} means were within the literature range while φ was slightly higher. While study conditions and methods do influence gas exchange measurements, the tendency of several photosynthetic parameters measured at LSP to be less than those from other locations suggests the photosynthetic capacity of the LSP trees may be limited in comparison to trees growing in non-contaminated soils. These lower rates could be attributed to stress from exposure to TE and/or the sub-optimal availability of some macro- and micro-nutrients observed in the study plots. Lack of nutrient availability and low water availability are common in degraded and anthropogenic soils and can hinder restoration efforts (Williamson et al. 2011; Wong 2003).

It was initially hypothesized that R_{dark} would increase with increasing TML similar to the results of other studies which posited higher R_{dark} indicates increased ion export rates and/or increased production of metal-binding molecules (Losch 2004; Romanowska et al. 2002; Vassilev et al. 1997). At LSP, R_{dark} tended to be lower in the HML group suggesting that leaves from these trees were not spending much additional energy on protection mechanisms against TE. Similar results were observed by Hermle et al. (2007) for *Salix vinimalis* and *Populus tremula* grown in soil contaminated with smelter dust. The decrease in R_{dark} can instead be attributed to the concurrent lower rate of A_{max} (and A_{net}) which means less substrate is available for respiration (Cannell and Thornley 2000). Given the lower rates of R_{dark} observed in the leaves from high metal load trees, evidence is lacking for a strong protection response by these *B. populifolia* leaves.

As expected, an increase in Γ_{comp} was observed in the high metal load (HML) trees. High Γ_{comp} can indicate an increase in photorespiration – the release of CO_2 during photosynthesis when O_2 rather than CO_2 binds to RuBP (Di Baccio et al. 2009). Photorespiration can increase as stomatal closure limits CO_2 supply, or it may also increase to reduce the effects of other stresses

(Wingler et al. 2000). HML g_s rates are in the lower range compared to low metal load (LML), an effect which is also manifested in the lower C_i/C_a and higher iWUE in the HML trees. This reduction in HML g_s makes it difficult to determine how much of the increase in Γ_{comp} is a direct result of stomatal limitation or of a stress response to elevated TE concentrations in the leaf.

TE exposure can affect plant-water relations in many ways, including causing ion imbalance, disrupting hormone signaling, or causing structural changes in water transport pathways (Poschenrieder and Barcelo 2004). Yet surprisingly when compared as an entire group, few differences were observed in E and g_s between HML and LML leaves though iWUE was higher for HML trees. Variable responses of iWUE to heavy metals have been reported in the literature. In some cases iWUE decreases with increasing metal exposure which is usually attributed to a reduction in net photosynthetic rates (Anjum et al. 2016; Hermle et al. 2006; Stancheva et al. 2014), while in other cases iWUE increased with increasing metal exposure usually because stomatal conductance has decreased (Nwugo and Huerta 2008; Stancheva et al. 2014). While both A_{net} and g_s are generally lower in the HML trees, it appears the increasing iWUE reflects a greater decrease in g_s. Other studies have observed correlations between reduced root biomass and rooting depth and reduced g_s which then increased iWUE (Köhler et al. 2016; Menon et al. 2007). The higher iWUE in HML trees at LSP may reflect greater water stress caused by metal exposure as well as a potential for different root responses in HML soils.

Since net carbon assimilation is fairly similar between the low and high metal groups, differences in whole plant growth and community productivity observed by previous research at the site could result from differences in carbon allocation between low metal and high metal load trees. Exposure to TE can alter patterns of biomass allocation within plants, though in some species allocation to below-ground biomass is favored (Brun et al. 2003; Zhang et al. 2014) while others increase allocation to above-ground or reproductive resources (Sánchez Vilas et al. 2016). Notably different mycorrhizal communities and soil enzymatic rates have been observed in other

study plots within LSP (Evans et al. 2015; Hagmann et al. 2015) suggesting that facilitative interactions with soil biota may also play an important role in tree growth in this site.

Leaf mass per area (LMA) in 2015 was the only measured parameter with a significant metal load only model. The decrease in LMA with increasing metal load could be an indication that the high metal load trees preferentially allocate resources to other compartments, such as roots. Alternatively since lower LMA is associated with shorter leaf longevity (Wright et al. 2004), the lower LMA in the high metal load (HML) trees may result from higher leaf turnover rates in these trees, which would also divert carbon from trunk biomass. Lower LMA can represent a decrease in the resources allocated to a leaf because of a change in leaf thickness and/or the concentrations of cellular compounds (Poorter et al. 2009). Some studies have found LMA to respond to metal exposure (Di Baccio et al. 2009; Renninger et al. 2015) while others found no effect (André et al. 2006; Shi and Cai 2009) or species specific effects (Hermle et al. 2006). Light availability is a strong driver of LMA variability within an organism or species (longer exposure to light leads to greater LMA), though LMA can also be influenced by water availability and salinity stress (Poorter et al. 2009). Other authors have found LMA for *B. populifolia* leaves ranging from 74 to 95 g m^{-2} (Chen et al. 2014; Wayne and Bazzaz 1993) which is at the upper range of leaf samples measured at LSP in 2015 (11 to 88 g m^{-2}) which suggests that LMA is negatively affected by exposure to TE even in the low metal load trees.

Hypothesis 2: Elevated ML will exacerbate effects of stressful weather

While there is evidence that heat response proteins confer protection of photosynthetic pathways from heavy metals (Heckathorn et al. 2017) and that plants exposed to heavy metals may have greater thermotolerance (Howarth 1990), it is also possible that heat and metal stress may produce an additive negative effect on photosynthesis. Between the ranges of 25 to 35^{o}C, no differences were observed in the relationships between leaf temperature and photosynthetic

parameters from the high metal (HML) and low metal load (LML) trees. It is possible that within this temperature range leaves were either not exposed to heat for a long enough period of time to induce heat shock or that higher temperatures were needed to induce a response. Within this range of temperatures and exposure time, the increasing V_{cmax} and J_{max} suggests little to no thermal damage occurred. However a concurrent increase in A_{net} was not observed since g_s declined in response to higher temperatures.

The invariant A_{net} across a temperature range of 25 to 35ºC observed for LSP *B. populifolia* is similar to temperature responses observed in studies of other *Betula* species. *B. papyrifera, B. pendula, B. jacquemontii*, and *B. nigra* had optimal temperatures for A_{net} ranging between 25 and 30ºC (Ranney and Peet 1994). Another study found *B. papyrifera's* optimal A_{net} temperature to be 24ºC in a mixed deciduous stand in Michigan (Jurik et al. 1988). Optimal temperatures for *B. platyphylla* tended to be lower, 25ºC in a common garden experiment in North Carolina (Ranney and Peet 1994) and 10 to 20ºC in Hokkaido, Japan (Koike and Sakagami 1986). An optimum temperature for V_{cmax} and J_{max} was not observed in the temperature range of this study which is consistent with findings for *B. pendula* which had optimal temperatures at 37.9 and 35.1ºC, respectively (Dreyer et al. 2001). At LSP, *B. populifolia* grows both at the southern end of its range and at a low altitude. The results of the temperature analysis and survey measurements following a heat wave suggest this population may be sensitive to higher temperatures and dry conditions as would be expected for its genus.

As more extreme weather events are expected in the coming century under various climate change scenarios, it is important to understand the ways abiotic soil stressors can interact with extreme weather events. During the July 2015 heat wave, while slightly above average temperatures occurred for only three days when temperatures decreased, ETo actually increased because of sunnier weather and θ_g measurements in three of the four plots continued to decrease in the following days. These conditions, while not particularly remarkable in the context of

regional weather trends, dramatically reduced photosynthesis rates for a period of several days. The positive relationships observed between soil water content and net photosynthesis, transpiration and conductance strongly suggests lack of water was an important driver for the reduction of photosynthesis rates in the second half of the 2015 growing season. The leaf temperature study suggests that while this population of *B. populifolia* is somewhat sensitive to this temperature range, it was probably the combination of elevated temperature plus the lack of antecedent rainfall and higher evaporative demand that produced the observed decline. In a study of mild drought stress on six birch species, *B. populifolia*, was moderately affected by lack of water in comparison with the other species (Ranney et al. 1991). A decrease in soil water content of potting mix from 45% to 10% effectively halved A_{net} of *B. populifolia* (Graves et al. 2002). Similarly imposition of a water deficit reduced *B. papyrifera* V_{cmax} by 46% (Gu et al. 2008).

The lower iWUE observed for the high metal load (HML) trees after the July 2015 heat wave and in August 2015 suggests the HML trees are more negatively affected by heat wave. There is a mix of reports on the interacting effects of trace elements and water stress on plant growth. Some researchers have suggested that metal induced changes in xylem structure, higher stomatal resistance, smaller and fewer leaves, and enhanced abscission effectively promote water conservation by the plant, countering the effects of drought (Poschenrieder and Barcelo 2004). In a pot experiment, the dry mass of *B. papyrifera* seedlings exposed to high concentrations Cu-Ni was less affected by drought compared to control seedlings (Santala and Ryser 2009). The authors posit that since the seedlings were already impaired by metal exposure, they had a lower overall water demand and consequently were less affected by drought stress. However additive effects of drought and heavy metal stress which reduce growth have been observed in other studies (de Silva et al. 2012).

Hypothesis 3: Differences in other edaphic conditions could offset TML effects

Contrary to the initial hypothesis, no interactions were observed between metal load and water content effects on photosynthesis. Anthropogenic and brownfield soils are known to frequently be limited in both their water and nutrient holding capacities (Jimenez et al. 2013; Pavao-Zuckerman 2008; Whelan et al. 2013; Williamson et al. 2011) in addition to their potential contamination. These limitations can hinder both the growth of plants and soil microbes. A suite of soil chemistry measurements were made on soils from the four study plots in order to assess the potential effects of other soil conditions in addition to total metal load (TML). However, since soil quality parameters did not vary consistently between plots (e.g. P is higher in L1 than H3, but K is higher in H3 than L1), it was difficult to draw conclusions about their potential effects on photosynthesis.

Study plots did tend to vary by water content, with the two low metal load plots having both the highest and lowest mean water content during the course of the 2015 growing season. *B. populifolia* is sensitive to prolonged inundation so it is possible that during some times of the year Plot L2 may be too wet which could explain some of the impaired photosynthetic parameters measured in that plot. Differences between plot water content were most pronounced earlier in the 2015 growing season while during the drier months of August and September differences between plots were minimized. The responses of maximum carboxylation rate, maximum net photosynthetic assimilation, quantum efficiency and dark respiration did vary by metal load in plants measured in 2015. It is difficult to conclude in this case if high metal soil stress is exacerbating the effects of low water content on photosynthesis parameters. Since plot L1 tends to be drier than the other plots it is possible its trees are better adapted to drier conditions or perhaps are tapping a deeper water source than what was measured in the upper soil horizon.

CONCLUSION

Anthropogenic soils can create novel ecosystems which may function differently when compared to more traditionally studied rural ecosystems. Consequently expectations of their function and resilience should be tailored to fit these unique conditions rather than based on assumptions from other environments. Our results suggest that in spite of increasing metal loads, leaf level photosynthesis efficiency is surprisingly robust. Even when trees are exposed to sub-optimal weather conditions, higher metal loads did not appear to exacerbate these effects. It is likely that differences along a metal gradient observed at a coarser scale at the site may have resulted from differences in resources allocation rather than photosynthetic capacity. It is also feasible that, while the differences observed between high and low metal load plots were small, when scaled up these small differences could become manifest as larger differences. A comparison of macro and micro-nutrients between plots highlights the heterogeneous availability of resources at the site but did not provide additional insight into the lack of difference in photosynthetic rates between plots. While some variability was observed in the gravimetric water content of the plots, more detailed study would be needed to develop a more direct connection between soil moisture and photosynthetic capacity.

Table 3-1: Photosynthetic parameters reported in the literature for members of the *Betula* section. A_{sat} is defined as the net photosynthetic assimilation rate at saturating light and ambient CO_2, and may have been collected as a point sample or calculated from a light response curve. With the exception of results from the Ranney et al (1991) study, all data was extracted from tables or text and not estimated from graphs. With the exception of studies on light availability effects, data represents average growing conditions (e.g. ambient CO_2, well-watered soil, etc.).

Parameter	**Value**	**Species**	**Setting**	**Temp. (ºC)**	**CO_2 (ppm)**	**Light (µmol m^2 s^{-1})**	**Source**
A_{sat} (µmol m^{-2} s^{-1})	4.08	*B. papyrifera*	Shade grown, Open top chamber (Michigan)	-	350	1000-1500	(Kubiske and Pregitzer 1996)
	9.1	*B. pendula*	Open grown trees, mature leaves (Poland)	24	379	1000-1500	(Oleksyn et al. 2000)
	9.7	*B. platyphylla* var. *japonica*	Low N regime, greenhouse (Japan)	25	360	1200	(Kitao et al. 2005)
	10.5	*B. papyrifera*	Forest, upper canopy	20-25	330-345	1000	(Jurik et al. 1988)
	10.53	*B. papyrifera*	Sun grown, Open top chamber (Michigan)	-	350	1000-1500	(Kubiske and Pregitzer 1996)
	10.8	*B. papyrifera*	Hydroponic system (pH = 5) (Canada)	20	400	400	(Zhang et al. 2016)
	11.58	*B. platyphylla* var. *japonica*	Seedlings, common garden (Japan)	25	370	1500	(Watanabe et al. 2016)
	12.2	*B. pendula*	Lower Canopy, Forest (Estonia)	25	370	800-1800	(Sellin et al. 2010)
	12.46	*B. pendula*	Seedling, hydroponic system (Sweden)	-	350	600	(Pettersson et al. 1992)
	12.5	*B. populifolia*	Greenhouse	-	330	1200	(Ranney et al. 1991)
	13.2	*B. platyphylla* var. *japonica*	High N regime, greenhouse (Japan)	25	360	1200	(Kitao et al. 2005)
	15.1	*B. platyphylla* var. *japonica*	Forest, June (Japan)	25	380	1500	(Hoshika et al. 2013)
	15.9	*B. pendula*	Upper Canopy, Forest (Estonia)	25	370	800-1800	(Sellin et al. 2010)
Mean	**11.5**						

Table 3-1 (con't)

Parameter	**Value**	**Species**	**Setting**	**Temp. (ºC)**	**CO_2 (ppm)**	**Light (µmol m^2 s^{-1})**	**Source**
g_s (mol m^{-2} s^{-1})	0.12	*B. platyphylla* var. *japonica*	Seedlings, common garden (Japan)	25	370	1500	(Watanabe et al. 2016)
	0.27	*B. platyphylla* var. *japonica*	Forest, June (Japan)	25	380	1500	(Hoshika et al. 2013)
	~0.6	*B. populifolia*	Greenhouse	-	330	1200	(Ranney et al. 1991)
	2.1 mm/s (?)	*B. papyrifera*	Forest, upper canopy	20-25	330-345	1000	(Jurik et al. 1988)
E (mmol m^{-2} s^{-1})	2.9	*B. papyrifera*	Hydroponic system (pH = 5) (Canada)	20	400	400	(Zhang et al. 2016)
R_{dark} (µmol m^{-2} s^{-1})	0.53	*B. pendula*	Lower Canopy, Forest (Estonia)	25ºC	370	800-1800	(Sellin et al. 2010)
	0.57	*B. papyrifera*	Forest, upper canopy	20-25	330-345	0	(Jurik et al. 1988)
	0.62	*B. pendula*	Potted, outdoors (Finland)	25	Var.	1500	(Aalto and Juurola 2001)
	0.69	*B. papyrifera*	Shade grown, Open top chamber (Michigan)	-	350	1000-1500	(Kubiske and Pregitzer 1996)
	0.76	*B. pendula*	Upper Canopy, Forest (Estonia)	25ºC	370	800-1800	(Sellin et al. 2010)
	0.9	*B. pendula*	Open grown trees, mature leaves (Poland)	24	379	1000-1500	(Oleksyn et al. 2000)
	1.27	*B. papyrifera*	Sun grown, Open top chamber (Michigan)	-	350	1000-1500	(Kubiske and Pregitzer 1996)
	1.65	*B. pendula*	Common garden (Germany)	25ºC	Var.	0	(Feng et al. 2007)
	1.91	*B. pendula*	Greenhouse (France)	25	35 Pa	0	(Dreyer et al. 2001)

Table 3-1 (con't)

Parameter	**Value**	**Species**	**Setting**	**Temp. (ºC)**	**CO_2 (ppm)**	**Light (µmol m^2 s^{-1})**	**Source**
V_{cmax} (µmol m^{-2} s^{-1})	70.5	*B. pendula*	Greenhouse (France)	25	Var.	1000	(Dreyer et al. 2001)
	78.8	*B. platyphylla* var. *japonica*	Forest, June (Japan)	25ºC	380	1500	(Hoshika et al. 2013)
	93.5	*B. pendula*	Common garden (Germany)	25ºC	Var.	2000	(Feng et al. 2007)
J_{max}	125.3	*B. pendula*	Greenhouse (France)	25	Var.	1000	(Dreyer et al. 2001)
	148.8	*B. platyphylla* var. *japonica*	Forest, June (Japan)	25ºC	380	1500	(Hoshika et al. 2013)
	151.6	*B. pendula*	Common garden (Germany)	25ºC	Var.	2000	(Feng et al. 2007)
I_{comp} (µmol m^{-2} s^{-1})	11	*B. pendula*	Lower Canopy, Forest (Estonia)	25ºC	370	800-1800	(Sellin et al. 2010)
	14	*B. pendula*	Upper Canopy, Forest (Estonia)	25ºC	370	800-1800	(Sellin et al. 2010)
	16.4	*B. papyrifera*	Shade grown, Open top chamber (Michigan)	-	350	1000-1500	(Kubiske and Pregitzer 1996)
	20	*B. pendula*	Open grown trees, mature leaves (Poland)	24	379	1000-1500	(Oleksyn et al. 2000)
	54.9	*B. papyrifera*	Sun grown, Open top chamber (Michigan)	-	350	1000-1500	(Kubiske and Pregitzer 1996)
φ (mol C mol^{-1} photons)	0.021	*B. papyrifera*	Shade grown, Open top chamber (Michigan)	-	350	1000-1500	(Kubiske and Pregitzer 1996)
	0.022	*B. papyrifera*	Sun grown, Open top chamber (Michigan)	-	350	1000-1500	(Kubiske and Pregitzer 1996)
	0.063	*B. pendula*	Lower & Upper Canopy, Forest (Estonia)	25ºC	370	800-1800	(Sellin et al. 2010)

Table 3-2: 2015 study plot names used in current paper along with names used in previous studies and total metal load (composite index based on concentrations of As, Cr, Cu, Pb, and Zn measured in 2005, see Gallagher et al. (2008).

Plot	**Previous label**	**Total Metal Load**
L1	TP-41	0.85
L2	TP-48	1.56
H2	TP-14/16	3.56
H3	TP-25	4.31

Table 3-3**:** Equation variables and photosynthesis parameters abbreviations.

Variable	Name	Units
A_c	Rubisco limited net photosynthesis rate	μmol CO_2 m^{-2} s^{-1}
A_{gmax}	Maximum gross photosynthetic assimilation rate	μmol CO_2 m^{-2} s^{-1}
A_J	RuBP regeneration limited net photosynthesis rate	μmol CO_2 m^{-2} s^{-1}
A_{max}	Maximum net photosynthetic assimilation rate	μmol CO_2 m^{-2} s^{-1}
A_{net}	Net photosynthetic assimilation rate	μmol CO_2 m^{-2} s^{-1}
A_P	TPU limited net photosynthesis rate	μmol CO_2 m^{-2} s^{-1}
C_a	Ambient CO_2 concentration	μmol CO_2 mol air
C_i	Intercellular CO_2 concentration	μmol CO_2 mol air
C_i/C_a	Ratio of intercellular to ambient CO_2 concentration	dimensionless
E	Transpiration rate	mmol H_2O m^{-2} s^{-1}
g_s	Stomatal conductance of water vapor rate	mol H_2O m^{-2} s^{-1}
iWUE	Intrinsic water use efficiency	μmol CO_2 mol^{-1} H_2O
I	Photosynthetic photon flux density	μmol photon m^{-2} s^{-1}
I_{comp}	Light compensation point	μmol photon m^{-2} s^{-1}
J_{max}	Maximum electron transport rate	μmol e- m^{-2} s^{-1}
K_C	Michaelis-Menten constant of Rubisco for CO_2	μmol CO_2 mol air (or Pa)
K_O	Michaelis-Menten constant of Rubisco for O_2	μmol CO_2 mol air (or Pa)
O	Oxygen concentration/partial pressure	μmol O_2 mol air (or Pa)
R_{dark}	Dark respiration rate	μmol CO_2 m^{-2} s^{-1}
TPU	Triose phosphate use	μmol CO_2 m^{-2} s^{-1}
V_{cmax}	Maximum Rubisco carboxylation rate	μmol CO_2 m^{-2} s^{-1}
Γ*	Photorespiratory compensation point	μmol CO_2 mol air
Γ_{comp}	CO_2 compensation point	μmol CO_2 mol air
θ	Convexity factor	dimensionless
φ	Quantum yield	μmol CO_2 μmol^{-1} photon
$\varphi_{(Io)}$	Quantum yield at I = 0	μmol CO_2 μmol^{-1} photon

Table 3-4: Temperature correction parameters for K_C, K_O, Γ^*, V_{cmax}, and J_{max} used in Equation 8. ΔH_a is the activation energy, and c is a scaling constant. The scaling constants for V_{cmax} and J_{max} were normalized so the parameters equal 1 at 25°C to facilitate the adjustment of values at leaf temperature to 25°C.

	Parameter at 25°C	**c (-)**	**ΔH_a (kJ mol^{-1})**
K_C (μmol CO_2 mol air)[1]	404.9	38.05	79.43
K_O (μmol O_2 mol air)[1]	278.4	20.30	36.38
Γ^* (μmol CO_2 mol air)[1]	42.75	19.02	37.83
V_{cmax} (μmol CO_2 m^{-2} s^{-1})[1]	1	26.35	65.33
J_{max} (μmol e- m^{-2} s^{-1})[2]	1	17.7	43.9

[1] (Bernacchi et al. 2001)

[2] (Bernacchi et al. 2003)

Table 3-5: Comparison of linear mixed effects models of photosynthesis parameters using metal load (ML) and month-year (MY) as fixed effects and plot and tree as random effects. Full model includes both ML and MY with interaction effects. The first four models were tested against the null model using an ANOVA test.

Parameter	**Statistic**	**Full**	**ML Only**	**MY Only**
Vcmax, 25oC (umol m-2 s-1)	Chisq	90.4	0.4	76.3
	Chi.Df	16	1	8
	Pr(>Chisq)	0	0.521	0
Ln(Jmax, 25oC (umol m-2 s-1))	Chisq	17.8	2.1	2.1
	Chi.Df	13	1	7
	Pr(>Chisq)	0.165	0.145	0.951
Ln(CO2 compensation point (ppm))	Chisq	125.1	0.3	110.3
	Chi.Df	16	1	8
	Pr(>Chisq)	0	0.556	0
Amax (umol m-2 s-1)	Chisq	72.8	1.7	63.4
	Chi.Df	17	1	8
	Pr(>Chisq)	0	0.191	0
Quantum efficiency (umol CO2 umol-1 photons)	Chisq	62.4	1.3	43.5
	Chi.Df	17	1	8
	Pr(>Chisq)	0	0.257	0
Ln(LCP (umol photons m-2 s-1))	Chisq	27.7	1.4	11
	Chi.Df	17	1	8
	Pr(>Chisq)	0.049	0.24	0.202
Rd (umol m-2 s-1)	Chisq	57.1	2.3	40.7
	Chi.Df	17	1	8
	Pr(>Chisq)	0	0.126	0
Ci/Ca (no units)	Chisq	72.7	1.6	57.9
	Chi.Df	17	1	8
	Pr(>Chisq)	0	0.207	0
Anet (umol m-2 s-1)	Chisq	98.3	0.9	85.9
	Chi.Df	19	1	9
	Pr(>Chisq)	0	0.337	0
Ln(Transpiration (mmol m-2 s-1))	Chisq	158.2	0.2	150.9
	Chi.Df	19	1	9
	Pr(>Chisq)	0	0.686	0
Ln(gs (mol H2O m-2 s-1))	Chisq	137.6	1.3	127.8
	Chi.Df	19	1	9
	Pr(>Chisq)	0	0.245	0

Table 3-5 (con't)

Parameter	**Statistic**	**Full**	**ML Only**	**MY Only**
iWUE (umol CO2 mol-1 H2O)	Chisq	72	0.2	53.9
	Chi.Df	19	1	9
	Pr(>Chisq)	0	0.686	0
LMA	Chisq	37.6	7	16.6
	Chi.Df	9	1	4
	Pr(>Chisq)	0	0.008	0.002

Table 3-6: Variance of random effects variables used in the linear mixed effects full interactive model for each photosynthetic parameter.

	Variance		
Parameter	**Tree**	**Plot**	**Residual**
Vcmax at 25ºC	17	0	146
Ln(Jmax at 25ºC)	0	0	0.03
Ln(CO2comp)	0.004	0	0.04
Amax	1	0	9.7
φ	2.00E-06	5.00E-06	0.0001
Ln(LCP)	0	0	0.14
Rd	0.008	0	0.076
Ci/Ca	0.002	0	0.008
Photo	1.1	0	9.7
Ln(Trmmol)	0.05	0	0.38
Ln(Cond)	0.07	0	0.44
iWUE	106	0	644

TABLE 3-7: Linear mixed effects model regression coefficients for full interaction model of the effects of metal load and measurement month and year on photosynthesis parameters. Standard errors shown in parentheses. Coefficients were included in the model if their 95% confidence interval did not include zero. Coefficients in italics had confidence intervals which included zero however are included because a related higher level term did. Month/year groups with no significant coefficients were excluded from table.

Param.	(Int.)	HML	Jun. 2014	Jul. 2014	Aug. 2014	Sep. 2014	May. 2015	Jun. 2015	Jul. 2015	Aug. 2015	Sep. 2015	HML Jul. 2014	HML Aug. 2014	HML Sep. 2014	HML May 2015	HML Jun. 2015	HML Jul. 2015
V_{cmax}	51.8 (4)	8.9 (5.7)		12.3 (5.4)		-8.1 (5.5)	21.6 (6.4)		-23.9 (8.2)	-26.5 (6)		-19.9 (7.6)		-12.6 (7.7)	-19.1 (8.4)		
$Ln(J_{max})$	4.55 (0.08)	0.23 (0.1)		0.25 (0.11)	0.29 (0.13)		0.14 (0.12)	0.14 (0.11)	NA			-0.5 (0.14)	-0.39 (0.16)	NA	-0.32 (0.15)	-0.32 (0.14)	
$Ln(\Gamma_{comp})$	4 (0.06)				0.21 (0.09)	0.21 (0.09)	0.31 (0.1)	0.57 (0.09)	0.91 (0.13)	0.52 (0.1)							
A_{max}	8.4 (1)				-3.5 (1.5)	-3.8 (1.4)			-6.6 (1.9)	-4.3 (1.5)							
φ	0.062 (0.004)	0.009 (0.005)		0.007 (0.005)	0.016 (0.005)	0.01 (0.005)	-0.001 (0.005)					-0.023 (0.006)	-0.018 (0.006)	-0.019 (0.006)	-0.014 (0.006)		
$Ln(I_{comp})$	2.96 (0.12)	-0.22 (0.17)	-0.35 (0.17)			-0.57 (0.17)								0.57 (0.24)			
R_{dark}	1.16 (0.09)					-0.41 (0.12)			-0.58 (0.17)	-0.37 (0.13)							
C_i/C_a	0.68 (0.03)			-0.08 (0.04)	-0.14 (0.04)	-0.21 (0.04)			-0.16 (0.06)								
A_{net}	8.88 (1.04)				-3.91 (1.41)	-4 (1.41)			-7.12 (1.45)	-4.36 (1.41)	-4.29 (1.42)						
Ln(E)	0.41 (0.21)					-0.68 (0.28)			-2.49 (0.3)	-0.98 (0.28)	-0.93 (0.28)						
$Ln(g_s)$	-2.13 (0.22)				-1.03 (0.3)	-1.17 (0.3)			-2.46 (0.33)	-1.12 (0.3)	-0.89 (0.3)						
iWUE	68.6 (8.6)	5.1 (12.2)			36.3 (11.5)	54.1 (11.5)	25.4 (11.5)		67.5 (13.4)								-41.4 (18.1)

Table 3-8: Monthly mean temperature and total precipitation at Jersey City in 2014 and 2015 with statewide monthly averages for comparison.

	Mean Temperature (ºC)			**Total Precipitation (cm)**		
Month	**2014**	**2015**	**State Average**	**2014**	**2015**	**State Average**
May	17	18	16	9.9	3.4	9.3
Jun	21	21	21	11.4	15.9	9.7
Jul	23	25	24	17.4	4.7	11.4
Aug	22	25	23	5.4	4.3	11.8
Sep	20	22	19	3.6	6.0	9.6
Oct	16	15	13	3.8	5.5	9.1

Table 3-9: Model parameters for linear and polynomial regression of weather variables and photosynthetic parameters. Note that only regressions with significant x or x^2 coefficients ($p < 0.05$) are included. Sqrt = square root transformation, rcp = reciprocal transformation, se = standard error

Parameter	Weather	Intercept (se)	Intercept p-value	x (se)	x p-value	x^2 (se)	x^2 p-value	Adj. r^2
rcp(Γ_{comp} (ppm))	Daily Mean Temp (°C)	0.021 (0.002)	0	-0.0002 (0)	0			0.05
	Reference ET (mm/day)	0.018 (0.001)	0	-0.0011 (0.0004)	0.01	0.0001 (0)	0.01	0.03
	Precip (cm, prev 24 hr)	0.015 (0.0004)	0	0.002 (0.001)	0.04			0.02
	Precip (cm, prev 72 hr)	0.01504 (0.00042)	0	0.002 (0.001)	0.03	-0.0005 (0.0002)	0.01	0.03
sqrt(A_{max} (μmol m^{-2} s^{-1}))	Precip (cm, prev 24 hr)	2.4 (0.07)	0	3.1 (0.9)	0	-2.0 (0.7)	0	0.06
	Daily Mean Temp (°C)	0.53 (1.1)	0.62	0.25 (0.11)	0.02	-0.007 (0.003)	0.01	0.07
sqrt(A_{net} (μmol m^{-2} s^{-1}))	Precip (cm, prev 24 hr)	2.4 (0.07)	0	3.2 (0.9)	0	-2.0 (0.7)	0	0.06
	Daily Mean Temp (°C)	1.3 (1.1)	0.23	0.17 (0.1)	0.1	-0.005 (0.002)	0.04	0.04
	Reference ET (mm/day)	2.8 (0.15)	0	-0.06 (0.02)	0.02			0.02
sqrt(R_d (μmol m^{-2} s^{-1}))	Daily Mean Temp (°C)	0.22 (0.22)	0.33	0.09 (0.02)	0	-0.0023 (0.0005)	0	0.12
	Precip (cm, prev 72 hr)	0.93 (0.02)	0	0.03 (0.01)	0.01			0.04
	Reference ET (mm/day)	0.97 (0.05)	0	-0.03 (0.02)	0.13	0.003 (0.002)	0.05	0.02
sqrt(E (mmol m^{-2} s^{-1}))	Daily Mean Temp (°C)	0.25 (0.56)	0.66	0.11 (0.06)	0.05	-0.003 (0.001)	0.02	0.03
	Precip (cm, prev 24 hr)	1.1 (0.04)	0	1.4 (0.5)	0	-0.87 (0.35)	0.01	0.05
	Precip (cm, prev 72 hr)	1.1 (0.04)	0	0.22 (0.10)	0.04	-0.04 (0.02)	0.05	0.01
	Reference ET (mm/day)	1.3(0.08)	0	-0.03 (0.01)	0.02			0.03
V_{cmax} (μmol m^{-2} s^{-1})	Daily Mean Temp (°C)	4.3 (21)	0.84	5.4 (2.0)	0.01	-0.14 (0.05)	0.01	0.04

Table 3-10: Linear regression coefficients, standard error (in parentheses), and p-values ($p < 0.05$) for A-Ci curve parameters using leaf temperature (Tleaf, ^oC) and metal load (ML) as predictors. Leaf temperature data was centered to 30^oC prior to regression. LML = low metal load, HML = high metal load.

Parameter	**Intercept (LML)**	**p**	**Tleaf**	**p**	**HML**	**p**	**Tleaf x ML**	**p**	**Adj. r^2**
V_{cmax}	128.28 (7.43)	0	15.11 (2.96)	0	-14.7 (10.27)	0.16	-5.8 (3.92)	0.15	0.55
J_{max}	145.05 (4.95)	0	5.59 (1.97)	0.01	-22.81 (6.83)	0	-1.99 (2.61)	0.45	0.37
Γ_{comp}	63.11 (2.3)	0	2.73 (0.92)	0.01	-1.49 (3.17)	0.64	1.95 (1.21)	0.12	0.58
A_{net}	13.46 (0.87)	0	-0.26 (0.35)	0.45	-2 (1.2)	0.11	-0.55 (0.46)	0.24	0.23
$Ln(g_s)$	-1.95 (0.12)	0	-0.1 (0.05)	0.04	-0.24 (0.16)	0.16	-0.01 (0.06)	0.82	0.31
C_i	211.17 (8.92)	0	-11.43 (3.55)	0	-7.77 (12.32)	0.53	1.74 (4.7)	0.72	0.39
Ln(E)	0.76 (0.12)	0	-0.07 (0.05)	0.16	-0.19 (0.17)	0.28	0.02 (0.07)	0.78	0.08
C_i/C_a	0.71 (0.02)	0	-0.01 (0.01)	0.08	-0.02 (0.02)	0.29	0 (0.01)	0.65	0.13

Table 3-11: Means and stand deviation (in parentheses) of physico-chemical soil properties of LAI plots. Means with the same letters are not significantly different according to a Tukey HSD test ($p < 0.05$) and can be compared between plots and between years.

Plot	pH	Conductivity ($mS\ s^{-1}$)	Sand (%)	Silt (%)	Clay (%)
L1	5.45 (0.29)b	0.11 (0.01)a	78.25 (5.8)a	19.75 (5.97)a	1.8 (2)b
L2	6.09 (0.3)a	0.09 (0.02)a	80.33 (0.58)a	14.33 (0.58)ab	5 (1)a
H2	5.37 (0.13)b	0.09 (0.01)a	81.75 (3.4)a	15 (2.58)ab	3.25 (1.26)ab
H3	5.43 (0.27)b	0.08 (0.01)a	85.5 (7.05)a	10.25 (5.62)b	4 (1.15)ab

Table 3-12: Means and stand deviation (in parentheses) Melich-3 extractable macronutrients as well as total nitrogen (TN) and total carbon (TC) in soils of LAI plots. TKN = total Kjeldahl nitrogen. Means with the same letters are not significantly different according to a Tukey HSD test ($p < 0.05$) and can be compared between plots and between years.

Plot	TKN %	P (ppm)	K (ppm)	Mg (ppm)	Ca (ppm)	TN (%)	TC (%)
L1	0.25 (0.1)a	79.88 (68.91)a	57.88 (13.65)a	93.75 (37.44)b	467 (417)a	0.31 (0.27)b	11.65 (8.25)b
L2	0.23 (0.06)a	6.67 (1.15)b	48.5 (9.66)a	77.67 (50.28)ab	395 (305)a	0.43 (0.16)ab	22.01 (2.01)a
H2	0.3 (0.03)a	82 (16.7)a	76.88 (8.94)a	101.62 (21.65)b	306 (142)a	0.55 (0.33)a	24.61 (7.77)a
H3	0.18 (0.1)a	5.75 (2.72)b	61.88 (25.54)a	96.5 (65.67)b	427 (299)a	0.37 (0.12)ab	18.4 (4.96)a

Table 3-13: Means and stand deviation (in parentheses) Melich-3 extractable micronutrients as well as soil quality index (SQI) values in soils of LAI plots. Means with the same letters are not significantly different according to a Tukey HSD test ($p < 0.05$) and can be compared between plots and between years.

Plot	Zn (ppm)	Cu (ppm)	B (ppm)	Fe (ppm)	Mn (activity index)
L1	53.93 (58.55)ab	23.57 (12.67)ab	0.42 (0.18)a	376.48 (196.34)a	37.36 (12.6)bc
L2	4.03 (3.87)b	22.26 (27.69)ab	0.52 (0.16)a	451.93 (43.96)a	19.93 (3.12)a
H2	6.56 (2.09)b	5.86 (0.59)b	0.33 (0.05)a	579.5 (29.27)a	27.46 (1.7)ab
H3	110.99 (81.1)a	124.81 (115.84)a	0.41 (0.05)a	486.65 (266.01)a	55.44 (12.9)c

Table 3-14: Linear mixed effects model regression coefficients for photosynthesis parameters modeled by water content (θ_g) and metal load (ML). Standard errors shown in parentheses. Coefficients were included in the model if their 95% confidence interval did not include zero. Parameters with no significant water content effects were excluded from table. HML = high metal load, LML = low metal load. Sqrt = square root transformation

Parameter	**LML (intercept)**	**HML**	**θ_g**	**HML x θ_g**
V_{cmax} (μmol CO_2 m^{-2} s^{-1})	33.8 (23.8)	-46.9 (26.5)	75.4 (85)	223.6 (100.9)
A_{max} (μmol CO_2 m^{-2} s^{-1})	0 (2.4)	-2.5 (3.7)	29.8 (9.2)	4.2 (15.5)
R_{dark} (μmol CO_2 m^{-2} s^{-1})	0.59 (0.19)	-0.31 (0.3)	1.67 (0.76)	0.31 (1.29)
A_{net} (μmol CO_2 m^{-2} s^{-1})	1.87 (1.36)		20.74 (7.02)	
Sqrt(E [mmol H_2O m^{-2} s^{-1}])	0.41 (0.16)		2.8 (0.82)	
Sqrt(g_s [mol H_2O m^{-2} s^{-1}])	0.14 (0.05)		0.61 (0.24)	

FIGURES

Figure 3-1: Photosynthesis parameter mean values for each metal load and each measurement month. Line length represents one standard deviation about the mean. Note data from light and A-C_i curves measured in Plot L1 in July 2015 were excluded from the calculation of the mean for this month since measurements were made prior to a heat wave. HML = high metal load, LML = low metal load.

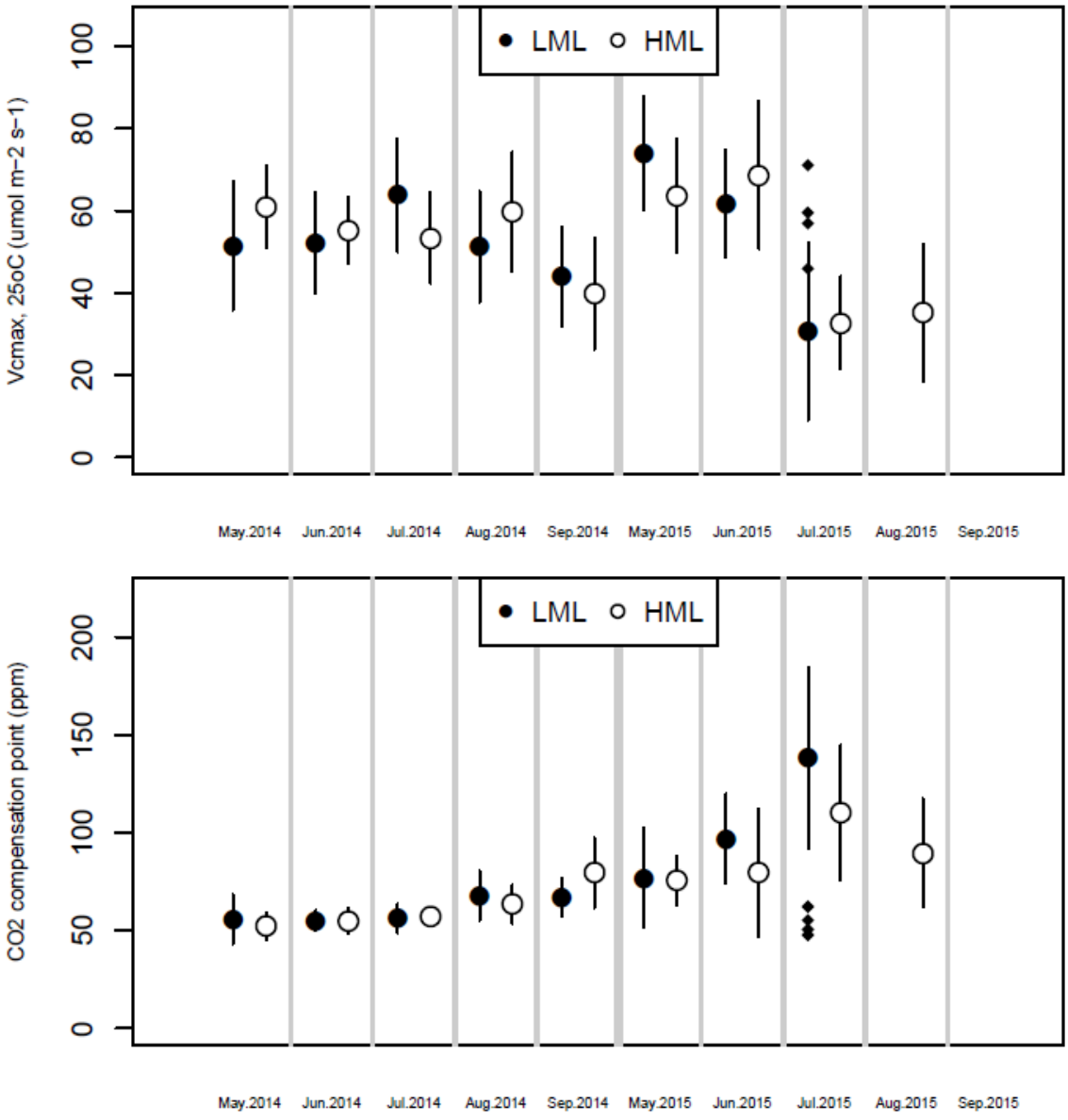

Figure 3-1 (con't)

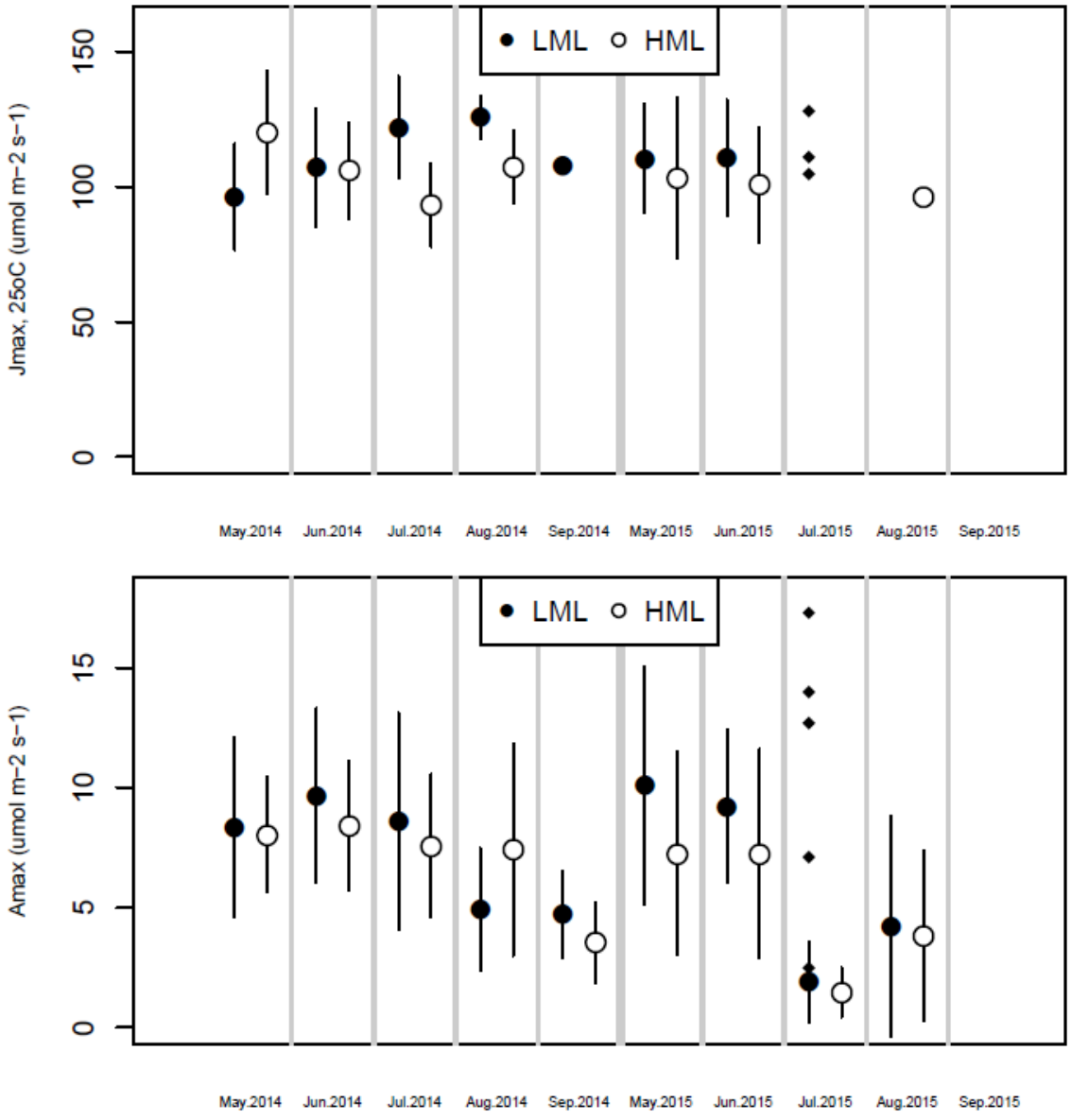

Figure 3-1 (con't)

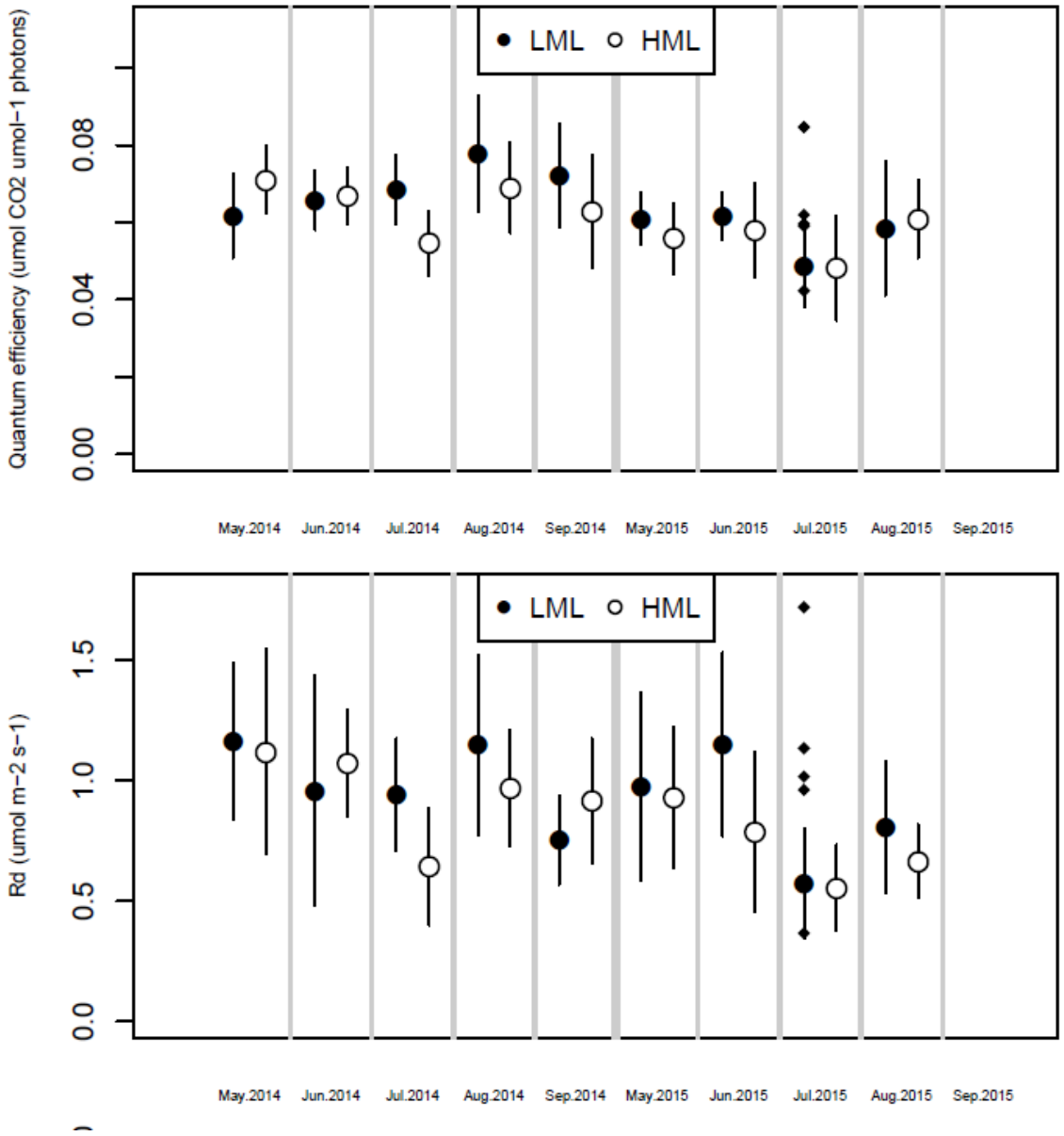

Figure 3-1 (con't)

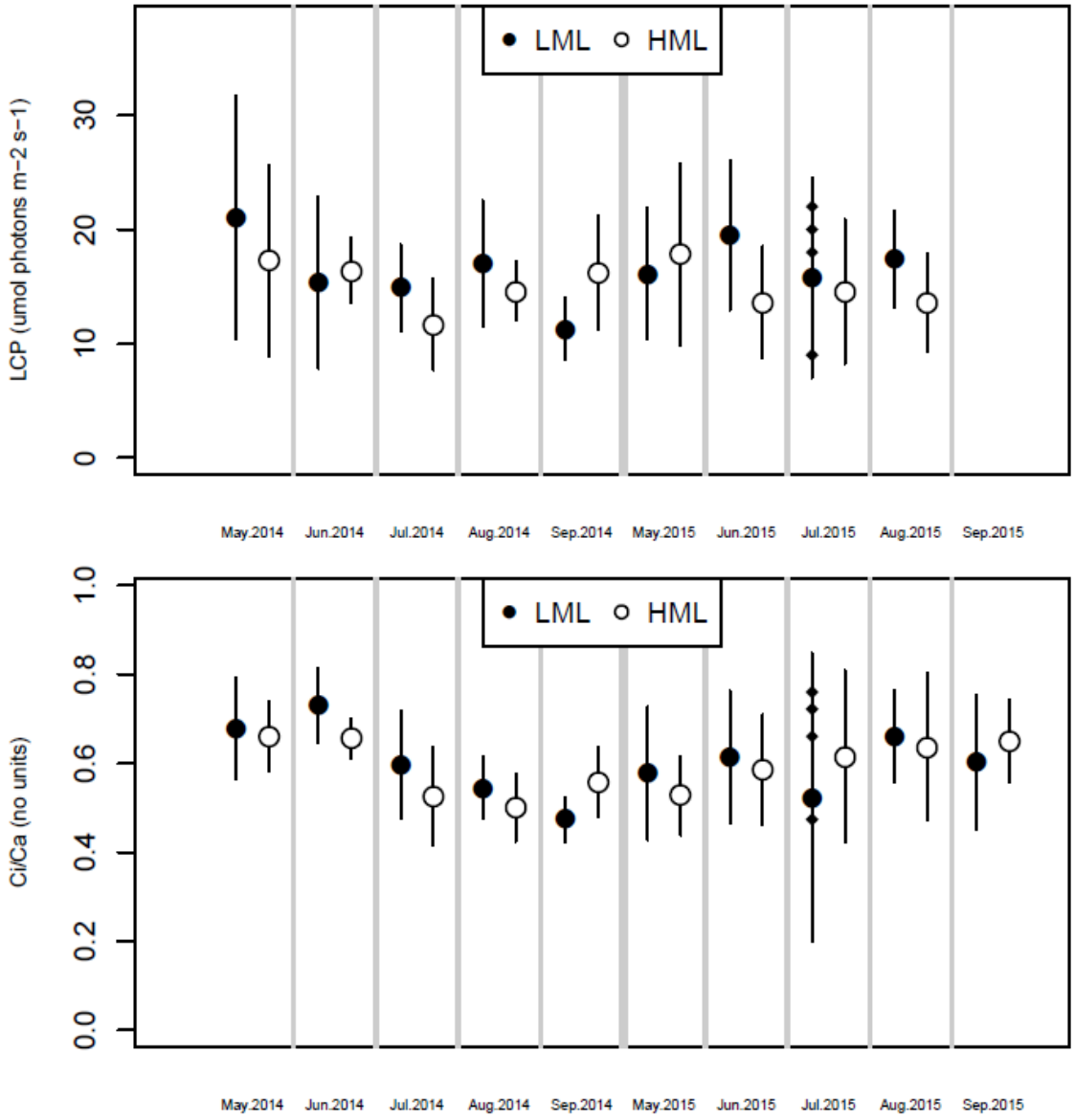

Figure 3-1 (con't)

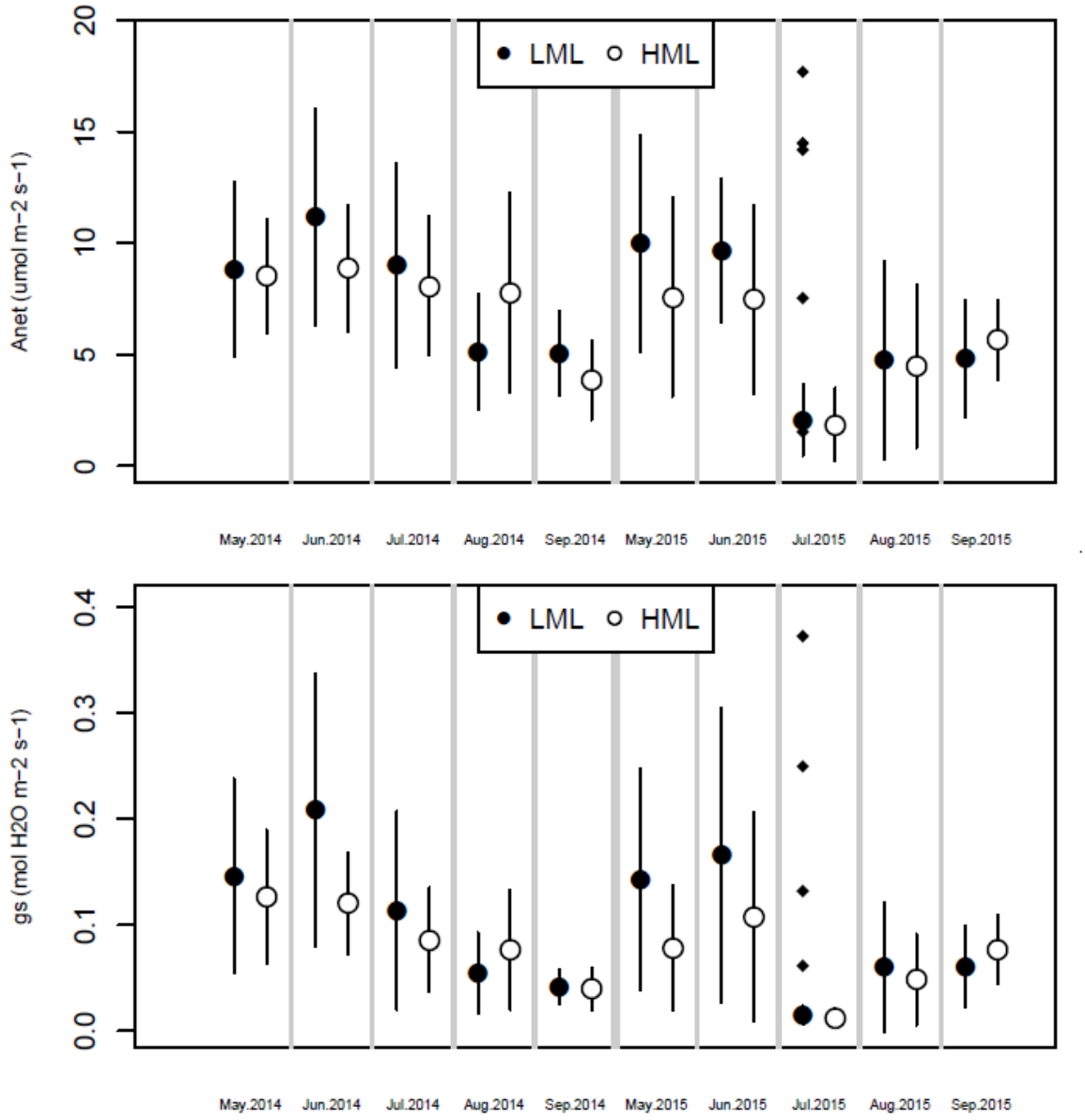

Figure 3-1 (con't)

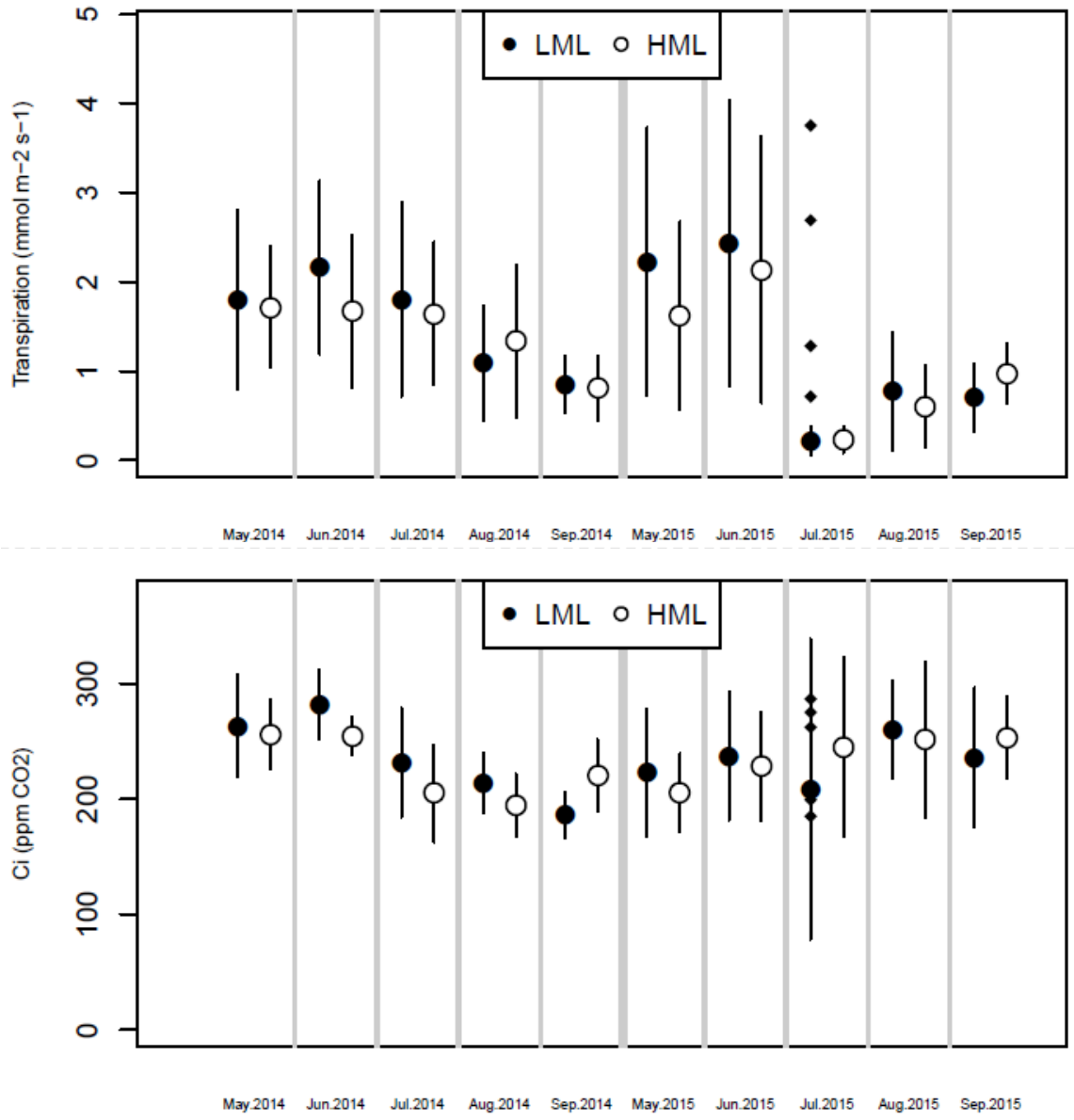

Figure 3-1 (con't)

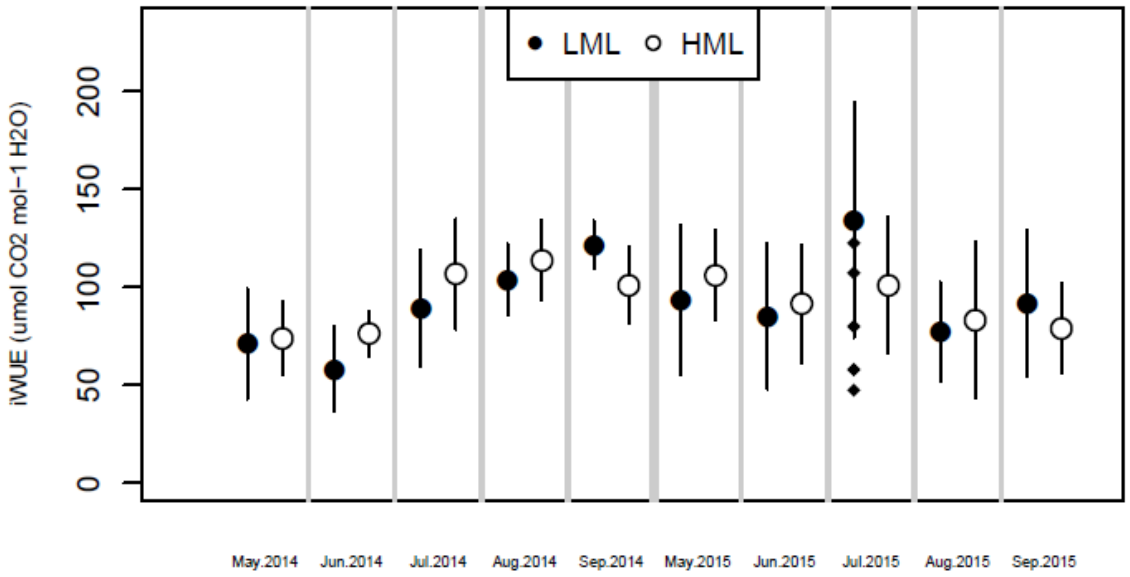

Figure 3-2: Box and whisker plots for each photosynthesis parameter split by metal load. Gray circles represent individual measurements. LML = low metal load. HML = high metal load.

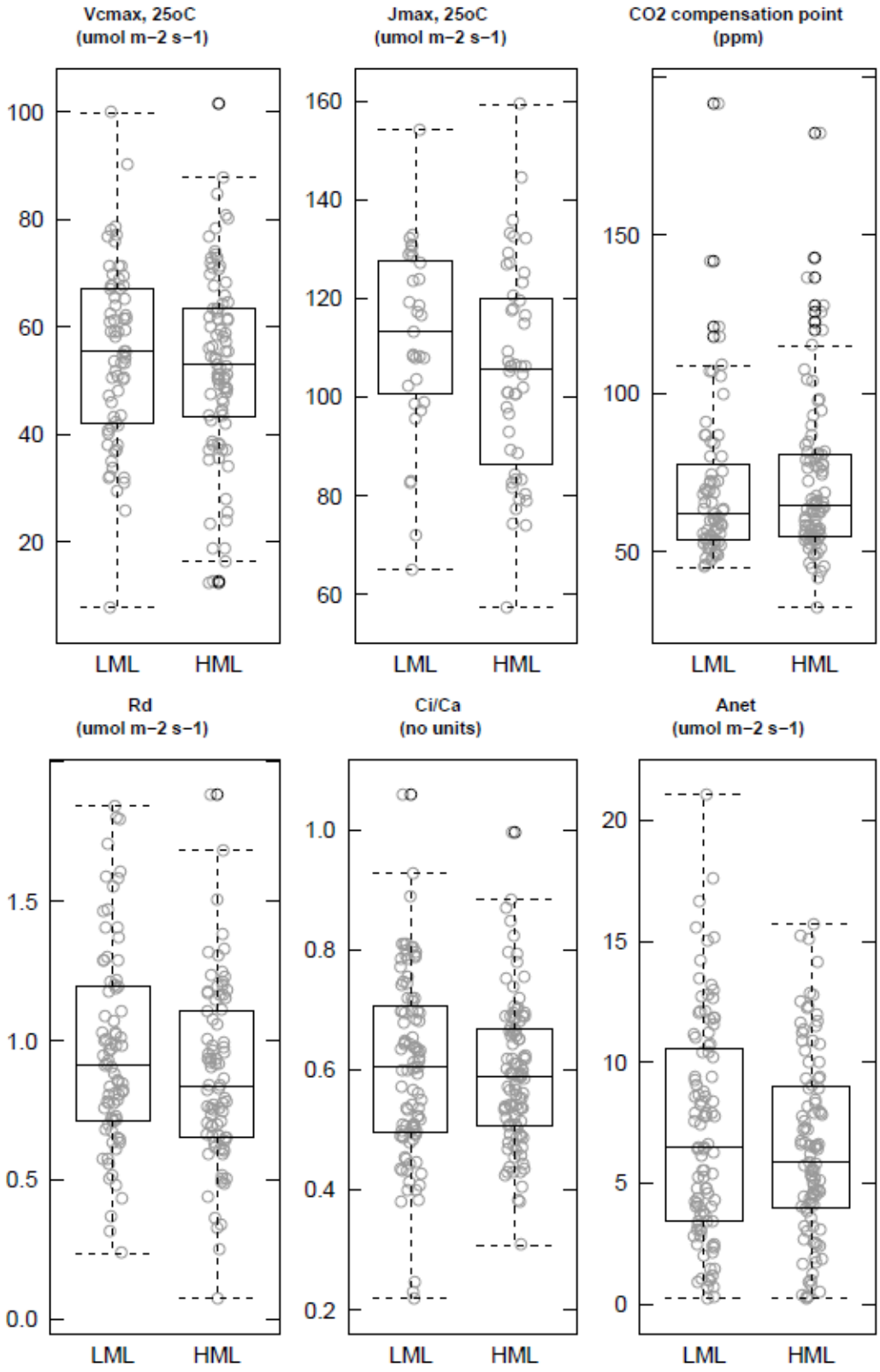

Figure 3-2 (con't)

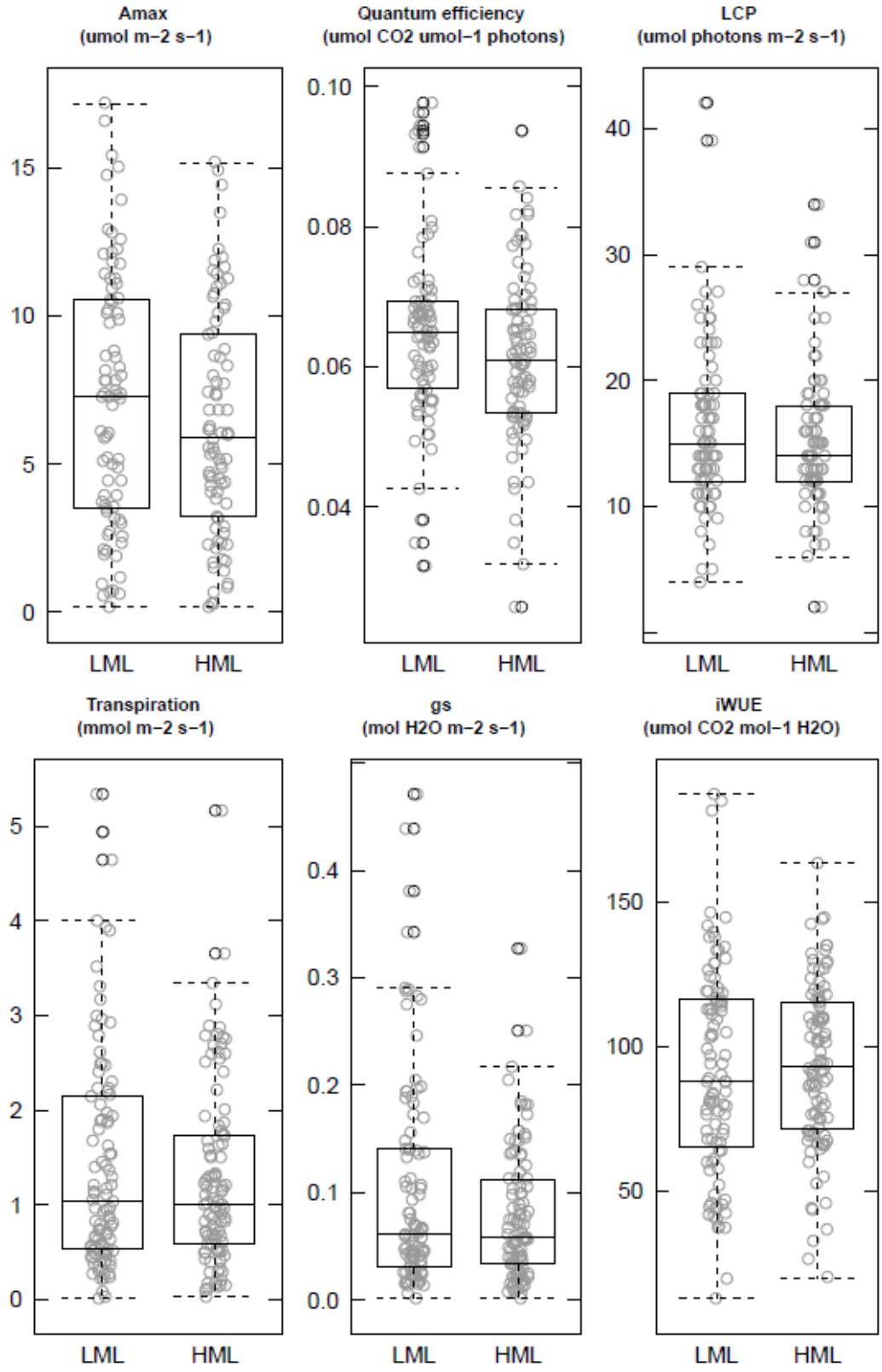

Figure 3-3: 2014 maximum and minimum daily temperatures and daily total precipitation. Data from New Jersey Weather & Climate Network (2016)

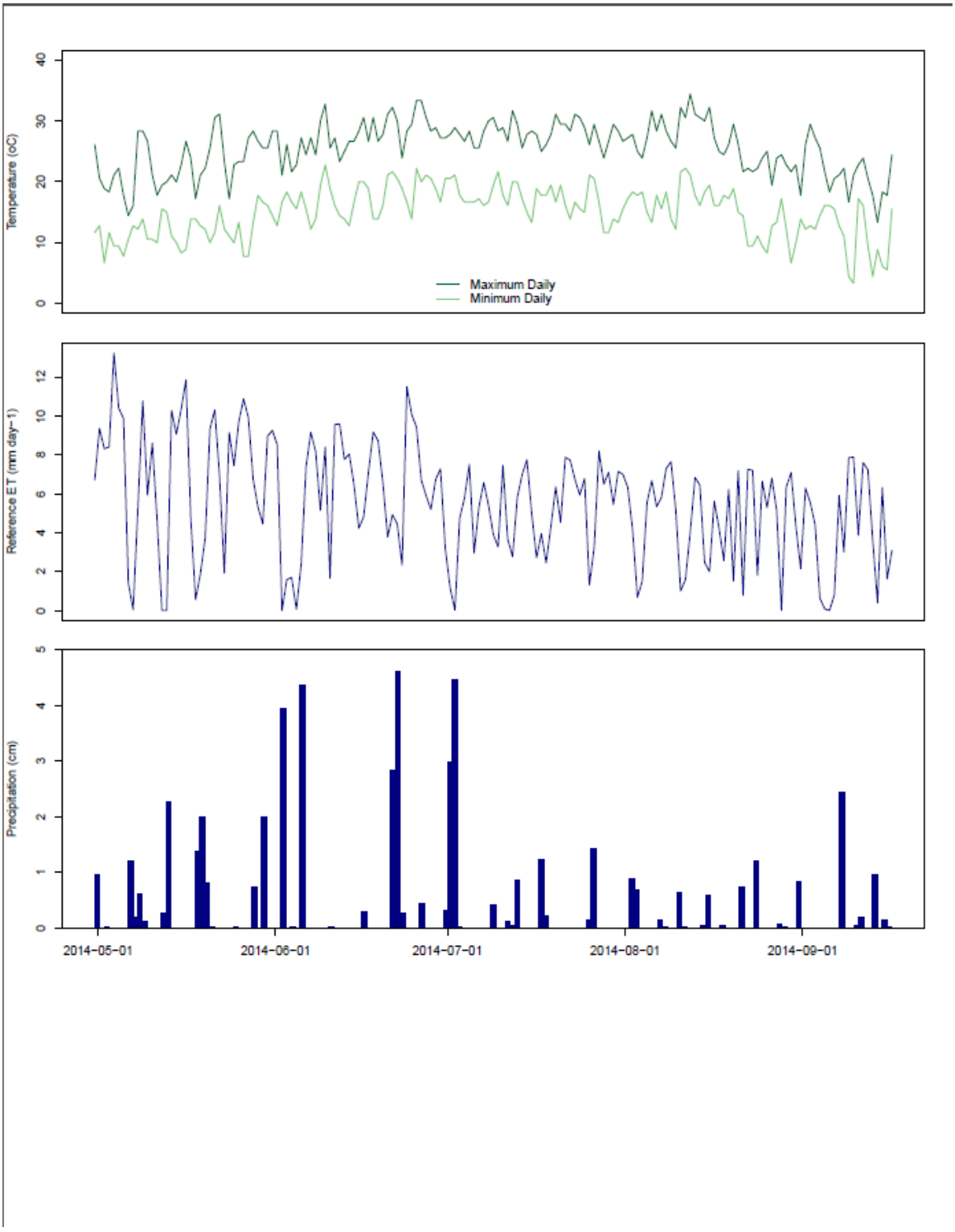

Figure 3-4: 2015 maximum and minimum daily temperatures and daily total precipitation. Data from New Jersey Weather & Climate Network (2016)

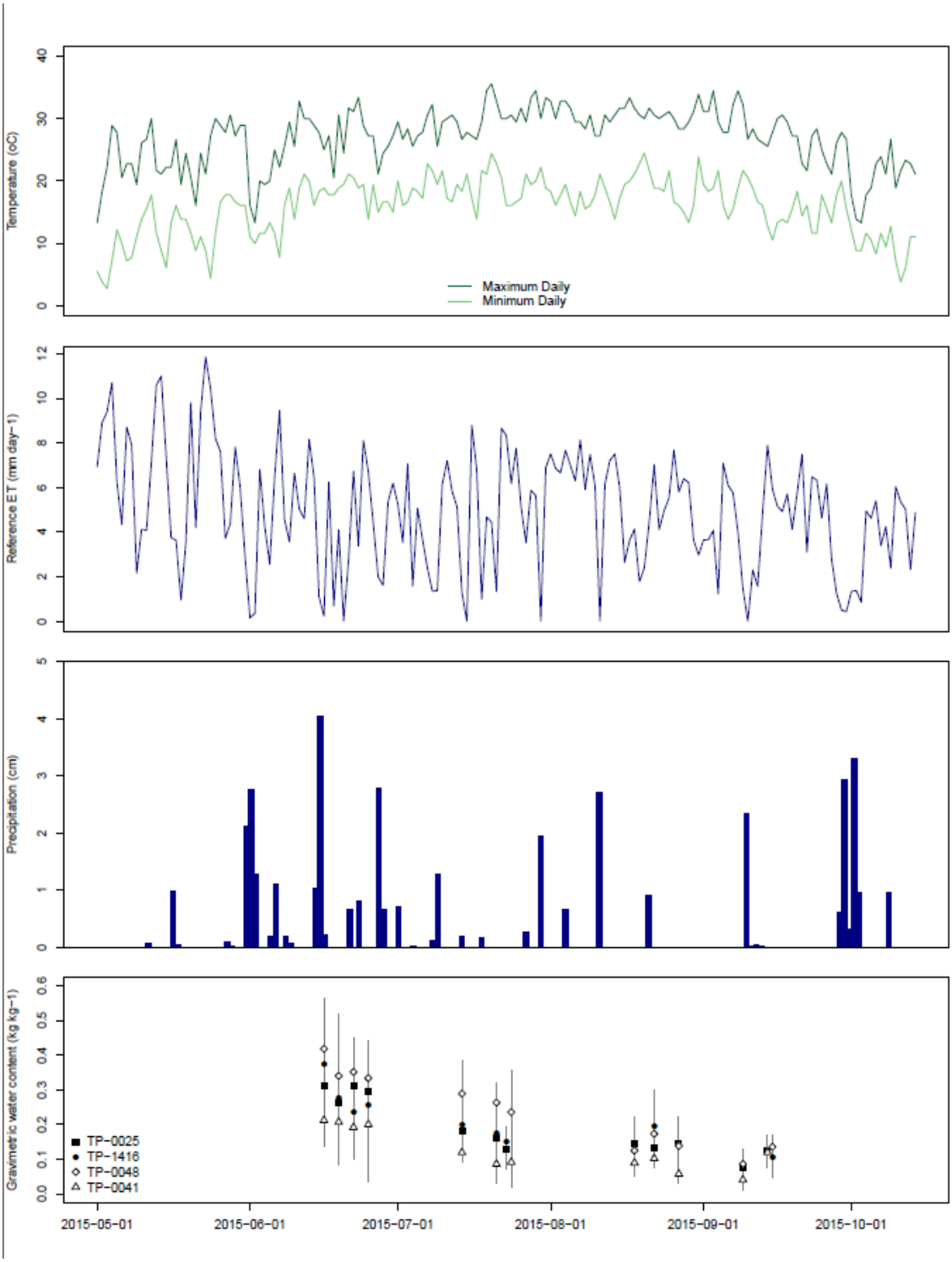

Figure 3-5: Photosynthesis parameters for Plot L1 in July 2014, and July 2015 before and after heat wave (July 20-21, 2015). Gray circles represent individual measurements.

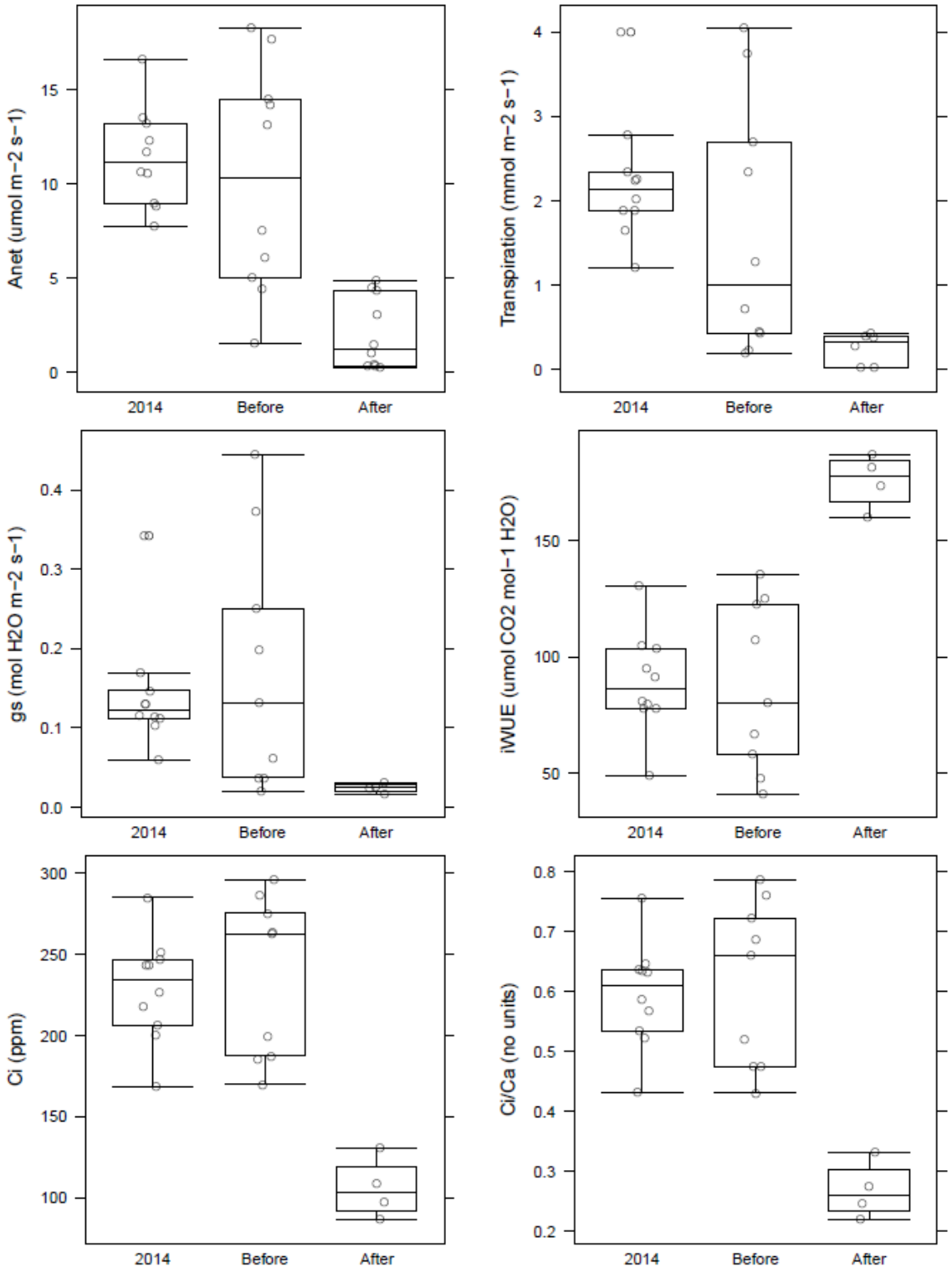

Figure 3-6: Mean net photosynthetic assimilation (A_{net}), stomatal conductance (g_s), intrinsic water use efficiency (iWUE), and transpiration (E) of low metal load (LML, closed circle) and high metal load (HML, open circle) trees in July through September. July measurements shown here were all made after the heat wave. Error bars represent one standard deviation.

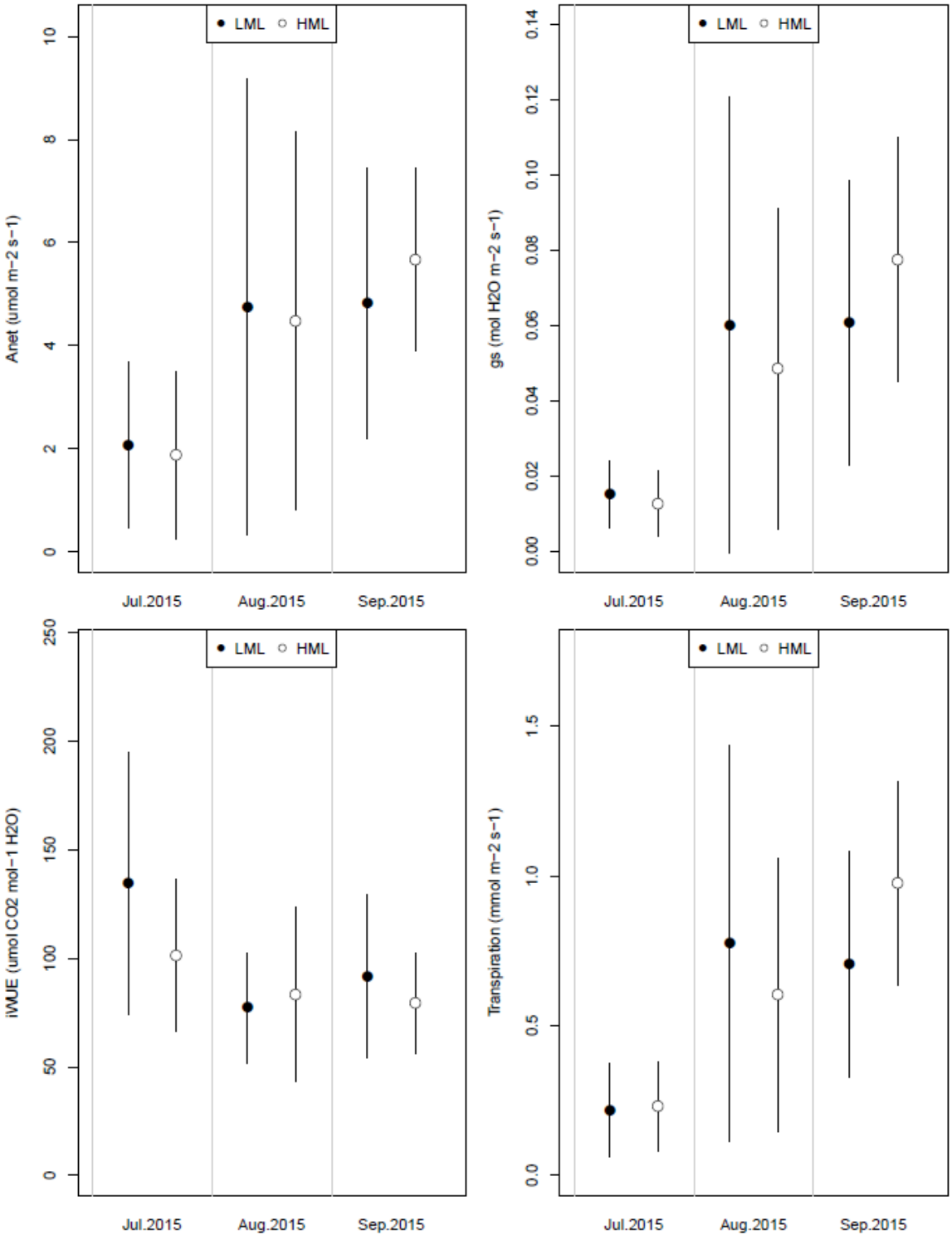

Figure 3-7: Stomatal conductance (g_s) versus C_i/C_a with an exponential rise to maximum function (Singh, et al 2011) for all data (black line) as well as high metal load (HML, red) and low metal load (LML, blue) measurements. Filled circles are measurements made in July 2015 after the heat wave while open circles are all other measurements. Curve was fitted using data where $g_s > 0.01$ mol H_2O m^{-2} s^{-1} (based on minimum C_i/C_a) for low metal load (LML), high metal load (HML), and combined data. The formula provided is based on combined data.

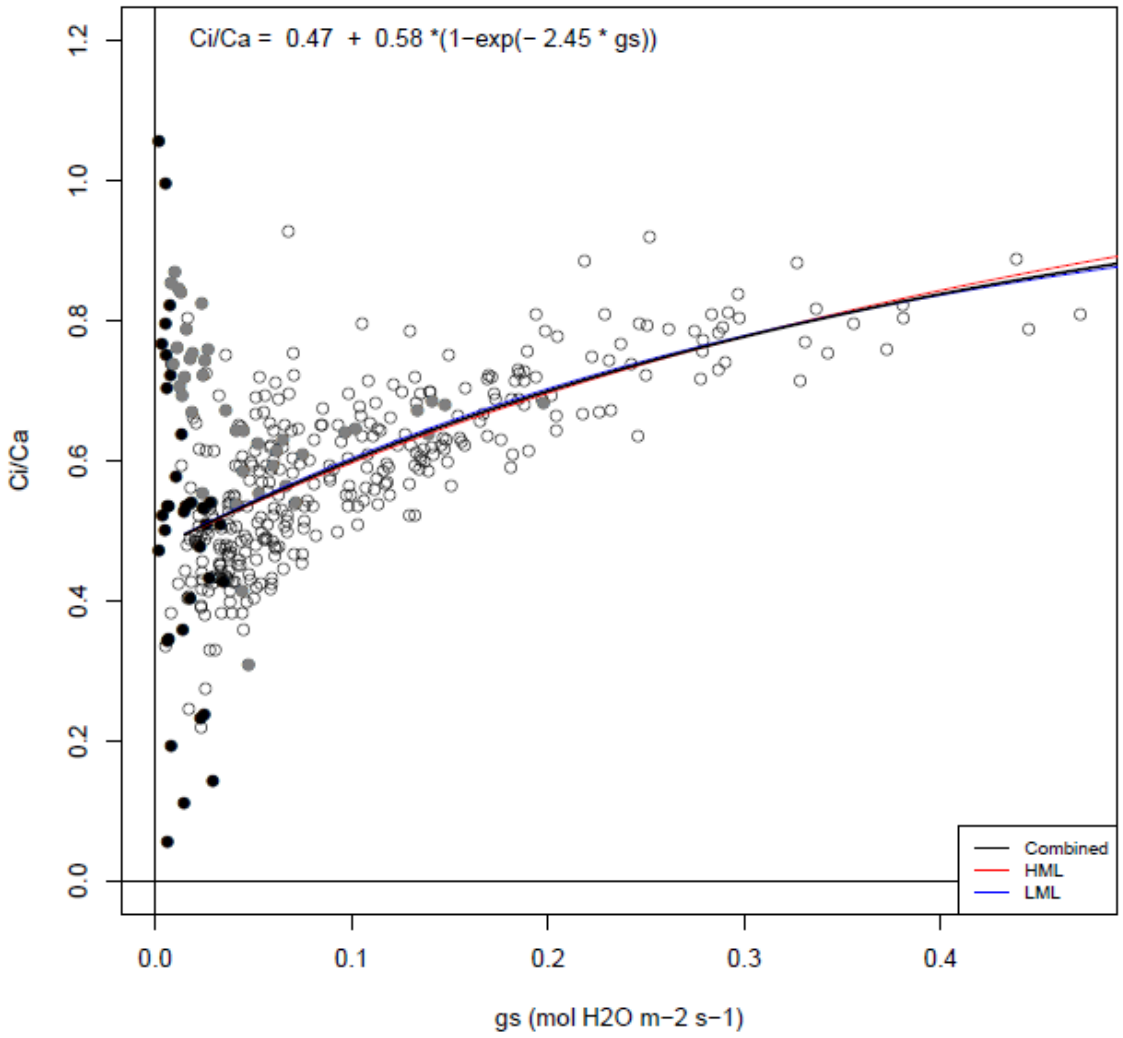

Figure 3-8: Linear and 2nd order polynomial regressions of weather variables and photosynthesis parameters. Note only pairs of variables with significant x or x^2 coefficients are shown.

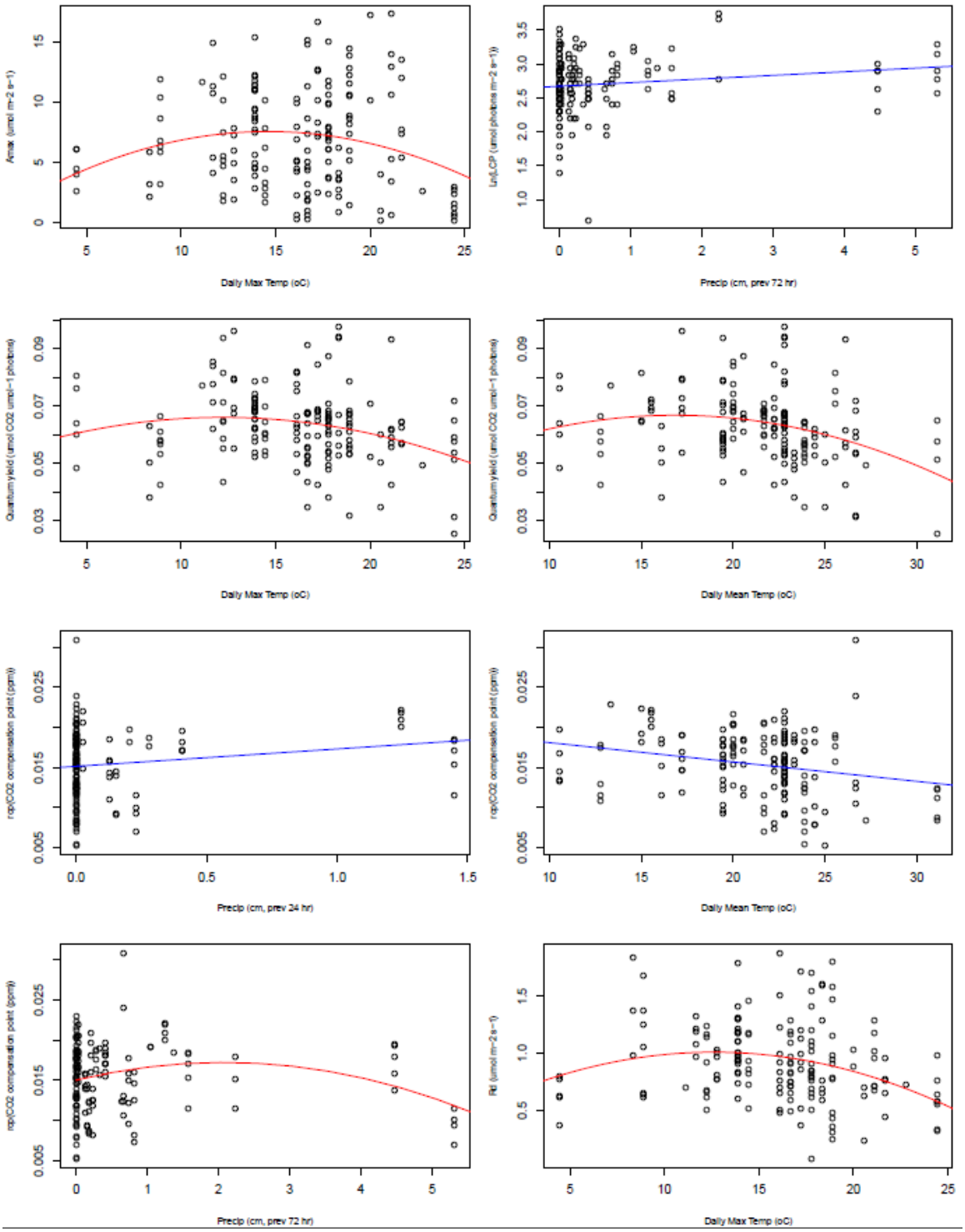

Figure 3-8 (con't)

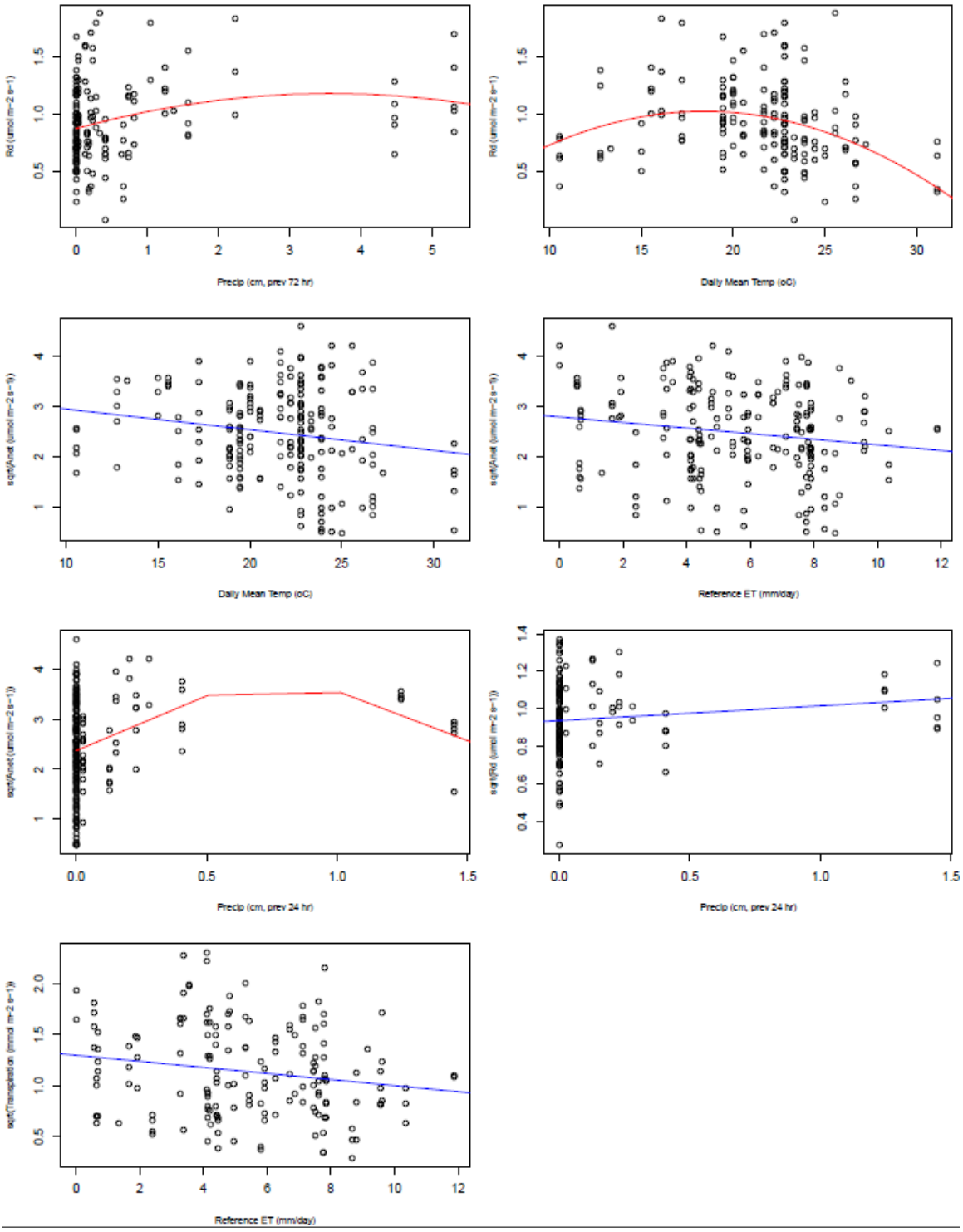

Figure 3-9: Response of A-Ci parameters to leaf temperature (ºC) based from trees in low metal load (LML) and high metal load (HML) plots.

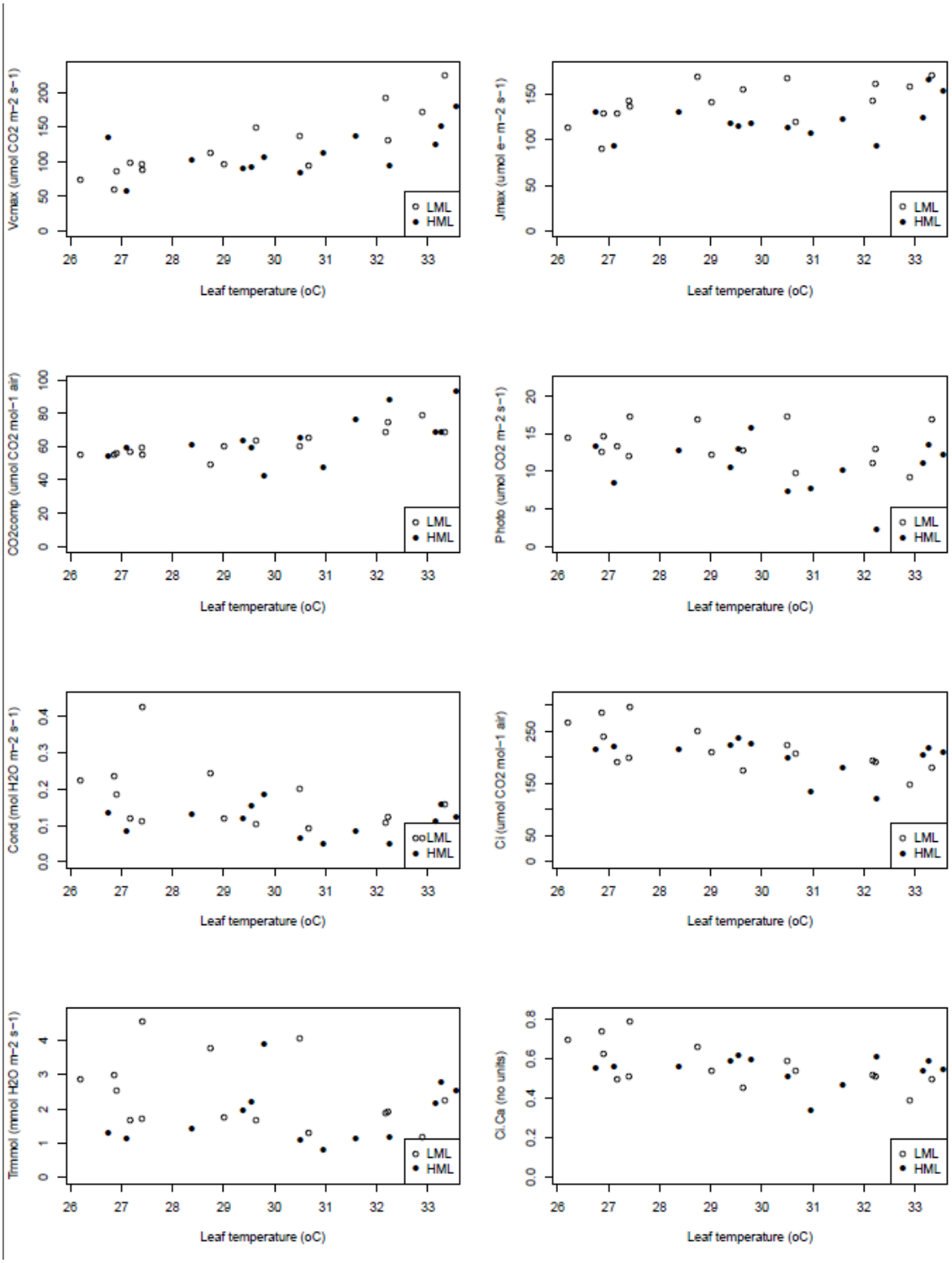

Figure 3-10: Response of photosynthesis parameters to gravimetric soil water content. TP-0041 (L1) and TP-0048 (L2) are low metal load plots. TP-1416 (H2) and TP-0025 (H3) are high metal load plots. Dashed line indicates linear regression through low metal load plots. Solid line is for high metal load plots.

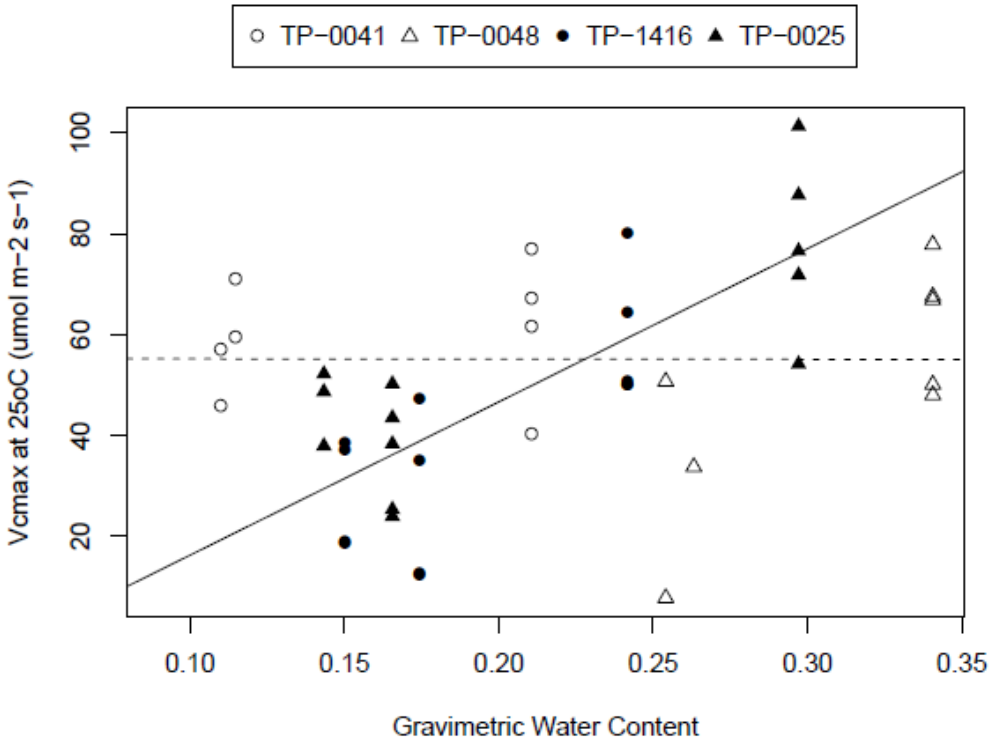

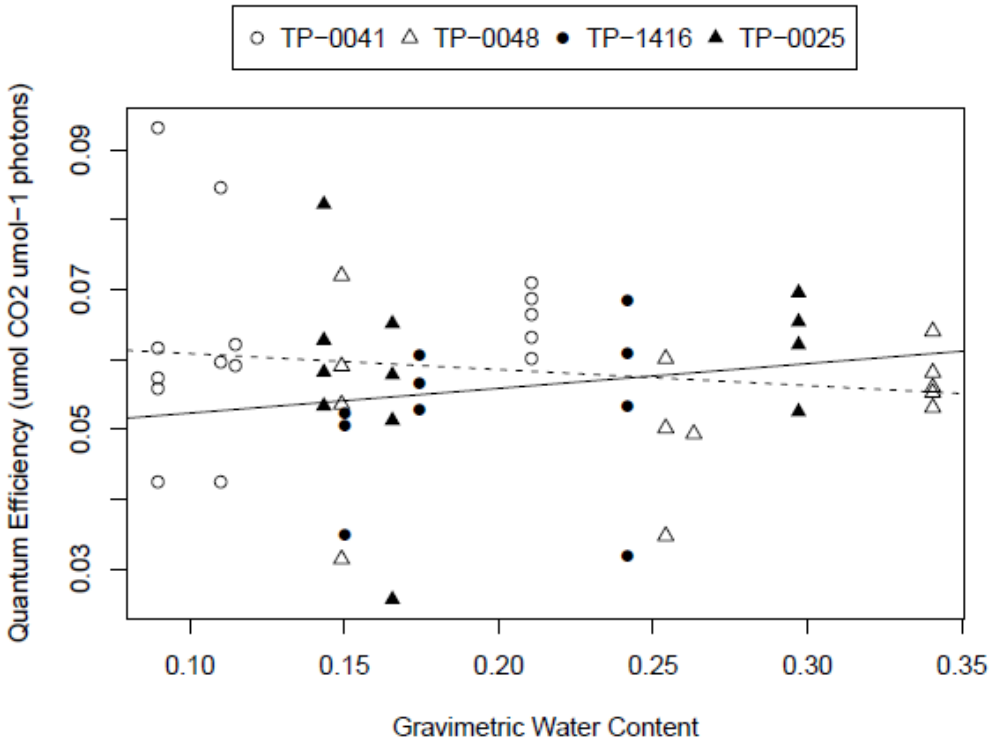

Figure 3-10 (con't)

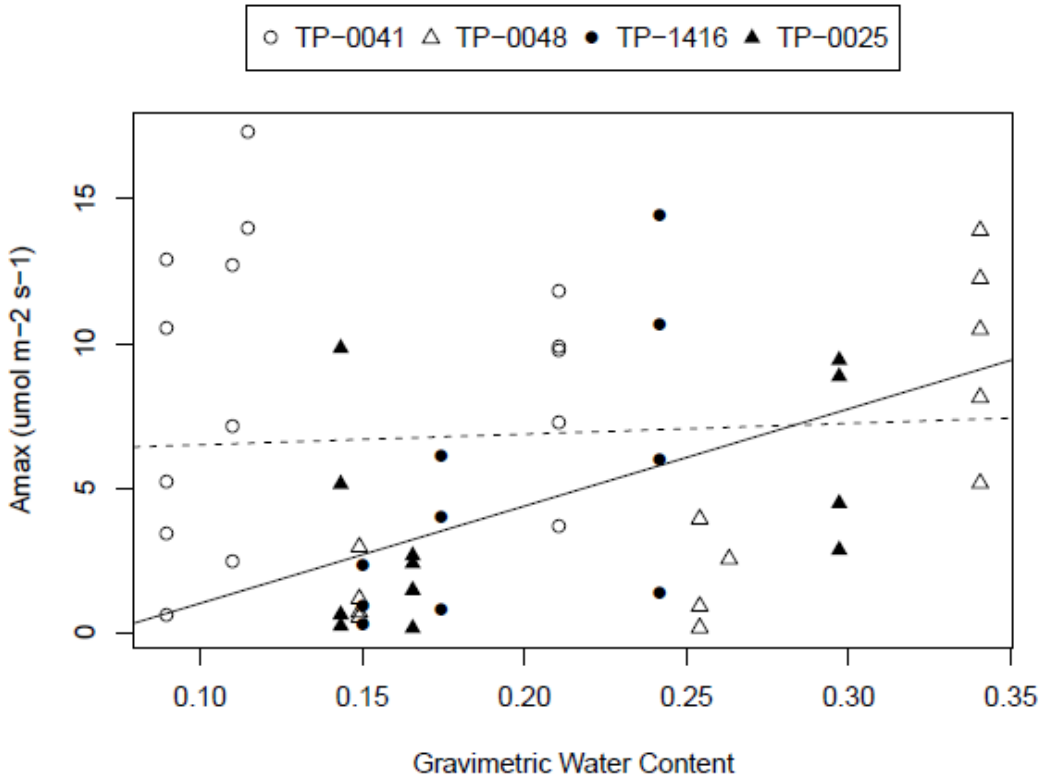

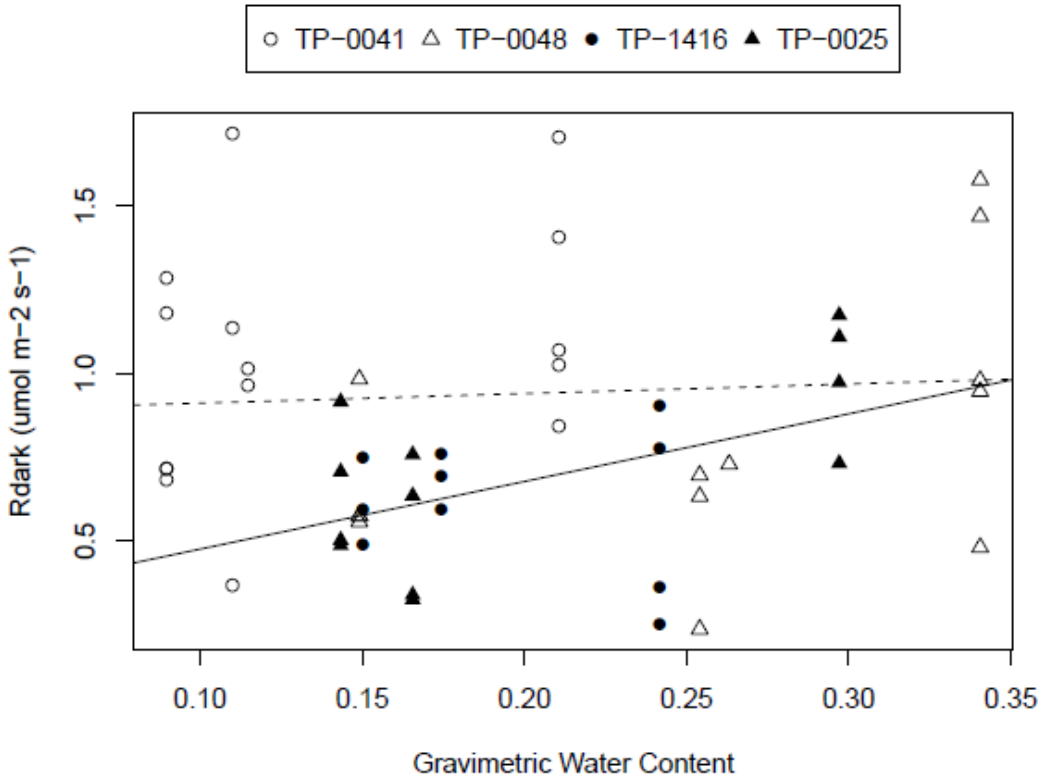

Figure 3-10 (con't)

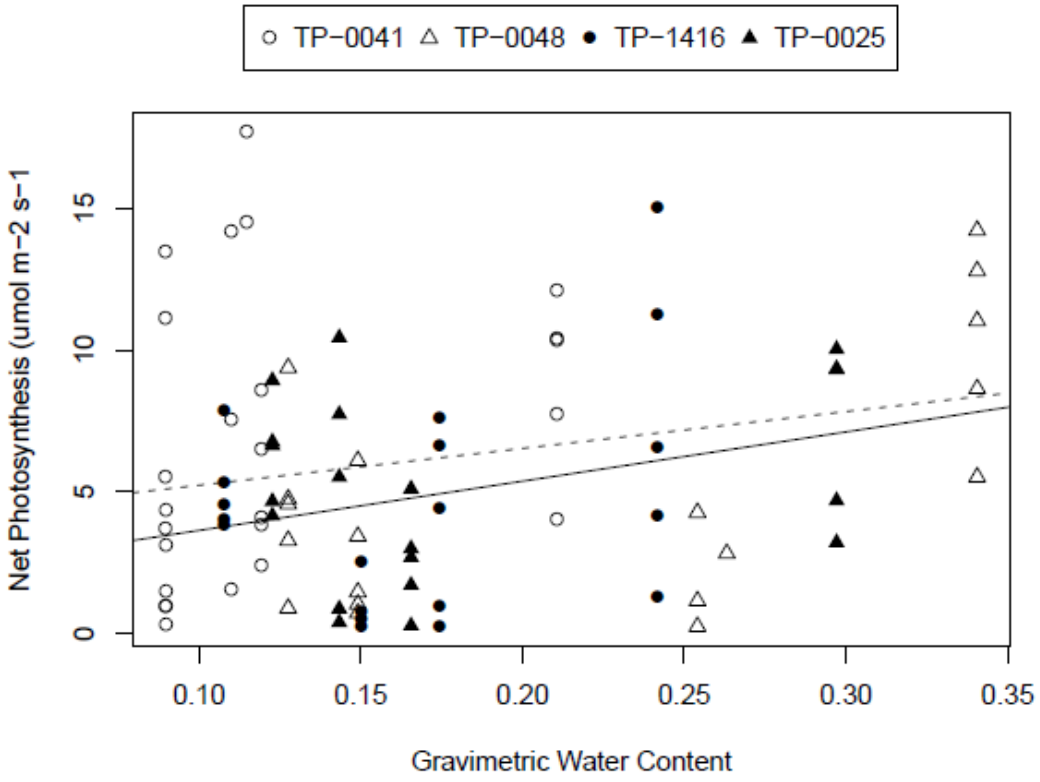

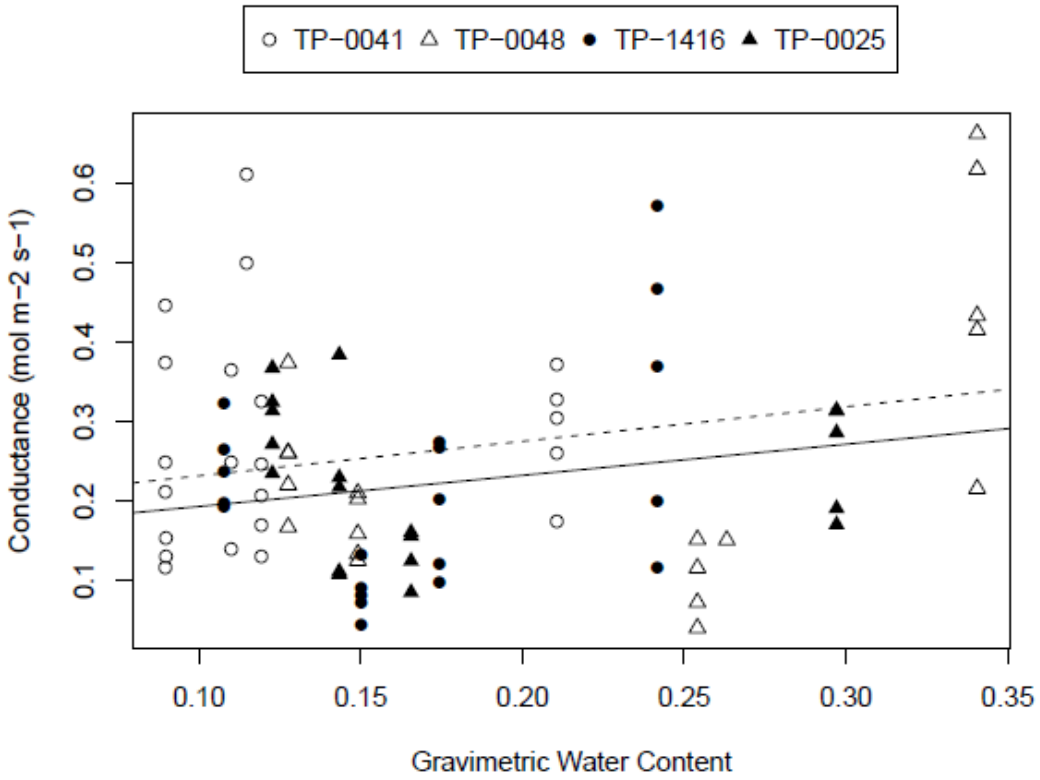

Figure 3-10 (con't)

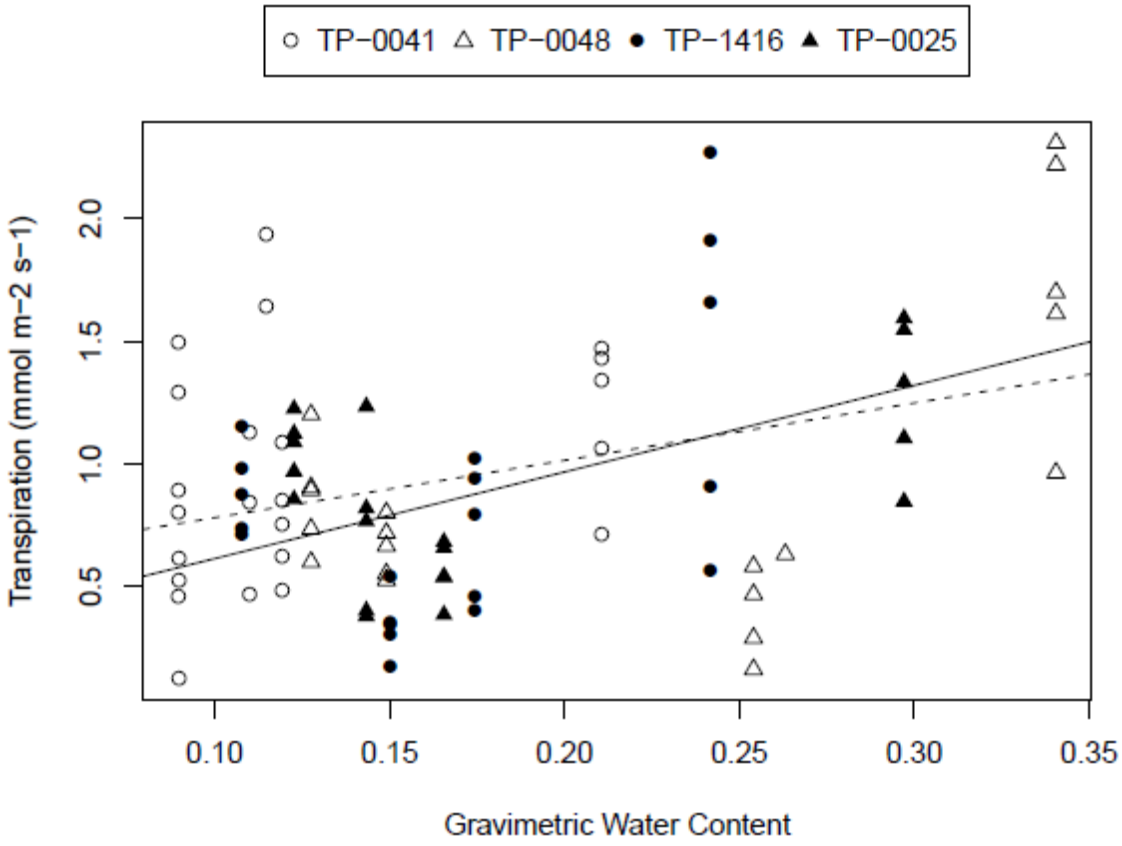

Chapter 4 - Spatial and temporal patterns of hardwood leaf area index in trace element contaminated soils

INTRODUCTION

Leaf area index (LAI) is the total one-sided area of leaf tissue per unit ground surface area which is a useful parameter for characterizing a variety of plant canopies, from cornfields to forests (Bréda 2003). It can be determined for a single plant or a group. As the plant canopy represents the primary interface between the atmosphere and the photosynthetic machinery of the plants, its characterization is a critical component of terrestrial biosphere models (Monson and Baldocchi 2014). In forestry, LAI can be used to assess both spatial and temporal changes in the canopy which may reflect forest responses to changing weather patterns or differences in soil quality (e.g. Gaydarova 2003; Strachan and McCaughey 1996).

Methods for measuring LAI fall into one of two categories: direct or indirect. Direct methods essentially involve measuring the area of individual leaves from part or all of a plant and scaling up those measurements as needed. Leaves may be collected as they fall off the tree using litterfall traps or by destructively harvesting all or part of the tree. Indirect methods estimate LAI based on the amount of light transmitted through the canopy or rely on aerial photography. Many studies have compared the accuracy of these methods (see Breda 2003 for review). Direct measurements are generally assumed to be more accurate at the expense of being labor intensive and potentially destroying the plant. The accuracy of indirect methods are dependent on how close a canopy comes to meeting assumptions used to calculate LAI and can also be sensitive to measurement conditions such as time of day. While LAI is a valuable metric for assessing canopy scale productivity, it has not been extensively used to assess the effects of pollution (but see Anda et al. 2013; Evans et al. 2015; Farrag et al. 2012).

Increased frequency of extreme weather events is one predicted consequence of climate change (Romero Lankao et al. 2014). Chambers et al. (2007) estimated that Hurricane Katrina caused the mortality of or structural damage to over 320 million large trees resulting in a loss of 105 ± 10 Tg C. It is unclear how disturbances caused by extreme weather patterns may interact with abiotic stress from soil pollution to affect forest structure and function, both in the short and long term. LAI has been extensively used to assess storm damage to forests using both on the ground measurements and aerial imagery. For example, Harrington et al. (1997) found that reductions of LAI in a Hawaiian *Acacia koa* forest correlated with pre-hurricane LAI and canopy height. Landscape position and forest composition were important predictors of ice damage in a forest in the northeastern US (Millward and Kraft 2004; Stueve et al. 2007).

Using data collected from hardwood study plots in Liberty State Park from 2010 to 2016, I tested three hypotheses: 1) total metal load will be the primary driver of hardwood canopy leaf area index; 2) soil nutrient availability will also be an important predictor of leaf area index; and 3) after damage caused by the Hurricane Sandy storm surge, the LAI of low metal load plots will recover to pre-hurricane values faster.

BACKGROUND

Hurricane Sandy affected the eastern seaboard of the US from October 22 to 29, 2012. While only effectively a post-tropical cyclone when it made landfall in New Jersey, Sandy was particularly devastating because of the coastal storm surge it caused (Blake et al. 2013). An analysis by FEMA Modeling Task Force (2013) as well as personal accounts indicate the majority of Liberty State Park was inundated with water from New York Harbor. Tide data from The Battery, New York (NOAA 2013) shows the surge lasted about 6-8 hours then retreated with the outgoing tide. The salinity of this portion of New York Harbor fluctuates on a daily basis as the tide mixes seawater with the outflow of the Hudson River. The salinity of the surge water

most likely ranged between 20 and 22 ppt (NYHOPS 2012). Tide data shows this is the only occurrence of an ocean surge at Liberty State Park between 1995 and 2015. According to a FEMA model (FEMA Modeling Task Force 2013) out of the six plots used in this study, Hurricane Sandy flooding was deepest in plot L2 (1.5 m) and shallowest in plot L3 (0.2 m) (Table 4-1).

METHODS

Leaf Area Index

This study focuses on four early successional northern hardwood plots in the LSP interior which range in total metal load index (TML, see Chapter 1 for explanation) from 0.85 to 4.31 (Table 4-1). LAI measurements were made during the growing seasons of 2010-2013, 2015-2016 though the measurement dates do not line up from year to year (Figure 4-1). Within each plot, a transect has been maintained over the course of the entire study period to ensure measurements are made in the same place every time samples are collected. LAI was measured using a LICOR LI-2000 (2010) and LI-2200 (2011-2016) Plant Canopy Analyzer. To minimize the effects of light scattering by leaves, measurements were made before 8:00 am while the sun was low in the horizon or when the sky was uniformly overcast. From 2010 to 2013, measurements were made using a single wand to first collect an above canopy measurement in an open field followed by five below canopy readings then a final above. In 2015 and 2016 a two wand system was implemented by leaving one wand in an open field to take above measurements automatically at regular intervals while a second wand was used to make below measurements. Four to five measurements were made at the same locations within each plot and data from these points were combined to calculate a single LAI value for each plot on a particular day. Additionally in 2015 a single set of measurements were made in plots L1 and H3 (similar plant community composition)

on July 16 & 17 to provide additional LAI data to complement a set of soil data analyzed for its nutrient composition (details in subsequent section).

Technically, the Plant Canopy Analyzer measures plant area index (PAI) since it cannot differentiate between the effects of foliage and woody biomass on light interception, though estimates have suggested branches account for less than 10% of light interception in the canopy (Kucharik et al. 1998). While there are many approaches to determining LAI from PAI (see Bréda (2003) for review), the additional data required for these calculations are not available for the LSP LAI data set so no corrections were made. However for the purposes of this paper, the Plant Canopy Analyzer output will be referred to as LAI to be more consistent with conventions in the literature.

The Plant Canopy Analyzer determines LAI indirectly using a gap fraction method. The tool measures light transmittance in an open field and under the forest canopy at five different zenith angles then calculates the probability of non-interception at each angle, P(θ) (the fraction of light reaching the ground). LAI is then calculated from a solution to the Beer-Lambert Law:

$$L = 2\sum_{i=1}^{5} \overline{K}_i W_i \qquad (1)$$

$$\overline{K}_i = \frac{1}{N_{obs}} \sum_{j=1}^{N_{obs}} \frac{-\ln\left(\frac{B_{ij}}{A_{ij}}\right)}{S_i} \qquad (2)$$

$$W_i = \sin\theta_i d\theta_i \qquad (3)$$

Where L is Leaf Area Index (LAI), K is the contact number, B_{ij} is the below canopy transmittance reading for zenith angle *i* and observation *j*, A_{ij} is the above canopy transmittance reading, S_i is the path length of zenith angle *i* (m, a function of canopy height and zenith angle), W_i is the weighting factor for angle *i*, and θ is zenith angle (LI-COR Biosciences 2013). These calculations

depend on two assumptions about the forest canopy. First, the foliage are very small compared to the overall canopy and second, the foliage is randomly distributed through the canopy (Bréda 2003). To address the first assumption, the analyzer was always held sufficiently far away from the foliage (recommended distance is at least four times the width of the nearest leaf). While foliage is never truly randomly distributed in a canopy, the randomness assumption is more problematic in crop and conifer canopies.

Soil nutrients

A total of 21 soil samples were collected from the six study plots in the fall of 2015 from the top 15 cm of soil (excluding intact leaf litter). The samples were analyzed for pH, soil texture, electrical conductivity, macro and micronutrients by the NJAES Soil Testing Lab. A separate set of soil samples from these plots were analyzed for total carbon (TC) and total nitrogen (TN). Details of these analyses are provided in Chapter 3.

Stand Age Estimation

Historic aerial photography used in Gallagher et al. (2011) to assess temporal trends in guild trajectory were used to estimate the relative ages of the hardwood forest plots used in this study. Community guild distribution maps made for 1969, 1976, 1984, 1993, 1996, 2000, 2003, 2009, and 2015 and GPS coordinates for each plot were combined in ArcMap 10 to determine the dominant guild of each plot in a given year. For situations where the plot appeared to be close to the boundary of two guilds, both guilds were recorded to represent the plot as in transition during that time period.

Weather Data

An analysis of the relationship between meteorological variables and LAI was made using temperature, precipitation, and relative humidity measurements from a weather station at Liberty Science Center, Jersey City, NJ (Station #3411) from 2010 to 2016. These measurements were used to calculate reference evapotranspiration (ETo) rates for each day following the FAO approach based on the Penman Monteith Equation and assuming a hypothetical reference crop with a height of 0.12 m, fixed surface resistance of 70 s m^{-1} and an albedo of 0.23 (Allen et al. 1998) (see Chapter 3 for full equations)**.** To account for lag effects that may influence canopy development, weather variables were averaged over 1 to 4 weeks prior to the LAI measurement date.

A series of drought indices calculated for northern New Jersey by the National Climatic Data Center (2017) were also used in the analysis. The indices included the Palmer Drought Severity Index (PDSI, reflects the duration and intensity of long-term drought), Palmer Hydrological Drought Index (PHDI, reflects impacts of drought on hydrological systems such as reservoirs), Palmer Z-index (ZNDX, measures short term drought), Modified Palmer Drought Severity Index (PMDI, based on current observations rather than historical records), and the standardized precipitation index (SPx, reflects probability of an observed precipitation event based on prior precipitation patterns analyzed for x months). The primary difference between the Palmer based and the SP indices is that the Palmer index is based on a water balance approach while the SP is purely probability based and focuses only on precipitation (Guttman 1998). To account for the lag effects of the drought indices, the analysis tested Palmer based variable calculated for the 1^{st} to 4^{th} week preceding the LAI measurement. The analysis also used SP indices calculated for 1, 2, 3, 6, 9, 12 and 24 months preceding LAI measurement.

Statistical analysis

The interacting effects of plot and measurement year were assessed using a linear model and Tukey HSD test. To better visualize changes in LAI during the summer between plots, LAI values from 2010 and 2012 were fitted using a moving average. Only 2010 and 2012 data were fitted with this method since they had the highest number of samples available. Differences in soil characteristics were compared between plots using a linear model and a Tukey HSD test. Since soil characteristic measurements were made in the Fall of 2015, these data were only compared to LAI data measured on July 16 and 17, 2015. These July data points were selected for analysis since they include extra measurements made in plots L1 and H3. Soil and LAI data were compared using a linear regression for both one soil property at a time and for pairs of soil properties. Weather and drought index parameters were compared against LAI data collected in 2010 and 2012 using a linear regression for one parameter at a time. This analysis only used the 2010 to 2012 LAI data to avoid potential confounding effects caused by Hurricane Sandy after 2012. The models reasonably fit assumptions for normality and homogeneity of variance so no transformations were needed.

RESULTS

LAI measurements made from 2010 to 2016 only partially supported the initial hypothesis that low metal load (LML) plots would have the higher LAI. Instead, from 2010 to 2012 the two LML plots (L2 and L3) tended to have similar LAI values to one of the high metal load (HML) plots (H2), ranging from around 2.5 to 3.5 (Figure 4-2, Table 4-2). Both plot and year and their interaction were significant predictors of LAI in the four study plots (F statistic = 180.5, $p < 0.001$, adjusted $r^2 = 0.82$). In 2010 a maximum LAI reading of 4.4 was made in H2, the plot with the highest metal load in the group. The second HML plot (H1) consistently had the lowest LAI in all study years which is in line with the initial hypothesis though contrarily H2

tends to have the highest LAI. Seasonal phenology of H2 appears to be slightly different from the other three plots (Figure 4-3). In 2010 H2's peak LAI occurs later and in 2012 its LAI decreased until June 06 and then increased while the other three plots' LAI mainly increased in this time period.

Most of the macro and micronutrients measured in the six study plots had greater within plot variation than between plot variation (Tables 4-3, 4-4, 4-5). Though P was one exception since it was significantly higher in L1 and H2 compared to the other for plots. H1, which consistently had the lowest LAI during the entire study, notably had the lowest mean soil pH out of all the plots based on samples collected in 2015 (Table 4-4). The Mg soil concentrations in H1 were also significantly lower than the other study plots. Though H1's exchangeable Zn and Cu are comparable to those in L2, L3, and H2 (Table 4-5). On the other hand, plot H2 with the consistently highest LAI had the highest mean P, K, and Mg (Table 4-4). H2 also had the highest mean Fe concentration, though the highest measured value in this group of soil samples was from H3 (Table 4-4). Forest stands also differed somewhat in age. Forest type cover had appeared in H2 by 1976 and in L2, L3 and H1 by 1993 (Figure 4-4).

While there were not significant between plot differences for K and B, these were the only two nutrients which showed a significant relationship with LAI in the six study plots sampled in July 2015 (Table 4-6, Figure 4-5). While the K relationship is positive, the negative relationship with B is surprising since all of the B concentrations are considered below optimum for plant nutrition. Though the slope of the Fe regression was not significant, it had the third highest r^2. When the effects of nutrient pairs were tested, the adjusted r^2 of the K regression was increased by sand, silt, electrical conductivity, exchangeable Cu and Fe while the B regression adjusted r^2 was increased with the addition of silt and sand (Table 4-7).

Several weather parameters were found to be predictors of LAI when between plot differences were accounted for by the model using 2010 to 2012 data (Table 4-8). Positive

relationships were observed between LAI and temperatures and reference ET averaged over the weeks preceding LAI measurement. Negative relationships were observed with the 12-month standardized precipitation index (SP12), though it should be noted that in the 2010 to 2012 dataset the SP12 ranged from about 0 (median conditions) to 2.5 (wetter conditions). LAI response to temperatures averaged over 7, 14, and 21 days prior, and the reference ET averaged 14 days prior was unique for H1 (Table 4-9, Figure 4-6). While LAI in L2, L3, and H2 varied positively with these parameters, LAI in H1 was not responsive to them. Only H2 had a significant negative relationship for the Z-index four weeks prior to the measurement date.

In the years following the Hurricane Sandy storm surge in October 2012, LAI values in L2, L3, and H2 were significantly lower compared to previous years (Figure 4-2, Table 4-2). However after the hurricane LAI in H1 remained effectively unchanged. Also contrary to the initial hypothesis, one of the LML plots (L2) had the greatest decrease in LAI after 2012 to the point where its LAI was equivalent to that of H1. As of 2016, none of the plots which had a significant decrease in LAI had recovered to pre-Sandy LAI levels. During the Hurricane Sandy storm surge, of the six plots L2 had the deepest floodwater while H1 had the least (Table 4-1). During this time period L3 and H2 continued to have similar values though by 2016 L3 LAI was greater, though the difference is not statistically significant.

Over half of the *B. populifolia* trees growing in L2 died between winter 2013 and winter 2016 according to a comparison of tagged trees surveyed in both years (Table 4-10). H1 had the lowest mortality rate in this time period, followed by L3 then H2 though it should be noted that many of the tags were missing in H2 so those trees were not included in calculations.

DISCUSSION

The seven year period of LAI data collected from four hardwood plots in LSP provide ambiguous results to the initial hypothesis which suggested high metal load (HML) plots should have the lowest LAI. These results were unexpected since NDVI analysis of aerial imagery showed a strong relationship between hardwood productivity and TML (Gallagher et al. 2008a). Though several authors have pointed out that NDVI may not be sensitive to higher LAI values (> 2-3) in deciduous environments (Fassnacht and Gower 1997; Gamon et al. 1995; Ludeke et al. 1991). Studies with agricultural species (maize, Brassica spp) have found exposure to TE reduces leaf area on a per plant basis (Anda et al. 2013; Farrag et al. 2012). Stress from salinity has also been associated with lower LAI in mangrove forests (Gutierrez et al. 2016).

The pattern of one HML plot having the highest LAI (H2) and the other HML having the lowest (H1) corresponds to results from Dahle et al. (2014) which found H2 had the highest standing density (stem volume per hectare) while H1 had the lowest, leaving L2 and L3 in the middle. This correlation suggests LAI in these plots more strongly reflects the number and size of trees in the stand rather than the size or number of leaves on a given tree, similar to Le Dantec et al. (2000). This interpretation is reasonable since each plot has a different stand density and consequently the contributions of LAI from entire trees (or lack thereof) overwhelms the measurement of LAI variation that may occur within a single tree. Drivers of LAI may be species specific with some responding more strongly to meteorological variables while others to stand characteristics such as stand age (Bequet et al. 2012).

The majority of weather based correlations observed in LSP LAI from 2010 to 2012 were based on temperature and reference ET, with the exception of the 12 month standardized precipitation index (SP12). This result is surprising considering other researchers have found parameters such as precipitation and soil water availability to be better predictors of LAI (Bequet et al. 2012; Le Dantec et al. 2000; Fassnacht and Gower 1997). The responses to temperature may

be reflecting the seasonal pattern in LAI rather than a direct effect of temperature on LAI. The negative relationship observed between LAI and SP12 is probably the result of the limited range of SP12 values in the study period – about 0 to 2 where 0 is median precipitation and 2 is more rainfall than average. LAI appears to be highest when annual precipitation is close to the region's median value. For some temperature variables, H1 had a unique response compared to the other three plots because while the other plots had a direct relationship with LAI and temperature H1 had effectively no relationship. This appears to stem from the smaller amplitude of change in LAI for H1 over the course of each growing season, again suggesting that temperature may be acting as a proxy for time of the year.

The connection between LAI and stand density at LSP is further supported by the loss of LAI following Hurricane Sandy and the high stand mortality in plots L2, L3, and H2. Contrary to the initial hypothesis that high metal stress would exacerbate the effects of Hurricane Sandy on LAI, three of the four plots were similarly affected while the least affected plot has a high metal load. It is difficult to pinpoint the precise causes of tree mortality in these LSP plots following Hurricane Sandy since the forest was subjected to both high winds and flooding with bay water from the storm surge. Tree death in coastal freshwater swamps in the Delmarva Peninsula also affected by a storm surge was primarily attributed to saltwater intrusion, though evidence of wind damage was apparent as well (Middleton 2016). It is possible that the storm surge of bay water exposed the trees to higher concentrations of salt than they are adapted for, though the low electrical conductivity measurements made in 2015 suggest that three years later the upper horizons of plot soils no longer had elevated salt levels. The plot which experienced the greatest decrease in LAI following the hurricane – L2 – was located both in a low lying area, had the deepest floodwater (Table 4-1) and also was one of the tallest stands according to Dahle et al. (2014). The relative heights of trees in L2 may have made them more susceptible to storm damage (Foster 1988; Harrington et al. 1997). The decrease in LAI after the hurricane appears to

be primarily driven by the loss of individuals within the stand rather than stress reducing leaf size or number in individual trees.

Clearly the pattern of standing density between the four plots also does not follow TML either, suggesting other factors may be interacting with TML to affect standing density, and by proxy LAI. Evans et al. (2015) assessed the relationship between ectomycorrhizal fungi (EMF) in the four LAI plots at LSP in 2012 and 2013. EMF community composition did vary by metal load suggesting that certain EMF communities may be better adapted to metalliferous soils. In a separate study on soil enzyme activity at LSP, the highest LAI plot (H2) also had significantly higher enzymatic activity, even when compared to a non-polluted reference site (Hagmann et al. 2015). Plot H2 is also unique since it has been forested for the longest period of time according to a review of historic aerial photography. Additionally because of its age, perhaps facilitative interactions between H2's plants and soil community may be more robust as they have had more time to develop. It is possible that the soil microbial community in H2 is not only well adapted to tolerate its conditions, but in the process also facilitate aboveground productivity as well. Some soil microbes do appear to be capable of facilitating plant growth in metal contaminated soils possibly by producing biomolecules which can sequester the metals and limit uptake (Khan 2005).

Differences in soil physical-chemical properties may also be influencing both above and belowground productivity in these four plots. The results of the soil nutrient analyses do lend support to the initial hypothesis that LAI would correlate with soil nutrient availability. The trees growing in H1 (lowest LAI) may experience the greatest nutrient limitation because of it low pH (4.74 ± 0.17) which may reduce nutrient availability in addition to its already low concentrations of P, K, and Mg (8.17 ± 7.01, 50.33 ± 3.79, and 37.67 ± 3.75). The higher concentrations of P, K, and Mg in H2 (82 ± 16.7, 76.88 ± 8.94, and 101.62 ± 21.65) along with the positive relationship between K and LAI further support the argument that nutrient availability may explain

differences observed between plots with similar metal load. Fassnacht and Gower (1997) also found significant relationships between LAI and pH, K and N in conifer and hardwood forests. K is a critical plant macronutrient need by plants in large quantities for many different functions, including respiration, transpiration, enzyme activity and root absorption (Kaufman 1989). When a combination of lime and pine bark mulch amendments were added around the dripline of *B. populifolia* trees growing in H1, an increase in pH, P, Mg and Ca or K (but not both Ca and K at the same time) led to altered root morphology which favored foraging (Gallagher et al. 2015). The trees growing with some nutrient limitation may be diverting more resources to foraging rather than aboveground productivity.

Ecosystems experiencing long term abiotic stresses such as soil pollution may be less resilient to short term disturbances (Folke et al. 2004). In a mixed conifer-deciduous forest downwind of a Cu smelter, plots with an experimental disturbance and high soil pollution had the lowest rates of re-colonization and lower species richness compared to a control site (Trubina 2009). The reduction of soil nutrients caused by acid deposition correlated with a decline in canopy density of a Norway spruce forest (Jonard et al. 2012). The authors posit that while acid deposition had decreased with time, the stresses it imposed on the forest led to a feedback cycle where soil stress reduced aboveground productivity which then reduced nutrient cycling leading to further losses in aboveground productivity. However microbial communities adapted to highly polluted soils were shown to be more resilient against the addition of new stressors, including As and salt (Azarbad et al. 2015). Continued monitoring of the LSP stands is needed to assess the long term resilience of this already stressed ecosystem to short term climate perturbations.

Previous work comparing plant guild trajectory between high and low metal load soils at LSP proposed that perhaps the additional abiotic stresses imposed by the high metal soils may lead to an alternative steady state community that differs from the typical succession community found in the region (Gallagher et al. 2011). In this young terrestrial system, the continued addition

of organic material as a result of plant growth may be acting as a sink, which would reduce the pool of available soil metals. If this concept is valid, then the strength of TML as the deterministic abiotic filter may decrease over time leading to the establishment of species with lower soil metal tolerance. The significant disturbance to forest structure in LSP caused by Hurricane Sandy may alter the anticipated trajectory pattern.

The creation of canopy gaps could enable new species to establish through altering light regimes (Schumann et al. 2003) and/or nutrient cycles (Scharenbroch 2009; Thiel and Perakis 2009). Though Carlton and Bazzaz (1998) found that *Betula papyrifera* seedlings, a close relative of *B. populifolia,* exhibited fast growth rates on artificially disturbed microsites provided they were not completely shaded. Two years following a hurricane which caused 70% canopy loss in a mixedwood urban forest, the majority of the site's soil seed bank and tree seedlings were early successional species (Burley et al. 2008), which suggests LSP's canopy loss could favor the development of a new generation of birch or other early successional species. At the same time, researchers at LSP have been observing increasing numbers of *Quercus rubra* and *Quercus coccinea* seedlings throughout the park which also suggests the possibility of a new shift in community composition. In the long run these gaps could also lead to greater structural heterogeneity in the forest (Lutz and Halpern 2006). A persistent challenge for land managers is deciding when efforts should be made to maintain a community in its current form or to allow it to change over time. Continued tracking of the long term changes in structure and function of these LSP plots could offer insight into the causes and effects of these changes.

CONCLUSIONS

An analysis of LAI of early successional hardwood forest plots along a gradient of metal contamination at LSP suggests the effects of soil metal stress on aboveground canopy productivity may be complicated by additional factors such as soil nutrients, stand age, and soil

community interactions. Higher nutrient levels may have some ameliorating effects on metal stress however time may also be an important factor enabling facilitative interactions to develop. A comparison of LAI before and after the 2012 Hurricane Sandy storm surge demonstrated the significant reductions in canopy at the site resulting from the death of trees within three of the four plots. As of 2016, no differences in canopy recovery have been observed between plots. It remains to be seen how this disturbance will influence the long term structure and functions of this forest.

TABLES

Table 4-1: Total metal load (TML) and estimated flood depth (m) caused by Hurricane Sandy Storm Surge in study plots at LSP. Flood depth based on FEMA Modeling Task Force (2013)

Plot	**TML**	**Flood Depth (m)**
L1	0.85	1
L2	1.56	1.5
L3	1.64	0.1
H1	3.08	0.2
H2	3.56	1.2
H3	4.31	1.3

Table 4-2: Mean leaf area index (LAI) for each LAI study plot from 2010 to 2016. Standard deviation shown in parentheses. Means with the same letters are not significantly different according to a Tukey HSD test ($p < 0.05$) and can be compared between plots and between years.

Year	**L2**	**L3**	**H1**	**H2**
2010	2.95 (0.19) bc	2.95 (0.23) bc	1.73 (0.29) ijk	3.44 (0.33) a
2011	3.01 (0.24) abc	2.84 (0.23) bcd	1.78 (0.39) hijk	3.16 (0.31) ab
2012	2.84 (0.36) bcd	2.69 (0.29) cde	1.68 (0.23) ijk	3.17 (0.26) ab
2013	2.06 (0.24) ghi	2.25 (0.26) fgh	1.59 (0.26) ijk	2.57 (0.27) cdef
2015	1.59 (0.16) ijk	2.42 (0.14) defg	1.45 (0.21) jk	2.6 (0.36) cdef
2016	1.38 (0.13) k	2.3 (0.11) efg	1.48 (0.15) jk	1.93 (0.23) ghij

Table 4-3: Means and stand deviation (in parentheses) of physico-chemical soil properties of LAI plots. Means with the same letters are not significantly different according to a Tukey HSD test ($p < 0.05$) and can be compared between plots and between years.

Plot	**pH**	**Conductivity (mS s^{-1})**	**Sand (%)**	**Silt (%)**	**Clay (%)**
L1	5.45 (0.29)b	0.11 (0.01)a	78.25 (5.8)a	19.75 (5.97)a	1.8 (2)b
L2	6.09 (0.3)a	0.09 (0.02)a	80.33 (0.58)a	14.33 (0.58)ab	5 (1)a
L3	5.05 (0.19)bc	0.1 (0.04)a	79 (0)a	16.33 (0.58)ab	4.67 (0.58)ab
H1	4.74 (0.17)c	0.08 (0.01)a	80.33 (2.08)a	14.67 (2.08)ab	5 (0)a
H2	5.37 (0.13)b	0.09 (0.01)a	81.75 (3.4)a	15 (2.58)ab	3.25 (1.26)ab
H3	5.43 (0.27)b	0.08 (0.01)a	85.5 (7.05)a	10.25 (5.62)b	4 (1.15)ab

TABLE 4-4: Means and stand deviation (in parentheses) Melich-3 extractable macronutrients as well as total nitrogen (TN) and total carbon (TC) in soils of LAI plots. TKN = total Kjeldahl nitrogen. Means with the same letters are not significantly different according to a Tukey HSD test ($p < 0.05$) and can be compared between plots and between years.

Plot	TKN %	P (ppm)	K (ppm)	Mg (ppm)	Ca (ppm)	TN (%)	TC (%)
L1	0.25 (0.1)a	79.88 (68.91)a	57.88 (13.65)a	93.75 (37.44)b	467 (417)a	0.31 (0.27)b	11.65 (8.25)b
L2	0.23 (0.06)a	6.67 (1.15)b	48.5 (9.66)a	77.67 (50.28)ab	395 (305)a	0.43 (0.16)ab	22.01 (2.01)a
L3	0.21 (0.03)a	6.83 (3.33)b	69.17 (14.64)a	75.5 (21.23)b	169 (48)a	0.46 (0.26)ab	23.43 (5.14)a
H1	0.36 (0.17)a	8.17 (7.01)b	50.33 (3.79)a	37.67 (3.75)a	289 (169)a	0.49 (0.31)ab	23.81 (4.72)a
H2	0.3 (0.03)a	82 (16.7)a	76.88 (8.94)a	101.62 (21.65)b	306 (142)a	0.55 (0.33)a	24.61 (7.77)a
H3	0.18 (0.1)a	5.75 (2.72)b	61.88 (25.54)a	96.5 (65.67)b	427 (299)a	0.37 (0.12)ab	18.4 (4.96)a

Table 4-5: Means and stand deviation (in parentheses) Melich-3 extractable micronutrients in soils of LAI plots. Means with the same letters are not significantly different according to a Tukey HSD test ($p < 0.05$) and can be compared between plots and between years.

Plot	Zn (ppm)	Cu (ppm)	B (ppm)	Fe (ppm)	Mn (activity index)
L1	53.93 (58.55)ab	23.57 (12.67)ab	0.42 (0.18)a	376.48 (196.34)a	37.36 (12.6)bc
L2	4.03 (3.87)b	22.26 (27.69)ab	0.52 (0.16)a	451.93 (43.96)a	19.93 (3.12)a
L3	2.81 (0.96)b	9.45 (1.29)ab	0.4 (0.03)a	402.8 (78.77)a	36.63 (2.34)bc
H1	3.44 (1.49)b	3.57 (0.53)b	0.43 (0.08)a	435.13 (125.12)a	51.3 (8.13)c
H2	6.56 (2.09)b	5.86 (0.59)b	0.33 (0.05)a	579.5 (29.27)a	27.46 (1.7)ab
H3	110.99 (81.1)a	124.81 (115.84)a	0.41 (0.05)a	486.65 (266.01)a	55.44 (12.9)c

Table 4-6: Linear regression coefficients and model r^2 values for leaf area index (LAI) predicted by individual soil nutrients. Coefficient standard errors shown in parentheses. P-values are for individual coefficients. TN = total nitrogen, TC = total carbon, and TKN = total Kjeldahl nitrogen. All elements with the exception of TC and TN are Mehlich 3 extractable concentrations.

Parameter	Intercept	p-value	Slope	p-value	r^2
K (ppm)	-0.42 (0.68)	0.57	0.04 (0.01)	0.02	0.8
B (ppm)	5.29 (1.1)	0.01	-7.31 (2.61)	0.05	0.66
Fe (ppm)	-0.23 (1.18)	0.85	0.01 (0)	0.1	0.53
Mg (ppm)	1.14 (0.76)	0.21	0.01 (0.01)	0.21	0.36
Sand (%)	-7.67 (6.8)	0.32	0.12 (0.08)	0.22	0.35
Silt (%)	3.33 (1.21)	0.05	-0.07 (0.08)	0.41	0.17
TN (%)	1.23 (1.25)	0.38	2.33 (2.84)	0.46	0.14
Conductivity (mS s^{-1})	3.55 (1.77)	0.11	-14.54 (19.39)	0.5	0.12
Cu (ppm)	2.11 (0.29)	0	0 (0.01)	0.52	0.11
TC (%)	1.56 (1.1)	0.23	0.03 (0.05)	0.56	0.09
Zn (ppm)	2.14 (0.3)	0	0 (0.01)	0.62	0.07
TKN (ppm)	2.72 (1.02)	0.06	-1.92 (3.92)	0.65	0.06
Ca (ppm)	2.66 (0.84)	0.03	0 (0)	0.63	0.06
P (ppm)	2.13 (0.32)	0	0 (0.01)	0.66	0.05
pH	3.03 (3.14)	0.39	-0.15 (0.58)	0.81	0.02
Clay (%)	2.48 (0.87)	0.05	-0.06 (0.21)	0.78	0.02
Mn (activity index)	2.09 (0.79)	0.06	0 (0.02)	0.85	0.01

Table 4-7: Linear regression coefficients and model adjusted r^2 values for leaf area index (LAI) predicted by pairs of soil nutrients. Coefficient standard errors shown in parentheses. All elements with the exception of TC and TN are Mehlich 3 extractable concentrations.

Nutrient 1	Nutrient 2	Correlation coefficient	Model p-value	Intercept	p-value	Nutrient 1 Slope	p-value	Nutrient 2 Slope	p-value	Adj. r^2
K (ppm)	Sand (%)	0.17	0.0002	-7.82 (0.55)	0	0.04 (0.002)	0	0.09 (0.007)	0.001	0.99
K (ppm)	Silt (%)	0.02	0.001	0.69 (0.25)	0.07	0.044 (0.003)	0.001	-0.08 (0.011)	0.006	0.98
K (ppm)	Conductivity (mS s^{-1})	0.06	0.007	1.03 (0.52)	0.14	0.045 (0.005)	0.004	-16.92 (4.585)	0.034	0.94
K (ppm)	Cu (ppm)	-0.03	0.02	-0.58 (0.49)	0.32	0.044 (0.008)	0.011	0 (0.002)	0.113	0.87
K (ppm)	Fe (ppm)	0.53	0.04	-1.07 (0.72)	0.23	0.035 (0.011)	0.054	0 (0.002)	0.219	0.81
B (ppm)	Silt (%)	-0.04	0.05	6.55 (0.99)	0.01	-7.483 (1.888)	0.029	-0.08 (0.037)	0.12	0.78
K (ppm)	Zn (ppm)	0	0.05	-0.51 (0.65)	0.49	0.044 (0.01)	0.025	0 (0.003)	0.315	0.77
B (ppm)	Sand (%)	-0.19	0.05	-2.62 (3.96)	0.56	-6.54 (1.983)	0.046	0.09 (0.046)	0.134	0.76

Table 4-8: Linear regression coefficients and model adjusted r^2 values for leaf area index (LAI) measured from 2010 to 2012 predicted by air temperatures and reference evapotranspiration (ET_o) average over periods of 1 to 4 weeks as well as the 12-month Standardized Precipitation Index . Table only shows model parameters with significant coefficients. Coefficient standard errors are shown in parentheses.

Variable	**Model p**	**Adj. r^2**	**Intercept**	**Slope**	**Plot H1**	**Plot H2**
Mean temp. 1 week (°C)	< 0.001	0.83	1.85 (0.28)	0.05 (0.01)		0.77 (0.39)
Mean temp. 2 week (°C)	< 0.001	0.83	1.94 (0.27)	0.04 (0.01)		0.89 (0.38)
Mean temp. 3 week (°C)	< 0.001	0.82	2.03 (0.26)	0.04 (0.01)		0.8 (0.37)
Mean temp. 4 week (°C)	< 0.001	0.82	2.12 (0.26)	0.04 (0.01)		0.78 (0.36)
Mean ET_o 1 Week (mm)	< 0.001	0.81	2.46 (0.21)	0.09 (0.04)	-0.76 (0.29)	
Mean ET_o 2 Week (mm)	< 0.001	0.81	2.08 (0.3)	0.16 (0.06)		
Mean ET_o 3 Week (mm)	< 0.001	0.81	1.95 (0.34)	0.18 (0.06)		
Mean ET_o 4 Week (mm)	< 0.001	0.82	1.86 (0.38)	0.2 (0.07)		
SP12	< 0.001	0.82	3.12 (0.09)	-0.18 (0.07)	-1.33 (0.13)	0.35 (0.14)

Table 4-9: Linear regression coefficients and model adjusted r^2 values for leaf area index (LAI) predicted by temperature and reference evapotranspiration (ET_o) averaged over 1 to 3 weeks and the Z-index (ZNDX) calculated four weeks prior to measurement date with significant interactions between plot and weather variable. Coefficient standard errors are shown in parentheses. Table only shows model parameters with significant coefficients.

Variable	**Model p**	**Adj. r^2**	**Intercept**	**Slope**	**Plot H1**	**Plot H2**	**Slope x H1**	**Slope x H2**
Mean temp. 1 week (°C)	< 0.001	0.83	1.85 (0.28)	0.05 (0.01)	-0.38 (0.39)	0.77 (0.39)	-0.04 (0.02)	
Mean temp. 2 week (°C)	< 0.001	0.83	1.94 (0.27)	0.04 (0.01)	-0.42 (0.38)	0.89 (0.38)	-0.03 (0.02)	
Mean temp. 3 week (°C)	< 0.001	0.82	2.56 (0.12)	0.03 (0.01)	-0.86 (0.17)	0.63 (0.17)	-0.03 (0.01)	
Mean ET_o 2 Week (mm)	< 0.001	0.81	2.08 (0.3)	0.16 (0.06)	-0.36 (0.42)	0.8 (0.42)	-0.16 (0.08)	
ZNDX four weeks prior	< 0.001	0.81	2.98 (0.07)	*0.06 (0.05)*	-1.19 (0.09)	0.15 (0.09)		-0.23 (0.07)

Table 4-10: Stand mortality based on a comparison of tagged tree inventories in Liberty State Park Study plots made in 2013 and 2016.

Plot	Died after 2013	Alive in 2016	Total trees surveyed	Percent died after 2013
L2	32	24	56	0.57
L3	22	59	81	0.27
H1	4	55	59	0.07
H2	12	16	28	0.43

FIGURES

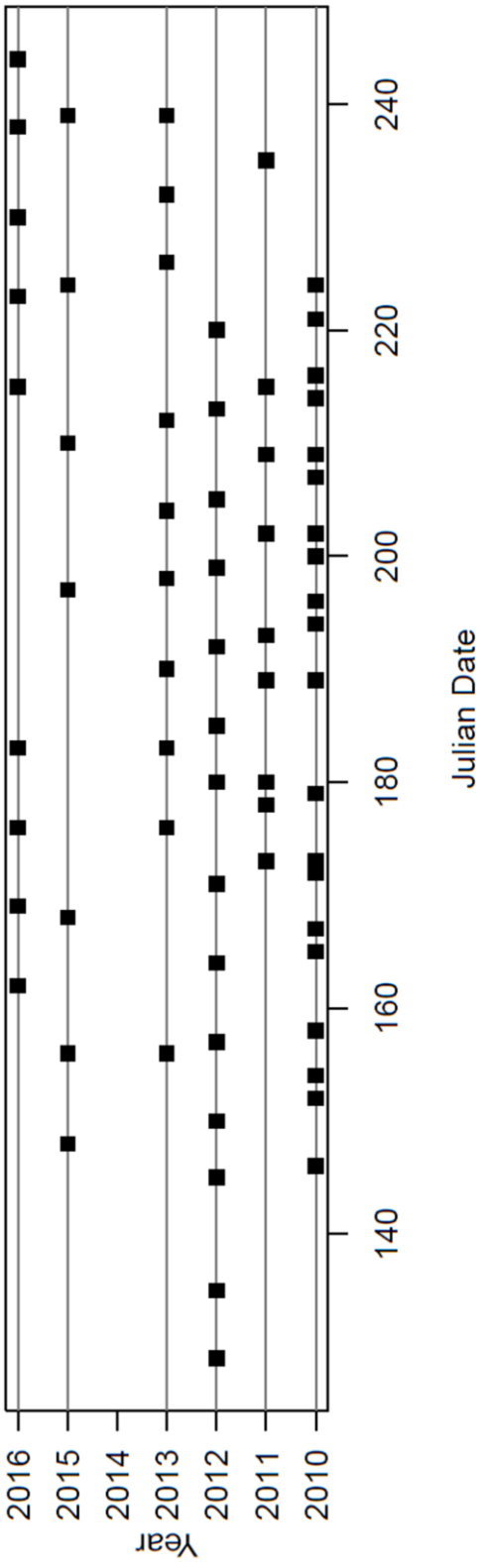

Figure 4-1: Leaf area index (LAI) measurement dates for four primary study plots from 2010 to 2016. Each square indicates a measurement date.

Figure 4-2: Leaf area index (LAI) of plots TP-48, TP-43, TP-14 and TP-1416 at LSP during the 2010-2016 growing seasons (excluding 2014). Circles represent measurement dates. TP-48 (L2) and TP-43 (L3) are low metal load plots while TP-14 (H1) and TP-1416 (H2) are high metal load plots.

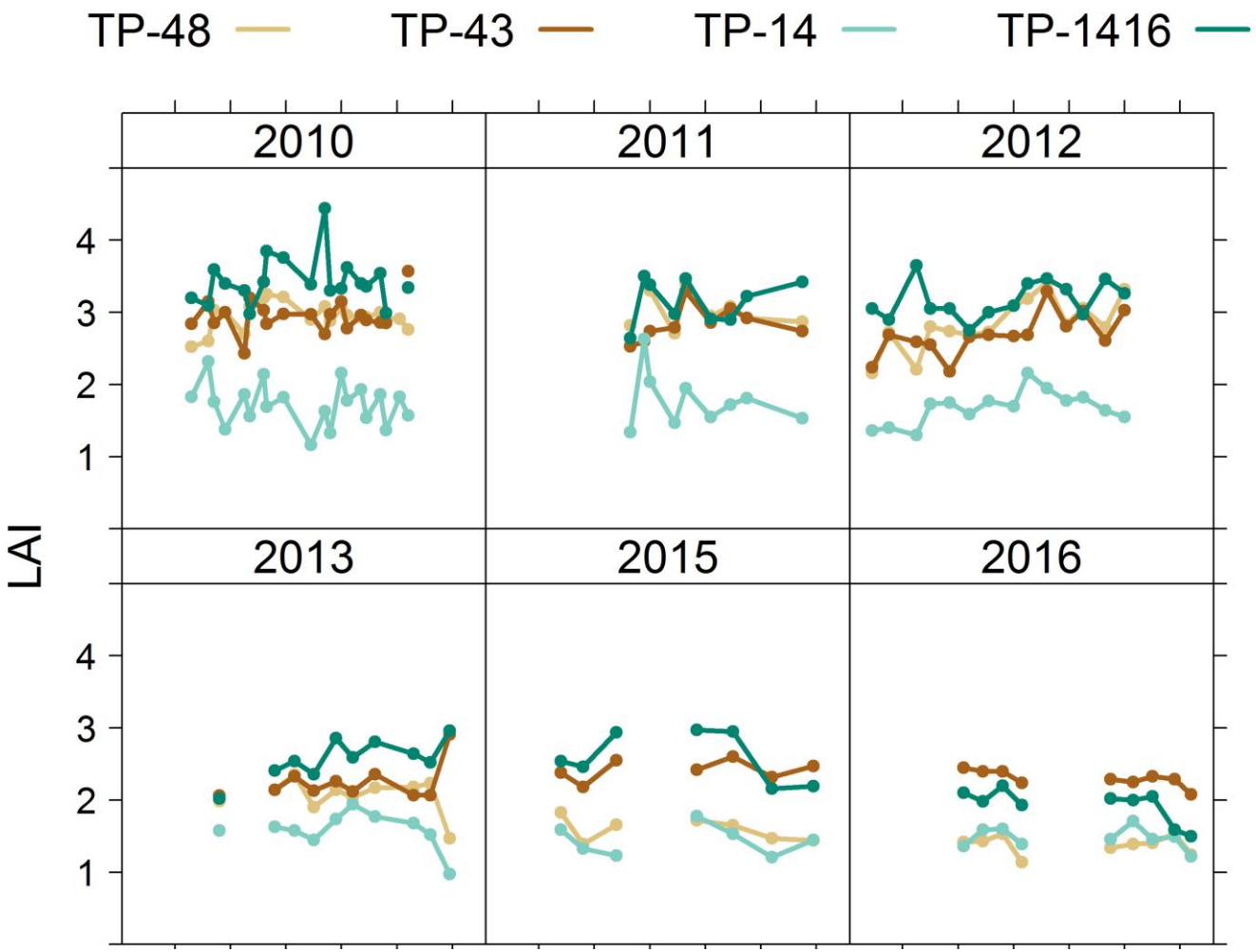

Figure 4-3: Moving averages of leaf area index (LAI) of four plots in 2010 and 2012.

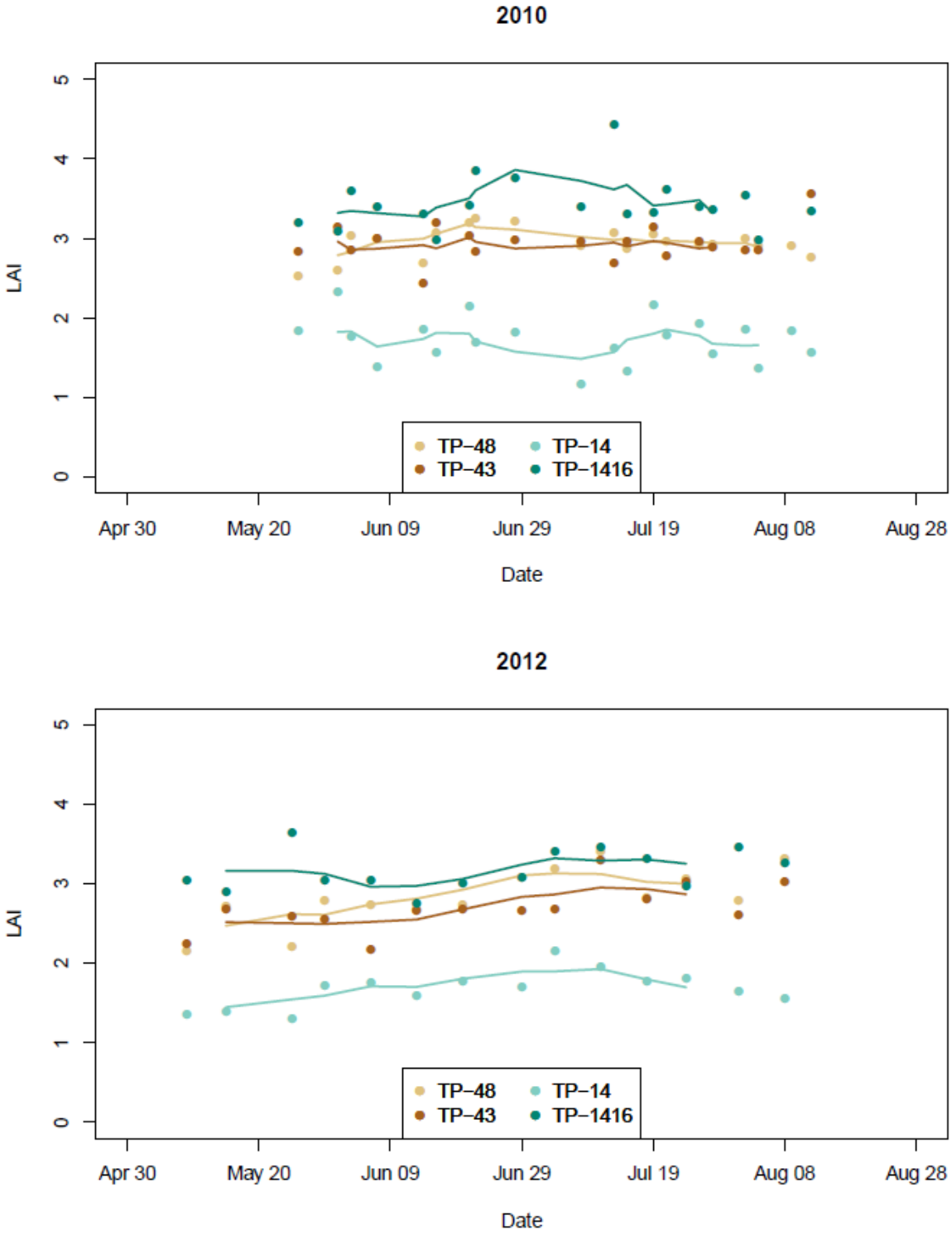

Figure 4-4: Plant guild trajectories for selected study plots in Liberty State Park based on an analysis of aerial photography in Gallagher et al. (2011). Solid lines indicate the years when aerial photographs were taken. Bare (light yellow) = bare soil, Hb (light green) = herb/forbe, Sh (medium green) = shrub, SNH (dark green) = successional northern hardwood. Plot total metal load increases down the chart.

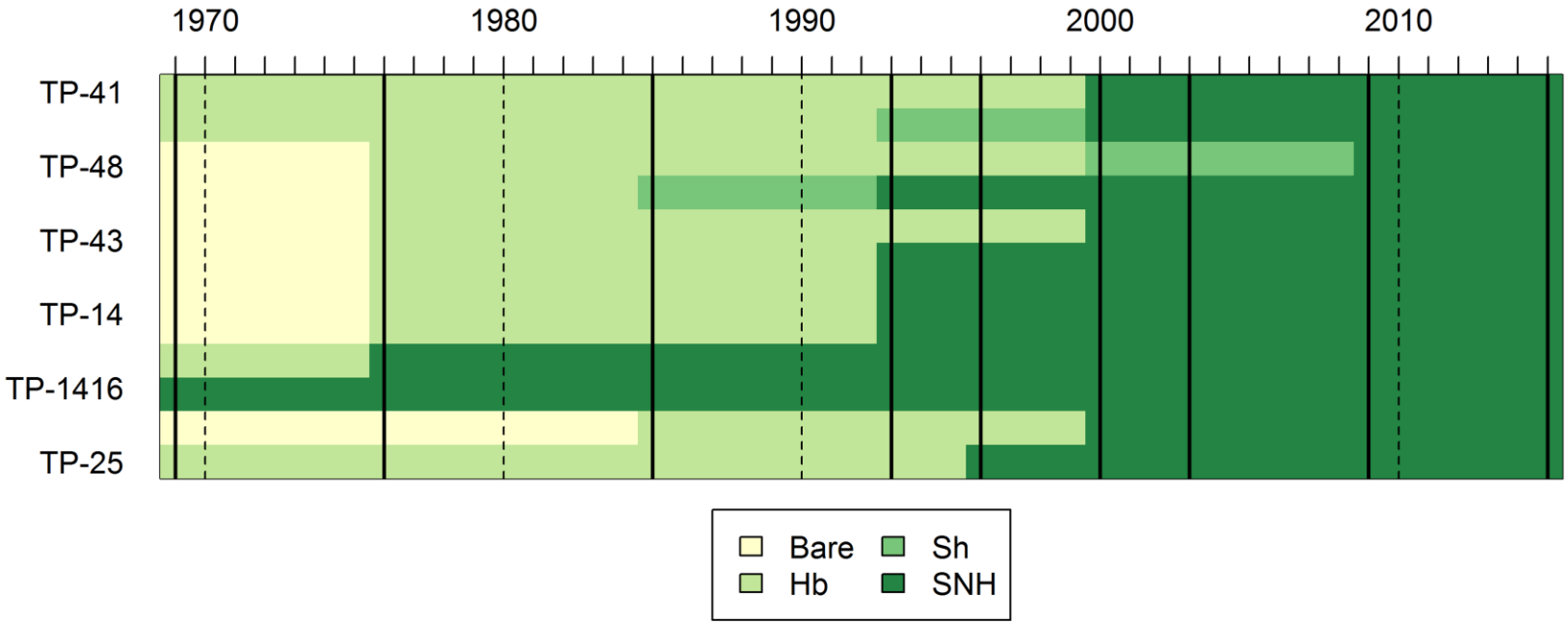

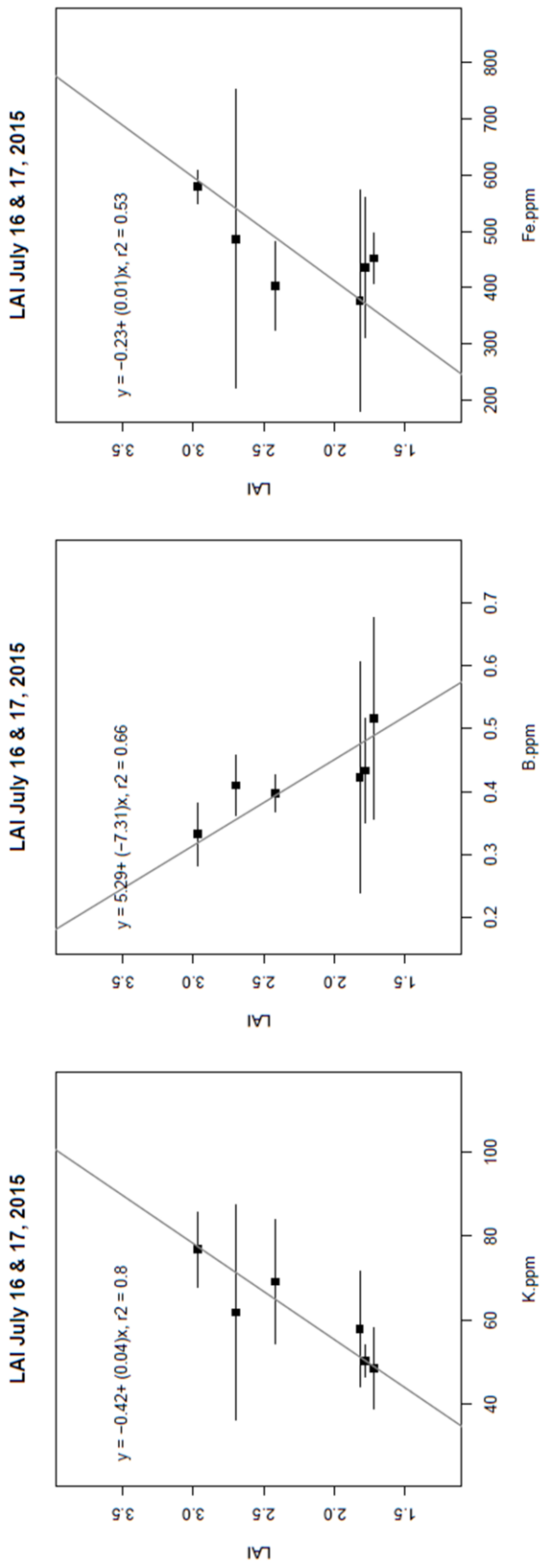

Figure 4-5: Leaf area index (LAI) of plots measured on July 16 and 17, 2015 predicted by Mehlich 3 extractable potassium, boron, and iron (ppm). Measurements were made in plots L1, L2, L3, H1, H2, and H3. Horizontal error bars represent one standard deviation about the mean SQI (n = 3 for L2, L3, H1 and n = 4 for L1, H2, H3).

FIGURE 5-6: Selected weather parameters with significant plot x parameter interactions for leaf area index (LAI) measured in 2010 to 2012. WeeklyTempAvg.C = temperature averaged over the 7 days preceding measurement date. BiWeeklyTempAvg.C = temperature averaged over the 14 days preceding measurement date. TriWeeklyTempMin.C = temperature minimum during the 21 days preceding measurement date. BiWeeklyEToAvg.mm = reference evapotranspiration averaged over the 14 days preceding the measurement date. ZNDX.n.28 = Z-index value four weeks prior to measurement date.

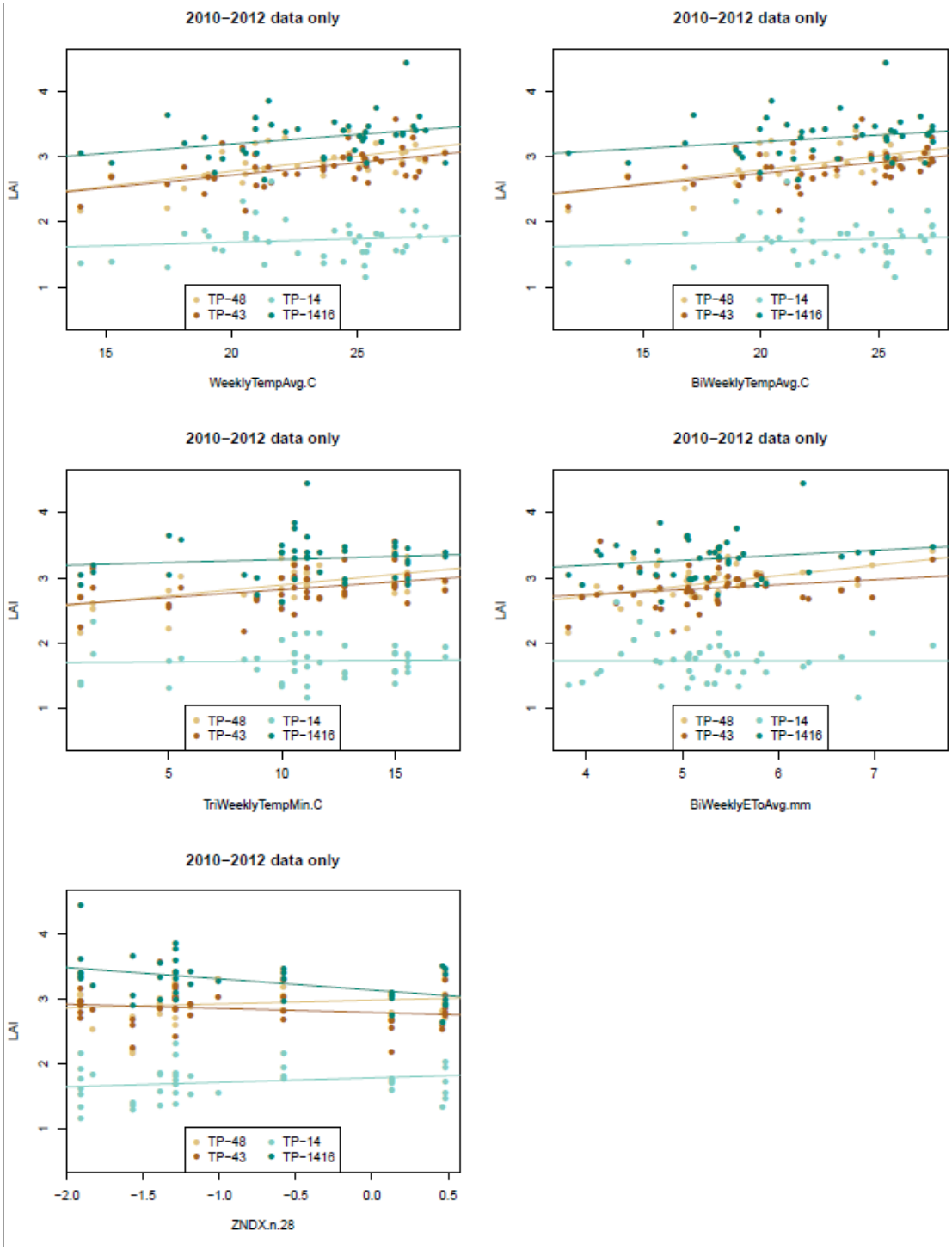

Chapter 5 - Synthesis & Conclusion

The goal of this dissertation was to begin addressing the question: What are the mechanisms by which soil trace element contamination affects primary forest productivity? The accurate quantification and prediction of ecosystem functions across a range of conditions is necessary for many applications, including terrestrial biosphere modelling (e.g. Medvigy et al. 2009), natural resource management (Cox et al. 2013), and restoration ecology (Hooper et al. 2016). Yet as Rohr et al. (2016) explain, there is a fundamental challenge to connect data collected on individual responses to environmental contaminants to the broader ecosystem functions of greatest interest to society. The interior forest in Liberty State Park (LSP) provides a unique opportunity to assess responses to TE contamination at multiple scales since the forest has been established for several decades in the contaminated soil. This site allows us to study TE effects as the ecosystem continues to develop and possibly goes through a transition phase rather than during the establishment phase of restoration which has been the focus of other studies (Baeten et al. 2010; Beesley et al. 2010; Dickinson 2000; Oldfield et al. 2015; Perez-de-Mora et al. 2006).

In particular, this research focused on testing the hypothesis that higher soil TE concentrations would reduce photosynthesis and related processes in *Betula populifolia*, thereby reducing overall net primary productivity and tree growth. Dramatic differences in leaf level photosynthesis were not observed between plots in LSP classed as having low and high metal load soils (see Chapter 1 for total metal load description), as had been expected based on differences in basal area growth rates observed in these groups by other studies at LSP (Dahle et al. 2014; Renninger et al. 2012). Some significant decreases in maximum carboxylation rate and electron transport rate of trees growing in high metal load plots were observed, however these

responses appear to only occur for short periods of time rather than lasting the entire growing season.

These findings suggest that one cannot draw a straight line between individual physiological responses to TE contamination and ecosystem level primary productivity, at least with mature hardwood trees. Instead, TE may exert greater influence as an abiotic filter during the establishment phase. TE may also affect multiple levels of biological organization which in turn interact with each other and respond to other environmental conditions. To understand the effects of TE on primary productivity based on the body of research conducted at LSP, I propose a conceptual model which accounts for both TE effects on multiple levels of biological organization as well as interacting effects which occur between levels in hardwood ecosystems (Figure 5-1). This model is based on work by Fattorini and Halle (2004) and Rohr et al. (2016).

The conceptual model accounts for TE impacts on community composition through the role of TE as an abiotic filter on species establishment (Figure 5-1 Part A). Community composition becomes limited to those species which possess traits which enable tolerance of the TE stress (or another condition typical of degraded soil such as nutrient deficiency) (Fattorini and Halle 2004). Hardwood biodiversity decreased with increasing TE concentrations at Liberty State Park (Gallagher et al. 2008b), and similarly in other sites plant distribution follows patterns of contamination (Desjardins et al. 2014). This filtering sets the stage for future interactions and the development of biodiversity within the site. It is well accepted that ecosystem functions generally scale positively with biodiversity (Hooper et al. 2005). However it is unclear how the addition of stress from soil pollution could influence that relationship.

In addition to filtering out entire species, TE contamination also acts a filter on genetic variation within species or local populations by favoring TE tolerant phenotypes. It is possible that the robust nature of photosynthesis rates between the low and high metal load trees at LSP stems from the site selecting for individuals with TE tolerant physiological processes. High

within species variability in TE tolerance has been observed in other species commonly planted in restoration and remediation settings, such as poplar (Gaudet et al. 2011). In order for spontaneous revegetation projects to be successful, the regional species and genetic pool need to contain material that is tolerant of stressful site conditions. It has been hypothesized that the original seeds of the LSP *Betula populifolia* trees may have travelled from as far as the coal mining regions of Pennsylvania. Though genetic material could have also travelled south out of the Hudson Valley as well. If this is indeed the case, then this would imply that the revegetation of novel anthropogenic soils may require a species pool from a large geographic region and possibly human intervention to access adequate genetic material. A genetic comparison of *B. populifolia* growing in LSP and from other populations in New Jersey, New York, and Pennsylvania could help to address this question and provide insight into the nature of regional species pools in urban environments.

In addition to an abiotic filter, biotic interactions undoubtedly have an effect on community composition through facilitative, competitive, and predator-prey interactions (Figure 5-1 Part B) (Fattorini and Halle 2004). More research is needed to understand how TE contamination may alter the magnitude and relative importance of these different types of interactions. Krumins et al. (2015) have suggested that in stressful environments, facilitation may play an important role in the development of communities. Research on leaf area index at LSP by Evans et al. (2015) suggests plant-mycorrhizal interactions may play a role in maintaining higher primary productivity in high metal load soils. As our ability to sequence and study soil microbial communities continues to improve, future research and modeling efforts can begin to account for the role of microbiota on aboveground ecosystem functions in degraded habitats.

TE contamination may directly influence organism physiology and growth (Figure 5-1 Part C). The *B. populifolia* photosynthesis data demonstrates that this effect may be seasonal or transient. Other photosynthesis research at LSP also suggests that these effects may be mediated

by other factors such as edaphic conditions or plant age (Radwanski et al. 2017; Renninger et al. 2012). While physiological responses of individual species to individual toxicants may be readily studied in laboratory and greenhouse settings (Rohr et al. 2016), the findings from LSP suggest that fine scale physiology may not be as important to the bigger picture of ecosystem function in well-established forest communities.

Allometry of individuals is likely influenced by both TE stress and interactions with other individuals (Figure 5-1 Part D). Direct exposure of roots to contaminants (Zhang et al. 2014), carbon demands of mycorrhizal fungi (Allen et al. 2003), and increased foraging in nutrient poor soil (Poorter et al. 2011) could all divert more carbon resources to the root zone rather than to aboveground growth. At the same time, stand density can exert a strong influence on aboveground resource allocation, altering tree height and diameter ratios and branch growth (Donoso and Nyland 2006). Stand density can be influenced by many factors, including succession or community trajectory patterns (Royo and Carson 2006). At LSP, vegetative guild trajectory varied between low and high metal load soils and may explain current patterns of stand density and allometry observed in study plots. If this is the case, then TE stress affects individual growth patterns both directly and indirectly which would further complicate modeling efforts.

Other edaphic conditions and disturbance events may also affect population characteristics and community composition (Figure 5-1 Part E). Many anthropogenic soils have multiple characteristics which can be detrimental to plant growth in addition to pollution, including low nutrient availability, extreme pH, and poor drainage (Morel et al. 2014). The leaf area index data at LSP highlighted the role nutrient availability may play in influencing canopy productivity. Major disturbances such as the Hurricane Sandy storm surge may lead to a state change in the system. As canopy was opened following tree mortality post-storm surge, it is possible new species may be able to gain a foothold in these canopy gaps (Muscolo et al. 2014). This situation will provide an interesting opportunity to see if TE contamination makes

established communities more or less resistant to invasion following a disturbance. The TE contamination may continue to act as a strong filter on species recruitment favoring the regrowth of species already in the site. Alternatively if ecosystem development over the past few decades has sufficiently influenced the availability of TE and/or mitigated other detrimental characteristics of the soil through the addition of organic matter, perhaps new species will be able to establish. If new species have different TE accumulation patterns or produce biomass with different decomposition rates, these changes could alter long term TE stability.

TE contamination affects primary productivity through its effects on community composition, individual physiology (possibly to a lesser degree), community trajectory and population characteristics (Figure 5-1 Part F). At the same time primary productivity is also influenced by other edaphic conditions within the site as well as the interactions of organisms within the community. These numerous interrelationships coupled with the longevity of trees makes developing a mechanistic understanding of TE impacts on hardwood primary productivity challenging. Given the long-lived nature of trees, the body of research at LSP suggests or demonstrates how the early effects of TE on community assembly (i.e. influencing species composition and guild trajectory) may have lasting consequences on the structure and function of the community.

Ecosystem functions may in turn influence TE concentrations and/or availability over time through TE uptake and the addition of organic matter to the soil (Figure 5-1 Part G). The results from the analysis of the 20 years of LSP soil data suggest the potential for plant growth (i.e. primary productivity) and possibly decomposition to stabilize concentrations of at least some of the TE at the site. It is unclear if this stability will mean that the TE will continue to act as an abiotic filter on species establishment. Alternatively, while pseudo-total TE concentrations have remained stable their availability may have increased or decreased which could then alter the nature of the TE-based filter. Concurrently, as the soil continues to develop with the addition and

subsequent decomposition of organic matter along with other soil forming processes, the role of the soil as a filter may change as well. Following up on previous biodiversity studies at the site could offer insight into the changing role of the soil as a filter on community composition over time.

Taken all together, this conceptual model highlights the potential for TE to influence hardwood primary productivity through multiple mechanisms, and equally important how primary productivity may influence the TE. In its current form, this model is derived from the pieces of many different research projects conducted at LSP. One approach to test the accuracy and utility of the model would be to use data from these LSP studies to parameterize it, possibly borrowing approaches from ecotoxicological (e.g. Forbes and Calow 2013; Martin et al. 2013), terrestrial biosphere (e.g. Medvigy et al. 2009) and/or community assembly models (e.g. Laughlin 2014) to assess how well these research pieces fit together. Fitting such model could reveal what components of the system may have been overlooked thus far or highlight which components are more or less important drivers of hardwood primary productivity in TE contaminated soil.

Another next step in studying the mechanisms by which TE contamination influence primary productivity will be to generalize findings from LSP in such a way as to be both comparable to and useful for other sites and projects. This next step could enable better prediction capabilities for environmental resource assessments (ERA) and improved expectations and treatment for restoration projects (Hooper et al. 2016). Trait-environment frameworks have been proposed as one strategy for enabling comparisons across sites and ecosystems (Perring et al. 2015). Trait-environment frameworks assess the distribution of selected traits (e.g. seed size) along an environmental gradient (e.g. soil moisture) (Pavoine et al. 2011). One could choose an environmental characteristic (or more likely a set of them) and then find where a site fits along that gradient in order to compare its community structure and function to other sites. Relatively new developments in the creation of soil taxonomies for urban and anthropogenic soils could also

be valuable in facilitating comparisons between sites. These taxonomies provide a richer vocabulary and framework to replace the rudimentary use of "urban" as a soil classifier. Morel et al. (2014) propose a set of broad classifications for soils in urban, industrial, transportation, and mining areas (collectively referred to as SUITMAs) and posit different ecosystem functions each could support. But this SUITMA-ecosystem function framework has not been tested. One could assess how biodiversity changes with level of anthropogenic impact using a metric such as the amount of anthropogenic material in a soil.

At LSP in particular, there are several other important directions for future research. Turner et al. (2003) contend a major limitation of many ecosystem service studies is their focus on one service at a time even though in reality many ecosystem functions occur together or may operate in opposition. The LSP hardwood studies have been essentially focused on primary production. Future research should assess other ecosystem functions across the trace element gradient such as nutrient cycling or habitat provisioning. Additionally as mentioned in Chapter 4**,** observations have been made of a growing number of mid-successional oak trees growing in the park. Research has started tracking the location and basal area growth of these trees including several transects of seedling location. Since research on other hardwoods at the site has highlighted the importance of other edaphic conditions along with metal load, additional measurements such as macronutrient availability could be made along these oak transects to complement TE data.

Conclusion

Trace element contaminated soils are a persistent problem and one that will continue to grow with increasing urbanization and global development. Consequently it is important to understand how the trace elements not only affect individual organisms but ecosystem functions

as a whole. Additionally, given the persistent nature of trace elements it is crucial for research to focus on the long term fate and effects of these contaminants. Research at Liberty State Park found that after several decades of plant community establishment, some soil trace element concentrations appear to have remained stable for at least two decades while others have become enriched in the C1 horizon. These finding emphasize the importance of long term monitoring for changing conditions that could affect the fate of these elements. Measurements of photosynthetic parameters of *Betula populifolia* growing at the site show that overall the photosynthetic parameters of these trees are fairly robust along a range of increasing trace element concentrations. When differences were observed they appear to last for a short period of time suggesting the possibility that trace element effects may be seasonal. Six years of leaf area index measurements demonstrated that other plot or stand specific characteristics such as nutrient availability, soil microbial community, and age may interact with or overwhelm trace element stress effects on canopy productivity. Taken together, these findings illustrate the complications of assessing trace element effects in field systems and the ways multiple factors may interact to influence primary productivity in trace element contaminated forests. They also demonstrate the potential of such ecosystems to function in spite of severe abiotic stresses.

FIGURES

Figure 5-1: Conceptual diagram representing the effects of trace element contamination on primary productivity through effects at lower levels of biological organization and interactions between levels in a hardwood ecosystem. A) Trace element contamination operates as an abiotic filter on community composition. B) Interactions such as symbiotic relationships with mycorrhizal fungi influence population characteristics and individual growth. C) Trace element influence individual physiology. D) Individual growth and allometry is affected by population or stand characteristics. E) Edaphic conditions and disturbance can influence population dynamics. F) Primary productivity is an emergent property from all of these relationships. G) Plant growth and addition of organic matter to sol can modify trace element concentrations and availability over time.

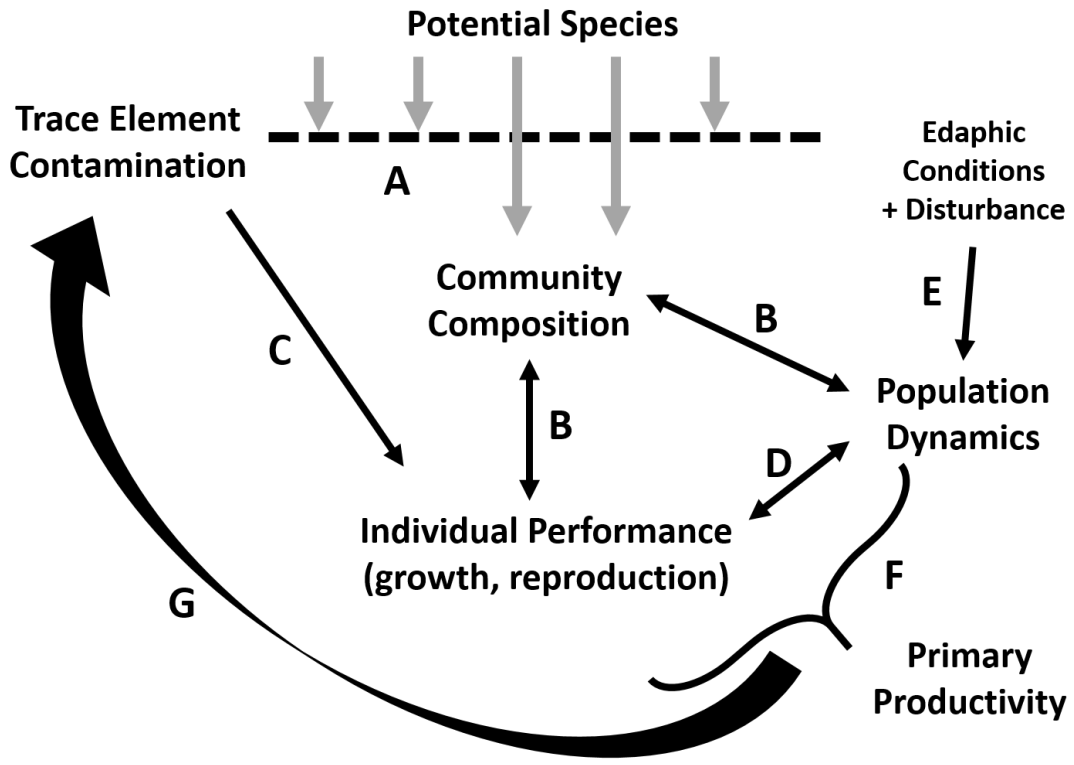

WORKS CITED

Aalto, T., and Juurola, E. (2001). “Parametrization of a biochemical CO 2 exchange model for birch (Betula pendula Roth .).” *Boreal Environment Research*, 6(March), 53–64.

Ajmone-Marsan, F., and Biasioli, M. (2010). “Trace elements in soils of urban areas.” *Water, Air, and Soil Pollution*, 213(1–4), 121–143.

Al-Tabbaa, A., Smith, S., Munck, C. De, Dixon, T., Doak, J., Garvin, S., and Raco, M. (2007). “Climate Change, Pollutant Linkage and Brownfield Regeneration.” *Sustainable Brownfield Regeneration*, T. Dixon, M. Raco, P. Catney, and D. Lerner, eds., Blackwell Publishing Ltd, Oxford, UK.

Allen, M. F., Swenson, W., Querejeta, J. I., and Treseder, K. K. (2003). “Ecology of Mycorrhizae: A Conceptual Framework for Complex Interactions Among Plants and Fungi.” *Annual Review of Phytopathology*, 41, 271–303.

Allen, R. G., Pereira, L. S., Raes, D., and Smith, M. (1998). *Crop evapotranspiration - Guidelines for computing crop water requirements - FAO Irrigation and drainage paper 56*. Rome, Italy.

Anda, A., Illes, B., and Soos, G. (2013). “Effect of cadmium pollution of atmospheric origin on field-grown maize in two consecutive years with diverse weather conditions.” *Acta biologica Hungarica*, 64(4), 476–489.

Anderson, P., Davidson, C. M., Littlejohn, D., Ure, A. M., Garden, L. M., and Marshall, J. (1998). “Comparison of techniques for the analysis of industrial soils by atomic spectrometry.” *International Journal of Environmental Analytical Chemistry*, 71(1), 19–40.

André, O., Vollenweider, P., and Günthardt-Goerg, M. S. (2006). “Foliage response to heavy metal contamination in Sycamore Maple (Acer pseudoplatanus L.).” *For. Snow Landsc. Res*, 80(3), 275–288.

Anjum, S. A., Ashraf, U., Saleem, M. F., and Wang, L. (2016). “Chromium Toxicity Induced Alterations in Growth, Photosynthesis, Gas Exchange Attributes and Yield Formation in Maize.” *Pakistan Journal of Agricultural Sciences*, 53(4), 751–757.

Ascher, J., Ceccherini, M. T., Landi, L., Mench, M., Pietramellara, G., Nannipieri, P., and Renella, G. (2009). “Composition, biomass and activity of microflora, and leaf yields and foliar elemental concentrations of lettuce, after in situ stabilization of an arsenic-contaminated soil.” *Applied Soil Ecology*, 41(3), 351–359.

Azarbad, H., Niklińska, M., Nikiel, K., van Straalen, N. M., and Röling, W. F. M. (2015). “Functional and compositional responses in soil microbial communities along two metal pollution gradients: does the level of historical pollution affect resistance against secondary stress?” *Biology and Fertility of Soils*, 51(7), 879–890.

Di Baccio, D., Tognetti, R., Minnocci, A., and Sebastiani, L. (2009). “Responses of the Populus x euramericana clone I-214 to excess zinc: Carbon assimilation, structural modifications, metal distribution and cellular localization.” *Environmental and Experimental Botany*, 67(1), 153–163.

Baeten, L., Velghe, D., Vanhellemont, M., De Frenne, P., Hermy, M., and Verheyen, K. (2010). “Early Trajectories of Spontaneous Vegetation Recovery after Intensive Agricultural Land

Use.” *Restoration Ecology*, 18(SUPPL. 2), 379–386.

Beesley, L., Moreno-Jiménez, E., Gomez-Eyles, J. L., and Moreno-Jimenez, E. (2010). “Effects of biochar and greenwaste compost amendments on mobility, bioavailability and toxicity of inorganic and organic contaminants in a multi-element polluted soil.” *Environmental Pollution*, 158(6), 2282–7.

Bequet, R., Kint, V., Campioli, M., Vansteenkiste, D., Muys, B., and Ceulemans, R. (2012). “Influence of stand, site and meteorological variables on the maximum leaf area index of beech, oak and Scots pine.” *European Journal of Forest Research*, 131(2), 283–295.

Van Den Berge, J., Naudts, K., Janssens, I. A., Ceulemans, R., and Nijs, I. (2011). “Does the stress tolerance of mixed grassland communities change in a future climate? A test with heavy metal stress (zinc pollution).” *Environmental Pollution*, Elsevier Ltd, 159(12), 3294–3301.

Bernacchi, C. J., Pimentel, C., and Long, S. P. (2003). “In vivo temperature response functions of parameters required to model RuBP-limited photosynthesis.” *Plant, Cell and Environment*, 26(9), 1419–1430.

Bernacchi, C. J., Singsaas, E. L., Pimentel, C., Portis, a. R. J., and Long, S. P. (2001). “Improved temperature response functions for mod- els of Rubisco-limited photosynthesis.” *Plant, Cell and Environment*, 24(2), 253–260.

Blake, E. S., Kimberlain, T. B., Berg, R. J., Cangialosi, J. P., and Beven, J. L. (2013). *Tropical Cyclone Report - Hurricane Sandy (AL182012)*.

Blake, L., and Goulding, K. W. T. (2002). “Effects of atmospheric deposition, soil pH and acidification on heavy metal contents in soils and vegetation of semi-natural ecosystems at Rothamsted Experimental Station, UK.” *Plant and Soil*, 240(2), 235–251.

Bleeker, P. M., Assunção, A. G. L., Teiga, P. M., De Koe, T., and Verkleij, J. A. C. (2002). “Revegetation of the acidic, As contaminated Jales mine spoil tips using a combination of spoil amendments and tolerant grasses.” *Science of the Total Environment*, 300(1–3), 1–13.

Bodek, I., Lyman, W. J., Reehl, W. F., and Rosenblatt, D. H. (1988). *Environmental Inorganic Chemistry: Properties, Processes and Estimation Methods*. (B. T. Walton and R. A. Conway, eds.), Pergamon Press, New York City, NY.

Bolan, N., Kunhikrishnan, A., Thangarajan, R., Kumpiene, J., Park, J., Makino, T., Kirkham, M. B., and Scheckel, K. (2014). “Remediation of heavy metal(loid)s contaminated soils – To mobilize or to immobilize?” *Journal of Hazardous Materials*, Elsevier B.V., 266, 141–166.

Boone, R., Tardif, J., and Westwood, R. (2004). “Radial growth of oak and aspen near a coal-fired station, Manitoba, Canada.” *Tree-Ring Research*, 60(1), 45–58.

Borgegard, S.-O., and Rydin, H. (1989). “Biomass, root penetration and heavy metal uptake in birch in a soil cover over copper tailings.” *Journal of Applied Ecology*, 26, 585–595.

Bréda, N. J. J. (2003). “Ground-based measurements of leaf area index: A review of methods, instruments and current controversies.” *Journal of Experimental Botany*, 54(392), 2403–2417.

Brodribb, T. (1996). “Dynamics of Changing Intercellular CO2 Concentration (ci) during Drought and Determination of Minimum Functional ci.” *Plant physiology*, 111(1), 179–185.

Brown, S., Chaney, R. L., Hallfrisch, J. G., and Xue, Q. (2000). “Effect of biosolids processing on lead bioavailability in an urban soil.” *Journal of environmental quality*, 32, 100–108.

Brun, L. A., Le Corff, J., and Maillet, J. (2003). “Effects of elevated soil copper on phenology, growth and reproduction of five ruderal plant species.” *Environmental Pollution*, 122(3), 361–368.

Buchter, B., Davidoff, B., Amacher, M. C., Hinz, C., Iskandar, I. K., and Selim, H. M. (1989). “Correlation of Freundlich Kd and retention parameter with soils and elements.” *Soil Science*, 148(5), 370–379.

Burley, S., Robinson, S. L., and Lundholm, J. T. (2008). “Post-hurricane vegetation recovery in an urban forest.” *Landscape and Urban Planning*, 85(2), 111–122.

von Caemmerer, S. (2000). *Biochemical Models of Leaf Photosynthesis*. CSIRO Publishing, Collingwood, Australia.

Cannell, M. G. R., and Thornley, J. N. M. (2000). “Modelling the Components of Plant Respiration : Some Guiding Principles.” *Annals of Botany*, 85, 45–54.

Carlton, G. C., and Bazzaz, F. A. (1998). “Regeneration of three sympatric birch species on experimental hurricane blowdown microsites.” *Ecological Monographs*, 68(1), 99–120.

Castro-Rodríguez, A., Carro-Pérez, M. E., Iturbe-Argüelles, R., and González-Chávez, J. L. (2015). “Adsorption of hexavalent chromium in an industrial site contaminated with chromium in Mexico.” *Environmental Earth Sciences*, 73(1), 175–183.

Cervelli, E. W., Lundholm, J. T., and Du, X. (2013). “Spontaneous urban vegetation and habitat heterogeneity in Xi’an, China.” *Landscape and Urban Planning*, 120, 25–33.

Chambers, J. Q., Fisher, J. I., Zeng, H., Chapman, E. L., Baker, D. B., and Hurtt, G. C. (2007). “Hurricane Katrina’s carbon footprint on U.S. Gulf Coast forests.” *Science*, 318(5853), 1107.

Chen, A., Lichstein, J. W., Osnas, J. L. D., and Pacala, S. W. (2014). “Species-independent down-regulation of leaf photosynthesis and respiration in response to shading: Evidence from six temperate tree species.” *PLoS ONE*, 9(4).

Chen, M., and Ma, L. Q. (1998). “Comparison of Four USEPA Digestion Methods for Trace Metal Analysis Using Certified and Florida Soils.” *Journal of Environment Quality*, 27(6), 1294–1300.

Clemente, R., Almela, C., and Bernal, M. P. (2006). “A remediation strategy based on active phytoremediation followed by natural attenuation in a soil contaminated by pyrite waste.” *Environmental Pollution*, 143(3), 397–406.

Clemente, R., Dickinson, N. M., and Lepp, N. W. (2008). “Mobility of metals and metalloids in a multi-element contaminated soil 20 years after cessation of the pollution source activity.” *Environmental Pollution*, 155(2), 254–261.

Clements, W. H., and Kiffney, P. M. (1994). “Assessing contaminant effects at higher levels of biological organization.” *Environmental Toxicology and Chemistry*, 13(3), 357–359.

Cox, L. M., Almeter, A. L., and Saterson, K. A. (2013). “Protecting our life support systems: An inventory of U.S. federal research on ecosystem services.” *Ecosystem Services*, Elsevier, 5, 163–169.

Dahle, G. A., Gallagher, F. J., Gershensond, D., Schäfer, K. V. R., and Grabosky, J. C. (2014). "Allometric and mass relationships of Betula populifolia in a naturally assembled urban brownfield: implications for carbon modeling." *Urban Ecosystems*, 1147–1160.

Le Dantec, V., Dufrêne, E., and Saugier, B. (2000). "Interannual and spatial variation in maximum leaf area index of temperate deciduous stands." *Forest Ecology and Management*, 134(1–3), 71–81.

Denny, H., and Wilkins, D. A. (1987). "Zinc Tolerance in Betula Spp. I. Effect of external concentration of zinc on growth and uptake." *New Phytologist*, 106(3), 517–524.

Derome, J., and Nieminen, T. (1998). "Metal and macronutrient fluxes in heavy-metal polluted Scots pine ecosystems in SW Finland." *Environmental Pollution*, 103(2–3), 219–228.

Desjardins, D., Nissim, W. G., Pitre, F. E., Naud, A., and Labrecque, M. (2014). "Distribution patterns of spontaneous vegetation and pollution at a former decantation basin in southern Québec, Canada." *Ecological Engineering*, Elsevier B.V., 64, 385–390.

DeSousa, C. A. (2003). "Turning brownfields into green space in the City of Toronto." *Landscape and Urban Planning*, 62(May 2002), 181–198.

Dickinson, N. M. (2000). "Strategies for sustainable woodland on contaminated soils." *Chemosphere*, 41(1–2), 259–263.

Dickinson, N. M., Baker, A. J. M., Doronila, A., Laidlaw, S., and Reeves, R. D. (2009). "Phytoremediation of Inorganics: Realism and Synergies." *International Journal of Phytoremediation*, 11(2), 97–114.

Doick, K. J., Sellers, G., Castan-Broto, V., and Silverthorne, T. (2009). "Understanding success in the context of brownfield greening projects: The requirement for outcome evaluation in urban greenspace success assessment." *Urban Forestry and Urban Greening*, Elsevier, 8(3), 163–178.

Donoso, P. J., and Nyland, R. D. (2006). "Interference to hardwood regeneration in northeastern North America: The effects of raspberries (Rubus spp.) following clearcutting and shelterwood methods." *Northern Journal of Applied Forestry*, 23(Farmer 1997), 288–296.

Dreyer, E., Le Roux, X., Montpied, P., Daudet, F. a, and Masson, F. (2001). "Temperature response of leaf photosynthetic capacity in seedlings from seven temperate tree species." *Tree physiology*, 21(4), 223–232.

Duursma, R. A. (2015). "Plantecophys - An R Package for Analysing and Modelling Leaf Gas Exchange Data." *PloS one*, 10(11), e0143346.

Evans, J. M., Parker, A., Gallagher, F., and Krumins, J. A. (2015). "Plant Productivity, Ectomycorrhizae, and Metal Contamination in Urban Brownfield Soils." *Soil Science*, 180(4/5), 198–206.

Farquhar, G. D., Caemmerer, S. Von, and Berry, J. A. (1980). "A Biochemical Model of Photosynthetic CO2 Assimilation in Leaves of C3 Species." *Planta*, 90, 78–90.

Farrag, K., Senesi, N., Nigro, F., Petrozza, A., Palma, A., Shaarawi, S., and Brunetti, G. (2012). "Growth responses of crop and weed species to heavy metals in pot and field experiments." *Environmental Science and Pollution Research*, 19(8), 3636–3644.

Fassnacht, K. S., and Gower, S. T. (1997). "Interrelationships among the edaphic and stand

characteristics, leaf area index, and aboveground net primary production of upland forest ecosystems in north central Wisconsin." *Canadian Journal of Forest Research*, 27(7), 1058–1067.

Fattorini, M., and Halle, S. (2004). "The Dynamic Environmental Filter Model: How Do Filtering Effects Change in Assembling Communities after Disturbance?" *Assembly Rules and Restoration Ecology*, V. M. Temperton, R. J. Hobbs, T. Nuttle, and S. Halle, eds., Island Press, Washington, 96–114.

FEMA Modeling Task Force. (2013). *Hurricane Sandy Impact Analysis – Storm Surge Products*.

Feng, Y. L., Auge, H., and Ebeling, S. K. (2007). "Invasive Buddleja davidii allocates more nitrogen to its photosynthetic machinery than five native woody species." *Oecologia*, 153(3), 501–510.

Folke, C., Carpenter, S., Walker, B., Scheffer, M., Elmqvist, T., Gunderson, L., and Holling, C. S. (2004). "Regime Shifts, Resilience, and Biodiversity in Ecosystem Management." *Annual Review of Ecology, Evolution, and Systematics*, 35, 557–581.

Forbes, V. E., and Calow, P. (2013). "Developing predictive systems models to address complexity and relevance for ecological risk assessment." *Integrated environmental assessment and management*, 9(3), e75-80.

Foster, D. R. (1988). "Species and stand response to catastrophic wind in Central New England, USA." *Journal of Ecology*, 76, 135–151.

Fox, J., and Weisberg, S. (2011). "An R Companion to Applied Regression, Second Edition." Sage, Thousand Oaks, Ca.

French, C. J., Dickinson, N. M., and Putwain, P. D. (2006). "Woody biomass phytoremediation of contaminated brownfield land." *Environmental Pollution*, 141(3), 387–395.

Frouz, J., Prach, K., Pizl, V., Hanel, L., Stary, J., Tajovsky, K., Materna, J., Balik, V., Kalcik, J., and Rehounkova, K. (2008). "Interactions between soil development, vegetation and soil fauna during spontaneous succession in post mining sites." *European Journal of Soil Biology*, 44(1), 109–121.

Gallagher, F. J., Caplan, J. S., Krumins, J. A., and Grabosky, J. C. (2015). "Root Growth Responses to Soil Amendment in an Urban Brownfield." *Ecological Restoration*, 33(1), 10–13.

Gallagher, F. J., Pechmann, I., Bogden, J. D., Grabosky, J., and Weis, P. (2008a). "Soil metal concentrations and productivity of Betula populifolia (gray birch) as measured by field spectrometry and incremental annual growth in an abandoned urban Brownfield in New Jersey." *Environmental Pollution*, Elsevier Ltd, 156(3), 699–706.

Gallagher, F. J., Pechmann, I., Bogden, J. D., Grabosky, J., and Weis, P. (2008b). "Soil metal concentrations and vegetative assemblage structure in an urban brownfield." *Environmental Pollution*, 153(2), 351–361.

Gallagher, F. J., Pechmann, I., Holzapfel, C., and Grabosky, J. (2011). "Altered vegetative assemblage trajectories within an urban brownfield." *Environmental Pollution*, Elsevier Ltd, 159(5), 1159–1166.

Gamon, J. A., Field, C. B., Goulden, M. L., Griffin, K. L., Hartley, A. E., Joel, G., Penuelas, J., and Valentini, R. (1995). "Relationships between NDVI, canopy structure, and

photosynthesis in three Californian vegetation types." *Ecological Applications*, 5(1), 28–41.

Gandois, L., Nicolas, M., VanderHeijden, G., and Probst, A. (2010). "The importance of biomass net uptake for a trace metal budget in a forest stand in north-eastern France." *Science of the Total Environment*, Elsevier B.V., 408(23), 5870–5877.

Gaudet, M., Pietrini, F., Beritognolo, I., Iori, V., Zacchini, M., Massacci, A., Mugnozza, G. S., and Sabatti, M. (2011). "Intraspecific variation of physiological and molecular response to cadmium stress in Populus nigra L." *Tree Physiology*, 31(12), 1309–1318.

Gaydarova, P. N. (2003). "Deciduous forest communities in the Black Sea coastal Strandzha region: temporal and spatial characteristics of leaf area index and density." *Trees*, 17(3), 237–243.

Gessner, M. O., and Chauvet, E. (2013). "A Case for Using Litter Breakdown To Assess Functional Stream Integrity." *Ecological Applications*, 12(2), 498–510.

Good, J. E. G., Williams, T. G., and Moss, D. (1985). "Survival and growth of selected clones of birch and willow on restored opencast coal sites." *Journal of Applied Ecology*, 22, 995–1008.

Graves, W. R., Kroggel, M. A., Widrlechner, M. P., and others. (2002). "Photosynthesis and shoot health of five birch and four alder taxa after drought and flooding." *Journal of Environmental Horticulture*, 20(1), 36–40.

Greger, M. (2004). "Metal Availability, Uptake, Transport and Accumulation in Plants." *Heavy Metal Stress in Plants: From Biomolecules to Ecosystems*, M. N. V Prasad, ed., Springer, Berlin, 1–27.

Gu, M., Robbins, J. A., Rom, C. R., and Choi, H. S. (2008). "Photosynthesis of birch genotypes (Betula L.) under varied irradiance and CO2 concentration." *HortScience*, 43(2), 314–319.

Guédron, S., Duwig, C., Prado, B. L., Point, D., Flores, M. G., and Siebe, C. (2014). "(Methyl)Mercury, Arsenic, and Lead Contamination of the World's Largest Wastewater Irrigation System: the Mezquital Valley (Hidalgo State—Mexico)." *Water, Air, & Soil Pollution*, 225(8), 2045.

Gustafsson, J. P., and Jacks, G. (1995). "Arsenic geochemistry in forsted soil profiles as revealsed by solid-phase studies." *Applied Geochemistry*, 10, 307–315.

Gutierrez, J. C. S., Ponce-Palafox, J. T., Pineda-Jaimes, N. B., Arenas-Fuentes, V., Arredondo-Figueroa, J. L., and Cifuentes-Lemus, J. L. (2016). "Comparison of the mangrove soil with different levels of disturbance in tropical Agua Brava Lagoon, Mexican pacific." *Applied Ecology and Environmental Research*, 14(4), 45–57.

Guttman, N. B. (1998). "Comparing the Palmer Drought Index and the Standardized Precipitation Index." *Journal of the American Water Resources Association*, 34(1), 113–121.

Hagmann, D. F., Goodey, N. M., Mathieu, C., Evans, J., Aronson, M. F. J., Gallagher, F., and Krumins, J. A. (2015). "Effect of metal contamination on microbial enzymatic activity in soil." *Soil Biology and Biochemistry*, Elsevier Ltd, 91, 291–297.

Harrington, R. A., Fownes, J. H., Scowcroft, P. G., and Vann, C. S. (1997). "Impact of Hurricane Iniki on Native Hawaiian Acacia koa Forests: Damage and Two-Year Recovery." *Journal of Tropical Ecology*, 13(4), 539–558.

Hartley, W., Dickinson, N. M., Clemente, R., French, C., Piearce, T. G., Sparke, S., and Lepp, N. W. (2009). "Arsenic stability and mobilization in soil at an amenity grassland overlying chemical waste (St . Helens , UK)." *Environmental Pollution*, Elsevier Ltd, 157(3), 847–856.

Hartley, W., Dickinson, N. M., Riby, P., and Shutes, B. (2012). "Sustainable ecological restoration of brownfield sites through engineering or managed natural attenuation? A case study from Northwest England." *Ecological Engineering*, Elsevier B.V., 40, 70–79.

Heckathorn, S. A., Mueller, J. K., Laguidice, S., Zhu, B., Heckathorn, S. A., Mueller, J. K., Laguidice, S., Zhu, B. I. N., Barrett, T., and Blair, B. (2017). "Chloroplast Small Heat-Shock Proteins Protect Photosynthesis during Heavy Metal Stress." *American Journal of Botany*, 91(9), 1312–1318.

Heinrichs, H., and Mayer, R. (1980). "The role of forest vegetation in the biogeochemical cycle of heavy metals." *Journal of Environment Quality*, 9(1), 111–118.

Hermle, S., Günthardt-Goerg, M. S., and Schulin, R. (2006). "Effects of metal-contaminated soil on the performance of young trees growing in model ecosystems under field conditions." *Environmental Pollution*, 144(2), 703–714.

Hermle, S., Vollenweider, P., Günthardt-Goerg, M. S., McQuattie, C. J., and Matyssek, R. (2007). "Leaf responsiveness of Populus tremula and Salix viminalis to soil contaminated with heavy metals and acidic rainwater." *Tree physiology*, 27(11), 1517–1531.

Hofer, C., Gallagher, F. J., and Holzapfel, C. (2010). "Metal accumulation and performance of nestlings of passerine bird species at an urban brownfield site." *Environmental pollution (Barking, Essex : 1987)*, Elsevier Ltd, 158(5), 1207–13.

Hooper, D. U., Chapin, F. S., Ewel, J. J., Hector, A., Inchausti, P., Lavorel, S., Lawton, J. H., Lodge, D. M., Loreau, M., Naeem, S., Schmid, B., Setala, H., Symstad, A. J., Vandermeer, J., and Wardle, D. A. (2005). "Effects of biodiversity on ecosystem functioning: a consensus of current knowledge." *Ecological Monographs*, 75(1), 3–35.

Hooper, M. J., Glomb, S. J., Harper, D. D., Hoelzle, T. B., Mcintosh, L. M., and Mulligan, D. R. (2016). "Integrated risk and recovery monitoring of ecosystem restorations on contaminated sites." *Integrated Environmental Assessment and Management*, 12(2), 284–295.

Hoshika, Y., Watanabe, M., Inada, N., Mao, Q., and Koike, T. (2013). "Photosynthetic response of early and late leaves of white birch (Betula platyphylla var. japonica) grown under free-air ozone exposure." *Environmental Pollution*, Elsevier Ltd, 182, 242–247.

Howarth, C. J. (1990). "Heat shock proteins in sorghum and pearl millet; ethanol, sodium arsenite, sodium malonate and the development of thermotolerance." *Journal of Experimental Botany*, 41(7), 877–883.

Huang, J. H., and Matzner, E. (2007). "Biogeochemistry of organic and inorganic arsenic species in a forested catchment in Germany." *Environmental Science and Technology*, 41(5), 1564–1569.

Itoh, Y., Noguchi, K., Takahashi, M., Okamoto, T., and Yoshinaga, S. (2007). "Estimation of lead sources in a Japanese cedar ecosystem using stable isotope analysis." *Applied Geochemistry*, 22(6), 1223–1228.

Jardine, P. M., Stewart, M. A., Barnett, M. O., Basta, N. T., Brooks, S. C., Fendorf, S., and Mehlhorn, T. L. (2013). "Influence of soil geochemical and physical properties on

chromium(VI) sorption and bioaccessibility." *Environmental Science and Technology*, 47(19), 11241–11248.

Jarvinen, P., Palme, A., Orlando Morales, L., Lannenpaa, M., Keinanen, M., Sopanen, T., and Lascoux, M. (2004). "Phylogenetic Relationshpis of Betula Species (Betulaceae) Based on Nuclear ADH and Chloroplast MATK Sequences." *American Journal of Botany*, 91(11), 1834–1845.

Jimenez, M. D., Ruiz-Capillas, P., Mola, I., Pérez-Corona, E., Casado, M. A., and Balaguer, L. (2013). "Soil development at the roadside: A case study of a novel ecosystem." *Land Degradation and Development*, 24(6), 564–574.

Joesting, H. M., McCarthy, B. C., and Brown, K. J. (2009). "Determining the shade tolerance of American chestnut using morphological and physiological leaf parameters." *Forest Ecology and Management*, 257(1), 280–286.

Johnson, D., MacDonald, D., Hendershot, W., and Hale, B. (2003). "Metals in northern forest ecosystems : Role of the vegetation in Sequenstration and Cycling, and Implications for Ecological Risk Assessment." *Human and Ecological Risk Assessment*, 9(4), 749–766.

Jonard, M., Legout, A., Nicolas, M., Dambrine, E., Nys, C., Ulrich, E., van der Perre, R., and Ponette, Q. (2012). "Deterioration of Norway spruce vitality despite a sharp decline in acid deposition: A long-term integrated perspective." *Global Change Biology*, 18(2), 711–725.

Jones, J. B. (2012). *Plant nutrition and soil fertility manual*. CRC Press, Boca Raton, Florida.

Juang, K. W., Lee, D. Y., and Ellsworth, T. R. (2001). "Using rank-order geostatistics for spatial interpolation of highly skewed data in a heavy-metal contaminated site." *Journal of Environmental Quality*, 30(3), 894–903.

Jurik, T. W., Weber, J. A., and Gates, D. M. (1988). "Effects of Temperature and Light on Photosynthesis of Dominant Species of a Northern Hardwood Forest." *Botanical Gazette*, 149(2), 203–208.

Khan, A. G. (2005). "Role of soil microbes in the rhizospheres of plants growing on trace metal contaminated soils in phytoremediation." *Journal of Trace Elements in Medicine and Biology*, 18(4), 355–364.

Kitao, M., Koike, T., Tobita, H., and Maruyama, Y. (2005). "Elevated CO2 and limited nitrogen nutrition can restrict excitation energy dissipation in photosystem II of Japanese white birch (Betula platyphylla var. japonica) leaves." *Physiologia Plantarum*, 125(1), 64–73.

Kitao, M., Lei, T. T., and Koike, T. (1997). "Comparison of photosynthetic responses to manganese toxicity of deciduous broad-leaved trees in northern Japan." *Environmental Pollution*, 97(1–2), 113–118.

Köhler, I. H., Macdonald, A. J., and Schnyder, H. (2016). "Last-Century Increases in Intrinsic Water-Use Efficiency of Grassland Communities Have Occurred over a Wide Range of Vegetation Composition, Nutrient Inputs, and Soil pH." *Plant Physiology*, 170(2), 881–890.

Koike, T., and Sakagami, Y. (1986). "Comparison of the photosynthetic responses to temperature and light of Betula maximowicziana and Betula platyphylla var. japonica." *Canadian Journal of Forest Research*, 16(6), 1397.

Kopponen, P., Utriainen, M., Lukkari, K., Suntioinen, S., Karenlampi, L., and Karenlampi, S. (2001). "Clonal differences in copper and zinc tolerance of birch in metal-supplemented

soils.” *Environmental Pollution*, 112, 89–97.

Krumins, J. A., Goodey, N. M., and Gallagher, F. (2015). “Plant–soil interactions in metal contaminated soils.” *Soil Biology and Biochemistry*, Elsevier Ltd, 80, 224–231.

Kubiske, M. E., and Pregitzer, K. S. (1996). “Effects of elevated CO2 and light availability on the photosynthetic light response of trees of contrasting shade tolerance.” *Tree Physiology*, 16(3), 351–358.

Kucharik, C. J., Norman, J. M., and Gower, S. T. (1998). “Measurements of branch area and adjusting leaf area index indirect measurements.” *Agricultural and Forest Meteorology*, 91(1–2), 69–88.

Kumpiene, J., Lagerkvist, A., and Maurice, C. (2008). “Stabilization of As, Cr, Cu, Pb and Zn in soil using amendments - A review.” *Waste Management*, 28(1), 215–225.

De Laender, F., De Schamphelaere, K. A. C., Vanrolleghem, P. A., and Janssen, C. R. (2008). “Validation of an ecosystem modelling approach as a tool for ecological effect assessments.” *Chemosphere*, 71(3), 529–545.

Landre, A. L., Watmough, S. a., and Dillon, P. J. (2009). “Metal Pools, Fluxes, and Budgets in an Acidified Forested Catchment on the Precambrian Shield, Central Ontario, Canada.” *Water, Air, & Soil Pollution*, 209(1–4), 209–228.

Landre, A. L., Watmough, S. A., and Dillon, P. J. (2010). “Metal pools, fluxes, and budgets in an acidified forested catchment on the precambrian shield, central Ontario, Canada.” *Water, Air, and Soil Pollution*, 209(1–4), 209–228.

Larson, C. (2014). “China Gets Serious About Its Pollutant-Laden Soil.” *Science*, 343(6178), 1415–1416.

Laughlin, D. C. (2014). “Applying trait-based models to achieve functional targets for theory-driven ecological restoration.” *Ecology Letters*, 17(7), 771–784.

LI-COR Biosciences. (2013). *LAI-2200C Plant Canopy Analyzer Instruction manual*. Lincoln, NE.

Li, J., Shoup, S., and Chen, Z. (2007). “Phylogenetic Relationships of Diploid Species of Betula (Betulaceae) Inferred from DNA Sequences of Nuclear Nitrate Reductase.” *Systematic Botany*, 32(2), 357–365.

Li, Y.-M., Chaney, R. L., Siebielec, G., and Kerschner, B. A. (1999). “Response of four turfgrass cultivars to limestone and biosolids-compost amendment of a zinc and cadmium contaminated soil at Palmerton, Pennsylvania.” *Journal of Environment Quality*, 29(5), 1440–1447.

Li, Z., and Huang, L. (2015). “Toward a new paradigm for tailings phytostabilization - nature of the substrates, amendment options, and anthropogenic pedogensis.” *Critical Reviews in Environmental Science and Technology*, 45(8), 813–839.

Linn, J. (2013). “The effect of voluntary brownfields programs on nearby property values: Evidence from Illinois.” *Journal of Urban Economics*, Elsevier Inc., 78, 1–18.

Liu, X., Song, Q., Tang, Y., Li, W., Xu, J., Wu, J., Wang, F., and Brookes, P. C. (2013). “Human health risk assessment of heavy metals in soil-vegetable system: A multi-medium analysis.” *Science of the Total Environment*, Elsevier B.V., 463–464, 530–540.

Lobo, F. de A., de Barros, M. P., Dalmagro, H. J., Dalmolin, Â. C., Pereira, W. E., de Souza, É. C., Vourlitis, G. L., and Rodríguez Ortíz, C. E. (2013). "Fitting net photosynthetic light-response curves with Microsoft Excel - a critical look at the models." *Photosynthetica*, 51(3), 445–456.

Losch, R. (2004). "Plant Mitochondrial Respiration Under the Influence of Heavy Metals." *Heavy Metal Stress in Plants: From Biomolecules to Ecosystems*, M. N. V. Prasad, ed., Springer, Berlin, 182–200.

Ludeke, M., Janecek, A., and Kohlmaier, G. (1991). "Modelling the seasonal CO2 uptake by land vegetation using the global vegetation index." *Tellus B*, 43(2), 188–196.

Lutz, J. A., and Halpern, C. B. (2006). "Tree Mortality during Early Forest Development : A Long-Term Study of Rates , Causes , and Consequences." *Ecological Monographs*, 76(2), 257–275.

Ma, Y., Prasad, M. N. V, Rajkumar, M., and Freitas, H. (2011). "Plant growth promoting rhizobacteria and endophytes accelerate phytoremediation of metalliferous soils." *Biotechnology Advances*, 29(2), 248–258.

MacFarlane, G. R., and Burchett, M. D. (2000). "Cellular distribution of Cu, Pb and Zn in the Grey Mangrove Avicennia marina (Forsk.). 68, 45 – 59." *Vierh. Aquat. Bot.*, 68, 45–59.

Maggio, A., and Joly, R. J. (1995). "Effects of mercuric chloride on the hydraulic conductivity of tomato root systems." *Plant Physiology*, 109, 331–335.

Margui, E., Queralt, I., Carvalho, M. L., and Hidalgo, M. (2007). "Assessment of metal availability to vegetation (Betula pendula) in Pb-Zn ore concentrate residues with different features." *Environmental Pollution*, 145(1), 179–184.

Martin, B. T., Jager, T., Nisbet, R. M., Preuss, T. G., Hammers-Wirtz, M., and Grimm, V. (2013). "Extrapolating ecotoxicological effects from individuals to populations: A generic approach based on Dynamic Energy Budget theory and individual-based modeling." *Ecotoxicology*, 22(3), 574–583.

McBride, M., Sauve, S., and Hendershot, W. (1997). "Solubility control of Cu, Zn, Cd and Pb in contaminated soils." *European Journal of Soil Science*, 48(2), 337–346.

McComb, J. Q., Rogers, C., Han, F. X., and Tchounwou, P. B. (2014). "Rapid Screening of Heavy Metals and Trace Elements in Environmental Samples Using Portable X-Ray Fluorescence Spectrometer, A Comparative Study." *Water, Air, & Soil Pollution*, 225(12).

Medlyn, B. E., Dreyer, E., Ellsworth, D., Forstreuter, M., Harley, P. C., Kirschbaum, M. U. F., Le Roux, X., Montpied, P., Strassemeyer, J., Walcroft, A., Wang, K., and Loustau, D. (2002). "Temperature respons of parameters of a biochemically based model of photosynthesis. II. A review of experimental data." *Plant, Cell and Environment*, 25, 1167–1179.

Medvigy, D., Wofsy, S. C., Munger, J. W., Hollinger, D. Y., and Moorcroft, P. R. (2009). "Mechanistic scaling of ecosystem function and dynamics in space and time: Ecosystem Demography model version 2." *Journal of Geophysical Research*, 114(G1), G01002.

Mench, M., Lepp, N., Bert, V., Schwitzguébel, J.-P., Gawronski, S. W., Schröder, P., and Vangronsveld, J. (2010). "Successes and limitations of phytotechnologies at field scale: outcomes, assessment and outlook from COST Action 859." *Journal of Soils and Sediments*, 10(6), 1039–1070.

Mendez, M. O., and Maier, R. M. (2008). “Phytostabilization of mine tailings in arid and semiarid environments--an emerging remediation technology.” *Environmental health perspectives*, 116(3), 278–83.

de Mendiburu, F. (2016). “agricolae: Statistical Procedures for Agricultural Research.” R package version 1.2-4.

Menon, M., Hermle, S., Abbaspour, K. C., Günthardt-Goerg, M. S., Oswald, S. E., and Schulin, R. (2005). “Water regime of metal-contaminated soil under juvenile forest vegetation.” *Plant and Soil*, 271(1–2), 227–241.

Menon, M., Hermle, S., Günthardt-Goerg, M. S., and Schulin, R. (2007). “Effects of heavy metal soil pollution and acid rain on growth and water use efficiency of a young model forest ecosystem.” *Plant and Soil*, 297(1–2), 171–183.

Micó, C., Recatalá, L., Peris, M., and Sánchez, J. (2006). “Assessing heavy metal sources in agricultural soils of an European Mediterranean area by multivariate analysis.” *Chemosphere*, 65(5), 863–872.

Middleton, B. A. (2016). “Differences in impacts of Hurricane Sandy on freshwater swamps on the Delmarva Peninsula, Mid-Atlantic Coast, USA.” *Ecological Engineering*, Elsevier B.V., 87, 62–70.

Millward, A. A., and Kraft, C. E. (2004). “Physical influences of landscape on a large-extent ecological disturbance: The northeastern North American ice storm of 1998.” *Landscape Ecology*, 19(1), 99–111.

Milton, A., Cooke, J. A., and Johnson, M. S. (2004). “A comparison of cadmium in ecosystems on metalliferous mine tailings in Wales and Ireland.” *Water, Air, and Soil Pollution*, 153(1–4), 157–172.

Moffat, A., and Hutchings, T. (2007). “Greening Brownfield Land.” *Sustainable Brownfield Regeneration*, T. Dixon, M. Raco, P. Catney, and D. N. Lerner, eds., Blackwell Publishing Ltd, Oxford, 143–176.

Monson, R., and Baldocchi, D. (2014). *Terrestrial Biosphere-Atmosphere Fluxes*. Cambridge University Press, Cambridge, UK.

Morel, J. L., Chenu, C., and Lorenz, K. (2014). “Ecosystem services provided by soils of urban, industrial, traffic, mining, and military areas (SUITMAs).” *Journal of Soils and Sediments*, 15(8), 1659–1666.

Moreno-Jiménez, E., Manzano, R., Esteban, E., and Peñalosa, J. (2010). “The fate of arsenic in soils adjacent to an old mine site (Bustarviejo, Spain): Mobility and transfer to native flora.” *Journal of Soils and Sediments*, 10, 301–312.

Moustakas, M., Ouzounidou, G., Symeonidis, L., and Karataglis, S. (1997). “Field study of the effects of excess copper on wheat photosynthesis and productivity.” *Soil Science and Plant Nutrition*, 43(3), 531–539.

Munns, W. R., Helm, R. C., Adams, W. J., Clements, W. H., Martin, A., Curry, M., Dipinto, L. M., Johns, D. M., Seiler, R., Williams, L. L., and Young, D. (2009). “Translating Ecological Risk to Ecosystem Service Loss.” *Integrated Environmental Assessment and Management*, 5(4), 500–514.

Munroe, M., Zheljazkov, V., Astatkie, T., and Stratton, G. (2012). “Comparison of Lead

Extraction and Detection Procedures for Six Canadian Soils." *Communications in Soil Science and Plant Analysis*, 43(17), 2303–2313.

Murray, P., Ge, Y., and Hendershot, W. H. (2000). "Evaluating three trace metal contaminated sites: a field and laboratory investigation." *Environmental pollution (Barking, Essex : 1987)*, 107(1), 127–35.

Muscolo, A., Bagnato, S., Sidari, M., and Mercurio, R. (2014). "A review of the roles of forest canopy gaps." *Journal of Forestry Research*, 25(4), 725–736.

Mysliwa-Kurdziel, B., Prasad, M. N. V., and Strzalka, K. (2004). "Photosynthesis in Heavy Metal Stressed Plants." *Heavy Metal Stress in Plants: From Biomolecules to Ecosystems2*, M. N. V. Prasad, ed., Springer, Berlin, 146–181.

Nabulo, G., Oryem-Origa, H., and Diamond, M. (2006). "Assessment of lead, cadmium, and zinc contamination of roadside soils, surface films, and vegetables in Kampala City, Uganda." *Environmental Research*, 101(1), 42–52.

National Climatic Data Center. (2017). "Divisional Data Select." <https://www7.ncdc.noaa.gov/CDO/CDODivisionalSelect.jsp#> (Feb. 1, 2017).

Navrátil, T., Shanley, J. B., Skřivan, P., Krám, P., Mihaljevič, M., and Drahota, P. (2007). "Manganese biogeochemistry in a central Czech Republic catchment." *Water, Air, and Soil Pollution*, 186(1–4), 149–165.

New Jersey Department of Environmental Protection. (1995). *Liberty State Park Soil Sampling Report*. Trenton, New Jersey.

New Jersey Department of Environmental Protection. (1999). *Soil Cleanup Criteria*.

New Jersey Weather & Climate Network. (2016). "Data Viewer - Jersey City Station #3411." *Office of the New Jersey State Climatologist*, <http://www.njweather.org/data> (Oct. 11, 2016).

Niemeyer, J. C., Nogueira, M. a., Carvalho, G. M., Cohin-De-Pinho, S. J., Outeiro, U. S., Rodrigues, G. G., da Silva, E. M., and Sousa, J. P. (2012). "Functional and structural parameters to assess the ecological status of a metal contaminated area in the tropics." *Ecotoxicology and Environmental Safety*, Elsevier, 86, 188–197.

NOAA. (2013). "The Battery, NY Station ID: 8518750." *Tides & Currents*, <http://www.tidesandcurrents.noaa.gov/stationhome.html?id=8518750> (May 25, 2016).

Nowack, B., Schulin, R., and Luster, J. (2010). "Metal fractionation in a contaminated soil after reforestation: Temporal changes versus spatial variability." *Environmental Pollution*, Elsevier Ltd, 158(10), 3272–3278.

Nowak, D. J., and Crane, D. E. (2002). "Carbon storage and sequestration by urban trees in the USA." *Environmental Pollution*, 116(3), 381–389.

Nwugo, C. C., and Huerta, A. J. (2008). "Effects of silicon nutrition on cadmium uptake, growth and photosynthesis of rice plants exposed to low-level cadmium." *Plant and Soil*, 311(1–2), 73–86.

NYHOPS. (2012). *NY/NJ Harbor Estuary Surface Salinity - Robbins Reef, NJ (NOS), 2012-10-29 to 2012-10-30*.

Oehlert, G. W. (2010). *A First Course in Design and Analysis of Experiments*. Creative

Commons License.

Oguma, A. Y., and Klerks, P. L. (2015). “Evidence for mild sediment Pb contamination affecting leaf-litter decomposition in a lake.” *Ecotoxicology*, Springer US, 24(6), 1322–1329.

Oldfield, E. E., Felson, A. J., Auyeung, D. S. N., Crowther, T. W., Sonti, N. F., Harada, Y., Maynard, D. S., Sokol, N. W., Ashton, M. S., Warren, R. J., Hallett, R. A., and Bradford, M. A. (2015). “Growing the urban forest: Tree performance in response to biotic and abiotic land management.” *Restoration Ecology*, 23(5), 707–718.

Oleksyn, J., Żytkowiak, R., Reich, P. B., Tjoelker, M. G., and Karolewski, P. (2000). “Ontogenetic patterns of leaf CO2 exchange, morphology and chemistry in Betula pendula trees.” *Trees*, 14(5), 271–281.

Olson, P. E., and Fletcher, J. S. (2000). “Ecological recovery of vegetation at a former industrial sludge basin and its implications to phytoremediation.” *Environmental science and pollution research international*, 7(4), 195–204.

Panagos, P., Liederkerke, M. Van, Yigini, Y., and Montanarella, L. (2013). “Contaminated Sites in Europe: Review of the Current Situation Based on Data Collected through a European Network.” *Journal of Environmental and Public Health*, 2013, 11.

Pastor, J., and Post, W. . (1988). “Response of Northern Forests to CO2-Induced Climate Change.” *Nature*, 334(6177), 55–58.

Pavao-Zuckerman, M. a. (2008). “The nature of urban soils and their role in ecological restoration in cities.” *Restoration Ecology*, 16(4), 642–649.

Pavoine, S., Vela, E., Gachet, S., De Bélair, G., and Bonsall, M. B. (2011). “Linking patterns in phylogeny, traits, abiotic variables and space: A novel approach to linking environmental filtering and plant community assembly.” *Journal of Ecology*, 99(1), 165–175.

Pereira, M. P., Rodrigues, L. C. de A., Corrêa, F. F., de Castro, E. M., Ribeiro, V. E., and Pereira, F. J. (2016). “Cadmium tolerance in Schinus molle trees is modulated by enhanced leaf anatomy and photosynthesis.” *Trees - Structure and Function*, 30(3), 807–814.

Perez-de-Mora, A., Madejon, E., Burgos, P., and Cabrera, F. (2006). “Trace element availability and plant growth in a mine-spill contaminated soil under assisted natural remediation I. Soils.” *Science of the Total Environment*, 363(1–3), 28–37.

Perring, M. P., Standish, R. J., Price, J. N., Craig, M. D., Erickson, T. E., Ruthrof, K. X., Whiteley, A. S., Valentine, L. E., and Hobbs, R. J. (2015). “Advances in restoration ecology: rising to the challenges of the coming decades.” *Ecosphere*, 6(8), art131.

Pettersson, R., McDonald, A. J. S., and Stadenberg, I. (1992). “Effects of elevated carbon dioxide concentration on photosynthesis and growth of small birch plants (*Betula pendula* Roth.) at optimal nutrition.” *Plant, Cell and Environment*, 15(8), 1115–1121.

Poorter, H., Niinemets, Ü., Poorter, L., Wright, I. J., Villar, R., Niinemets, U., Poorter, L., Wright, I. J., and Villar, R. (2009). “Causes and consequences of variation in leaf mass per area (LMA):a meta-analysis.” *New phytologist*, 182(3), 565–588.

Poorter, H., Niklas, K. J., Reich, P. B., Oleksyn, J., Poot, P., and Mommer, L. (2011). “Biomass allocation to leaves, stems and roots: meta-analysis of interspecific variation and environmental control.” *New Phytologist*, 193(1), 30–50.

Poschenrieder, C., and Barcelo, J. (2004). “Water relations in heavy metal stressed plants.” *Heavy Metal Stress in Plants: From Biomolecules to Ecosystems*, M. N. V. Prasad, ed., Springer, Berlin, 223–248.

Prioul, J. L., and Chartier, P. (1977). “Partitioning of Transfer and Carboxylation Components of Intracellular Resistance to Photosynthetic CO2 Fixation: A Critical Analysis of the Methods Used.” *Ann. Bot.*, 41(4), 789–800.

Pyle, S. M., Nocerino, J. M., Deming, S. N., Palasota, J. a., Palasota, J. M., Miller, E. L., Hillman, D. C., Kuharic, C. a., Cole, W. H., Fitzpatrick, P. M., Watson, M. a., and Nichols, K. Y. D. (1996). “Comparison of AAS, ICP-AES, PSA, and XRF in determining lead and cadmium in soil.” *Environmental Science and Technology*, 30(1), 204–213.

Qian, Y., Gallagher, F. J., Feng, H., and Wu, M. (2012). “A geochemical study of toxic metal translocation in an urban brownfield wetland.” *Environmental Pollution*, 166, 23–30.

R Core Team. (2016). “R: A Language and Environment for Statistical Computing.” R Foundation for Statistical Computing, Vienne, Austria.

Radu, T., and Diamond, D. (2009). “Comparison of soil pollution concentrations determined using AAS and portable XRF techniques.” *Journal of Hazardous Materials*, 171, 1168–1171.

Radwanski, D., Vanderklein, D. W., and Schäfer, K. V. R. (2017). “Physiology and carbon allocation of two co-occurring poplar species in an urban brownfield.” *Environmental Pollution*, 223, 497–506.

Ramos Arroyo, Y. R., and Siebe, C. (2007). “Weathering of sulphide minerals and trace element speciation in tailings of various ages in the Guanajuato mining district, Mexico.” *Catena*, 71(3), 497–506.

Ramsey, P. W., Rillig, M. C., Feris, K. P., Gordon, N. S., Moore, J. N., Holben, W. E., and Gannon, J. E. (2005). “Relationship between communities and processes; new insights from a field study of a contaminated ecosystem.” *Ecology Letters*, 8(11), 1201–1210.

Ranney, T. G., Bir, R. E., and Skroch, W. A. (1991). “Comparative Drought Resistance Among 6 Species of Birch (Betula) - Influence of Mild Water Stress on Water Relations and Leaf Gas Exchange.” *Tree Physiology*, 8, 351–360.

Ranney, T. G., and Peet, M. (1994). “Heat tolerance of five taxa of birch (Betula): Physiological responses to supraoptimal leaf temperatures.” *Journal of the American Society for Horticultural Science*, 119(2), 243–248.

Rawlins, B. G., Vane, C. H., Kim, A. W., Tye, A. M., Kemp, S. J., and Bellamy, P. H. (2008). “Methods for estimating types of soil organic carbon and their application to surveys of UK urban areas.” *Soil Use and Management*, 24(1), 47–59.

Reich, P. B., Ellsworth, D. S., and Uhl, C. (1995). “Leaf carbon and nutrient assimilation and conservation in species of differing successional status in an oligotrophic Amazonian forest.” *Functional Ecology*, 9(1), 65–76.

Renninger, H. J., Carlo, N. J., Clark, K. L., and Schäfer, K. V. R. (2015). “Resource use and efficiency, and stomatal responses to environmental drivers of oak and pine species in an Atlantic Coastal Plain forest.” *Frontiers in Plant Science*, 6(May), 1–16.

Renninger, H. J., Wadhwa, S., Gallagher, F. J., Vanderklein, D., and Schäfer, K. V. R. (2012).

"Allometry and photosynthetic capacity of poplar (Populus deltoides) along a metal contamination gradient in an urban brownfield." *Urban Ecosystems*, 16(2), 247–263.

Robb, J., Busch, L., and Rauser, W. E. (1980). "Zinc toxicity and xylem vessel wall alteration in white beans." *Annals of Botany*, 46(1), 43–50.

Robinson, B. H., Bañuelos, G., Conesa, H. M., Evangelou, M. W. H., and Schulin, R. (2009). "The Phytomanagement of Trace Elements in Soil." *Critical Reviews in Plant Sciences*, 28(4), 240–266.

Robinson, S. L., and Lundholm, J. T. (2012). "Ecosystem services provided by urban spontaneous vegetation." *Urban Ecosystems*, 15(3), 545–557.

Rohr, J. R., Salice, C. J., Nisbet, R. M., Rohr, J. R., Salice, C. J., and Nisbet, R. M. (2016). "The pros and cons of ecological risk assessment based on data from different levels of biological organization." *Critical Reviews in Toxicology*, 8444(June).

Romanowska, E., Igamberdiev, A. U., Parys, E., and Gardestrom, P. (2002). "Stimulation of respiration by Pb2+ in detached leaves and mitochondria of C-3 and C-4 plants." *Physiologia Plantarum*, 116, 148–154.

Romero Lankao, P., Davidson, D. J., Diffenbaugh, N. S., Kinney, P. L., Kirshen, P., Kovacs, P., and Ruiz, L. V. (2014). "North America." *Climate Change 2014: Impacts, Adaptation, and Vulnerability. Part B: Regional Aspects.*, V. R. Barros, C. B. Field, D. J. Dokken, M. D. Mastrandrea, K. J. Mach, T. E. Bilir, M. Chatterjee, K. L. Ebi, Y. O. Estrada, R. C. Genova, B. Girma, E. S. Kissel, A. N. Levy, S. MacCracken, P. R. Mastrandrea, and L. L. White, eds., Cambridge University Press, Cambridge, UK and New York, NY, USA, 1439–1498.

Royo, A. a, and Carson, W. P. (2006). "On the formation of dense understory layers in forests worldwide: consequences and implications for forest dynamics, biodiversity, and succession." *Canadian Journal of Forest Research*, 36(6), 1345–1362.

Ruttens, A., Colpaert, J. V., Mench, M., Boisson, J., Carleer, R., and Vangronsveld, J. (2006). "Phytostabilization of a metal contaminated sandy soil. II: Influence of compost and/or inorganic metal immobilizing soil amendments on metal leaching." *Environmental Pollution*, 144, 533–539.

Sánchez Vilas, J., Campoy, J. G., and Retuerto, R. (2016). "Sex and heavy metals: Study of sexual dimorphism in response to soil pollution." *Environmental and Experimental Botany*, Elsevier B.V., 126, 68–75.

Santala, K. R., and Ryser, P. (2009). "Influence of heavy-metal contamination on plant response to water availability in white birch, Betula papyrifera." *Environmental and Experimental Botany*, 66(2), 334–340.

Santana, K. B., de Almeida, A. A. F., Souza, V. L., Mangabeira, P. A. O., Silva, D. da C., Gomes, F. P., Dutruch, L., and Loguercio, L. L. (2012). "Physiological analyses of Genipa americana L. reveals a tree with ability as phytostabilizer and rhizofilterer of chromium ions for phytoremediation of polluted watersheds." *Environmental and Experimental Botany*, Elsevier B.V., 80, 35–42.

Sarkar, D. (2008). *Lattice: Multivariate Data Visualization with R*. Springer, New Y.

Sauve, S., Hendershot, W., and Allen, H. E. (2000). "Solid-Solution Partitioning of Metals in Contaminated Soils : Dependence on pH , Total Metal Burden , and Organic Matter." *Environmental Science & Technology*, 34(7), 1125–1131.

Schadek, U., Strauss, B., Biedermann, R., and Kleyer, M. (2009). “Plant species richness, vegetation structure and soil resources of urban brownfield sites linked to successional age.” *Urban Ecosystems*, 12(2), 115–126.

Scharenbroch, B. C. (2009). “A meta-analysis of studies published in arboriculture & urban forestry relating to organic materials and impacts on soil, tree, and environmental properties.” *Arboriculture and Urban Forestry*, 35(5), 221–231.

Schumann, M. E., White, A. S., and Witham, J. W. (2003). “The effects of harvest-created gaps on plant species diversity, composition, and abundance in a Maine oak-pine forest.” *Forest Ecology and Management*, 176(1–3), 543–561.

Sellin, A., Eensalu, E., and Niglas, A. (2010). “Is distribution of hydraulic constraints within tree crowns reflected in photosynthetic water-use efficiency? An example of Betula pendula.” *Ecological Research*, 25(1), 173–183.

Sessitsch, A., Kuffner, M., Kidd, P., Vangronsveld, J., Wenzel, W. W., Fallmann, K., and Puschenreiter, M. (2013). “The role of plant-associated bacteria in the mobilization and phytoextraction of trace elements in contaminated soils.” *Soil Biology and Biochemistry*, Elsevier Ltd, 60, 182–194.

Sharkey, T. D., Bernacchi, C. J., Farquhar, G. D., and Singsaas, E. L. (2007). “Fitting photosynthetic carbon dioxide response curves for C 3 leaves.” *Plant, Cell & Environment*, 30(9), 1035–1040.

Shi, G., and Cai, Q. (2009). “Leaf plasticity in peanut (Arachis hypogaea L.) in response to heavy metal stress.” *Environmental and Experimental Botany*, 67(1), 112–117.

de Silva, N. D. G., Cholewa, E., and Ryser, P. (2012). “Effects of combined drought and heavy metal stresses on xylem structure and hydraulic conductivity in red maple (Acer rubrum L.).” *Journal of experimental botany*, 63(16), 5957–5966.

Singh, S. K., and Raja Reddy, K. (2011). “Regulation of photosynthesis, fluorescence, stomatal conductance and water-use efficiency of cowpea (Vigna unguiculata [L.] Walp.) under drought.” *Journal of Photochemistry and Photobiology B: Biology*, Elsevier B.V., 105(1), 40–50.

Smith, K. S. (1999). “Metal Sorption on Mineral Surfaces: An Overview with Examples Relating to Mineral Deposits.” *Review in Economic Geology*, 6A–6B, 161–182.

Smith, T. T., Zaitchik, B. F., and Gohlke, J. M. (2013). “Heat waves in the United States: Definitions, patterns and trends.” *Climatic Change*, 118(3–4), 811–825.

Soil Survey Staff. (2010). *LadyLiberty Soil Series: Primary Characterization Data*.

Sparks, D. L. (2003). *Environmental Soil Chemistry*. Academic Press, Amsterdam.

Stancheva, I., Geneva, M., Markovska, Y., Tzvetkova, N., Mitova, I., Todorova, M., and Petrovl, P. (2014). “A comparative study on plant morphology, gas exchange parameters, and antioxidant response of Ocimum basilicum L. And Origanum vulgare L. Grown on industrially polluted soil.” *Turkish Journal of Biology*, 38(1), 89–102.

Strachan, I. B., and McCaughey, J. H. (1996). “Spatial and vertical leaf area index of a deciduous forest resolved using the LAI-2000 plant canopy analyzer.” *Forest Science*, 42(2), 176–181.

Stueve, K. M., Lafon, C. W., and Isaacs, R. E. (2007). “Spatial patterns of ice storm disturbance

on a forested landscape in the Appalachian Mountains, Virginia." *Area*, 39(1), 20–30.

Tack, F. M. G., and Vandecasteele, B. (2008). "Cycling and ecosystem impact of metals in contaminated calcareous dredged sediment-derived soils (Flanders, Belgium)." *Science of the Total Environment*, Elsevier B.V., 400(1–3), 283–289.

Takeno, N. (2005). *Atlas of Eh-pH diagrams: Intercomparison of thermodynamic databases*. *Geological Survey of Japan Open File Report No. 419*.

Tang, X., Shen, C., Shi, D., Cheema, S. a., Khan, M. I., Zhang, C., and Chen, Y. (2010). "Heavy metal and persistent organic compound contamination in soil from Wenling: An emerging e-waste recycling city in Taizhou area, China." *Journal of Hazardous Materials*, 173(1–3), 653–660.

Thiel, A. L., and Perakis, S. S. (2009). "Nitrogen dynamics across silvicultural canopy gaps in young forests of western Oregon." *Forest Ecology and Management*, 258(3), 273–287.

Tipping, E., Rieuwerts, J., Pan, G., Ashmore, M. R., Lofts, S., Hill, M. T. R., Farago, M. E., and Thornton, I. (2003). "The solid-solution partitioning of heavy metals (Cu, Zn, Cd, Pb) in upland soils of England and Wales." *Environmental Pollution*, 125(2), 213–225.

Tredici, P. Del. (2010). "Spontaneous Urban Vegetation: Reflections of Change in a Globalized World." *Nature and Culture*, 5(3), 299–315.

Trubina, M. R. (2009). "Species richness and resilience of forest communities: Combined effects of short-term disturbance and long-term pollution." *Forest Ecology: Recent Advances in Plant Ecology*, 339–350.

Turner, R. K., Paavola, J., Cooper, P., Farber, S., Jessamy, V., and Georgiou, S. (2003). "Valuing nature: Lessons learned and future research directions." *Ecological Economics*, 46(3), 493–510.

Tyler, G., and Olsson, T. (2001). "Concentrations of 60 elements in the soil solution as related to the soil acidity - Tyler - 2002 - European Journal of Soil Science - Wiley Online Library." *European Journal of Soil Science*, 52(1), 151–165.

U.S. Army Corps of Engineers. (2004). *Liberty State Park hydrology and hydraulics of freshwater wetlands*.

U.S. Army Corps of Engineers. (2005). *Hudson-Raritan Estuary, Liberty State Park Ecosystem Restoraiton: Integrated Feasibility Report and Environmental Impact Statement Vol. 1*. New York City, NY.

United States Army Corps of Engineers. (2004). *Hudson-Raritan Estuary Environmental Restoration Study, Liberty State Park, Jersey City, Hudson County, Sub-Surface Soil Characterization*.

United States Environmental Protection Agency. (2003). *Guidance for developing ecological soil screening levels. OSWER-Directive 9285*.

United States General Accounting Office. (1987). *SUPERFUND: Extent of Nation's Potential Hazardous Waste Problem Still Unknown*. Washington D.C.

Ussiri, D. A. N., Jacinthe, P. A., and Lal, R. (2014). "Methods for determination of coal carbon in reclaimed minesoils: A review." *Geoderma*, Elsevier B.V., 214–215, 155–167.

Utriainen, M. A., Karenlampi, L. V., Karenlampi, S. O., and Schat, H. (1997). "Differential

tolerance to copper and zinc of micropropagated birches tested in hydroponics." *New Phytologist*, 137(3), 543–549.

Vassilev, A., Yordanov, I., and Tsonev, T. (1997). "Effects of Cd2+ on the physiological state and photosynthetic activity of young barley plants." *Photosynthetica*.

Vázquez, S., Hevia, A., Moreno, E., Esteban, E., Peñalosa, J. M., and Carpena, R. O. (2011). "Natural attenuation of residual heavy metal contamination in soils affected by the Aznalcóllar mine spill, SW Spain." *Journal of Environmental Management*, Elsevier Ltd, 92(8), 2069–2075.

Vesk, P. A., Nockolds, C. E., and Allaway, W. G. (1999). "Metal localization in water hyacinth roots from an urban wetland." *Plant, Cell and Environment*, 22(2), 149–158.

Wang, W., Qu, J. J., Hao, X., Liu, Y., and Stanturf, J. A. (2010). "Post-hurricane forest damage assessment using satellite remote sensing." *Agricultural and Forest Meteorology*, 150(1), 122–132.

Watanabe, Y., Wakabayashi, K., Kitaoka, S., Satomura, T., Eguchi, N., Watanabe, M., Nakaba, S., Takagi, K., Sano, Y., Funada, R., and Koike, T. (2016). "Response of tree growth and wood structure of Larix kaempferi, Kalopanax septemlobus and Betula platyphylla saplings to elevated CO2 concentration for 5 years exposure in a FACE system." *Trees - Structure and Function*, Springer Berlin Heidelberg, 30(5), 1569–1579.

Watmough, S. A. (2008). "Element mobility and partitioning along a soil acidity gradient in central Ontario forests, Canada." *Environmental Geochemistry and Health*, 30(5), 431–444.

Watmough, S. A., and Dillon, P. J. (2007). "Lead biogeochemistry in a central Ontario Forested watershed." *Biogeochemistry*, 84(2), 143–159.

Wayne, P. M., and Bazzaz, F. A. (1993). "Birch seedling responses to daily time courses of light in experimental forest gaps and shadehouses." *Ecology*, 74(5), 1500–1515.

Wennerberg, S. (2004). *Plant Guide: Gray Birch Betula populifolia Marsh.* Baton Rouge, Louisiana.

Whelan, A., Kechavarzi, C., Coulon, F., Sakrabani, R., and Lord, R. (2013). "Influence of compost amendments on the hydraulic functioning of brownfield soils." *Soil Use and Management*, 29(2), 260–270.

Williamson, J. C., Rowe, E. C., Hill, P. W., Nason, M. A., Jones, D. L., and Healey, J. R. (2011). "Alleviation of Both Water and Nutrient Limitations is Necessary to Accelerate Ecological Restoration of Waste Rock Tips." *Restoration Ecology*, 19(2), 194–204.

Wingler, A., Lea, P. J., Quick, W. P., and Leegood, R. C. (2000). "Photorespiration: metabolic pathways and their role in stress protection." *Philosophical transactions of the Royal Society of London. Series B, Biological sciences*, 355(1402), 1517–29.

Wong, M. H. (2003). "Ecological restoration of mine degraded soils, with emphasis on metal contaminated soils." *Chemosphere*, 50(6), 775–80.

Wright, I. J., Reich, P. B., Westoby, M., Ackerly, D. D., Baruch, Z., Bongers, F., Cavender-bares, J., Chapin, T., Cornelissen, J. H. C., Diemer, M., Flexas, J., Garnier, E., Groom, P. K., and Gulias, J. (2004). "The worldwide leaf economics spectrum." *Nature*, 428, 821–827.

Wu, C.-M., Tsai, H.-T., Yang, K.-H., and Wen, J.-C. (2012). "How Reliable is X-Ray

Fluorescence (XRF) Measurement for Different Metals in Soil Contamination?" *Environmental Forensics*, 13(2), 110–121.

Yang, Y., Han, X., Liang, Y., Ghosh, A., Chen, J., and Tang, M. (2015). "The combined effects of arbuscular mycorrhizal fungi (AMF) and lead (Pb) stress on Pb accumulation, plant growth parameters, photosynthesis, and antioxidant enzymes in robinia pseudoacacia L." *PLoS ONE*, 10(12), 1–24.

Zhang, L., Pan, Y., Lv, W., and Xiong, Z. ting. (2014). "Physiological responses of biomass allocation, root architecture, and invertase activity to copper stress in young seedlings from two populations of Kummerowia stipulacea (maxim.) Makino." *Ecotoxicology and Environmental Safety*, Elsevier, 104(1), 278–284.

Zhang, W., Zwiazek, J. J., and Pfautsch, S. (2016). "Effects of root medium pH on root water transport and apoplastic pH in red-osier dogwood (Cornus sericea) and paper birch (Betula papyrifera) seedlings." *Plant Biology*, 18(6), 1001–1007.

APPENDIX A
Supplementary Data

Table A-1: Mean, minimum, and maximum As, Cr, Cu, Pb, and Zn concentrations (mg/kg) measured in 1995 (n = 7), 2005 (n = 21), and 2015 (n = 35) A horizon in seven research plots.

Year	As	Cr	Cu	Pb	Zn
	Mean (Minimum – Maximum) mg/kg				
1995	103.9 (5.8-545)	34.1 (11.1-57.1)	711 (30.1-3790)	2152.3 (37-11800)	3109.1 (19.9-16000)
2005	68.3 (3.84-429.32)	50.2 (1.4-271.74)	329.8 (47.19-1684.63)	940.5 (55.3-5441.54)	353.4 (3.5-3153.24)
2015	111.0 (28.04-772.11)	179.6 (41.11-395.37)	393.6 (61.3-2473.38)	822.4 (167.59-2820.75)	365.5 (48.67-1550.54)